Review

Current principles, challenges, and new metrics in pH-responsive drug delivery systems for systemic cancer therapy

Roman A. Verkhovskii [1], Alexey N. Ivanov [2], Ekaterina V. Lengert [2,3], Ksenia A. Tulyakova [4], Natalia Yu. Shilyagina [4], and Alexey V. Ermakov [2,3,*]

[1] Science Medical Center, Saratov State University, 83 Astrakhanskaya Str., 410012 Saratov, Russia; r.a.verhovskiy@mail.ru

[2] Central Research Laboratory, Saratov State Medical University of V. I. Razumovsky, Ministry of Health of the Russian Federation, 410012 Saratov, Russia; lex558452@gmail.com, lengert_e_v@staff.sechenov.ru, ermakov_a_v_2@staff.sechenov.ru

[3] Institute of Molecular Theranostics, I. M. Sechenov First Moscow State Medical University, 8 Trubetskaya Str., 119991 Moscow, Russia lengert_e_v@staff.sechenov.ru, ermakov_a_v_2@staff.sechenov.ru

[4] Institute of Biology and Biomedicine, Lobachevsky State University of Nizhny Novgorod, 23 Gagarin Ave., Nizhny Novgorod 603950, Russia, tulyakova.ksenia@gmail.com, nat-lekanova@yandex.ru

* Correspondence, ermakov_a_v_2@staff.sechenov.ru.

Abstract: The paradigm of drug delivery via nano- and microcarriers is one of the leading ideas that enable overcoming the limitations of traditional chemotherapy. The trend toward more complex drug carriers capable of multifunctionality is observed in the literature. To date, prospects of stimuli-responsive systems to control the cargo release in the lesion nidus are widely accepted. Both endogenous and exogenous stimuli are employed for this purpose, however, endogenous pH is one of the most common triggers. Unfortunately, scientists face difficulties in the implementation of this idea since a range of biological barriers, drug bioavailability issues, and challenges in the synthesis of carriers with required properties have arisen. Here, we discuss fundamental strategies of pH-responsive drug delivery as well as limits in its application and reveal the main problems, weak sides, and reasons for poor clinical results. Also, we have made an attempt to formulate the profiles of "ideal" drug carrier in the frame of different strategies and considered recently published studies through the lens of these profiles. This approach enables the identification of current trends and promising vectors in the development of pH-responsive drug delivery systems, as well as challenges to be resolved in the next generation of carriers.

Keywords: cancer therapy; nanomedicine; drug delivery; pH-responsiveness; EPR; intratumoral delivery; intracellular delivery; nanoparticles; metal-organic frameworks

1. Introduction

To date, the development and improvement of methods for cancer therapy occupy a large place in biomedical sciences. However, despite significant advances in both clinical and laboratory research, we are still far from a breakthrough in this field [1–4]. Research in this area goes along various vectors, from trying to achieve a fundamental understanding of disease processes and developing new drugs to "programming" the body to fight the disease[5–9]. Enormous efforts are devoted to the development of drug delivery systems (DDS), which sometimes represent a bigger problem than the drugs themselves. Nevertheless, such systems enable circumventing a range of shortcomings of traditional therapeutic agents including low bioavailability, susceptibility to the aggressive influence of surrounding media, accelerated blood clearance, and off-target toxicity[10–12].

 doi:10.20944/preprints202305.0289.v1

The application of such DDS for drug delivery through the systemic administration produces new challenges in therapy, which are often difficult to predict in advance. Various factors affect the behavior of carriers in the body. Multiple studies have shown that the nature, size, surface potential, and other characteristics of carriers fundamentally affect their biodistribution, cell interaction, circulation time, and hydrodynamics in the blood flow[13–16]. Often, features of the carrier that provide effective administration procedure such as prolonged circulation in the blood flow impede the other functions of the DDS such as uptake and drug release. In this regard, researchers have to take in consideration a huge number of parameters in order to obtain the optimal carrier for a particular task. In this way, the drug delivery paradigm has been applied to encapsulate all sorts of drugs from cytostatics to photodynamic agents [17–21]. Understanding drug bioavailability issues in the body and fundamental disease mechanisms is driving researchers to develop increasingly complex drug delivery systems designed to provide increased internalization into a specific cell type, prolonged circulation time, enhanced drug stability, tolerability, and retention in lesion area, controlled release profile, responsiveness to a specific endogenous and exogenous triggers (IR radiation, magnetic field, electric field, ultrasound, temperature, pH, enzymes) and others [22–25]. In general, targeting of drug-loaded carriers to tumors in the organism can be divided into active and passive. The passive approach is based on the accumulation of the carriers in pathological sites with affected vasculature such as tumors, inflammations, and infarcted areas [26]. In this case, drug carriers are supposed to circulate in the blood as long as possible to increase the probability of their accumulation in pathological sites via the enhanced permeability and retention (EPR) effect. Active targeting employs a modification of carriers with specific ligands or different nanostructures possessing certain physical properties, which ensure a specific recognition and bind of DDS with pathological cells [27,28], promotion of their uptake [29], or manipulation over their distribution and drug release by external stimuli like a magnetic field [30,31]. Usually, researchers employ hybrid approach when EPR-mediated accumulation promotes the delivery of actively targeted carriers into poorly accessible sites of interest.

A huge body of research dedicated to DDS application for chemotherapeutic compounds delivery suggests the release of encapsulated substances in response to external stimuli in addition to the EPR effect. The results of drug delivery via thermosensitive liposomes as externally activated carriers showed a significant increase in drug concentration in the tumor up to 17 times relative to the free form of the drug [32]. However, this method is applicable only to surgically accessible tumors, and not to systemic therapy at the stage of metastasis, which is paramount importance for cancer therapy. Other studies suggest the use of non-invasive methods for the activation of carriers and the induction of therapeutic agents release by exposure to external physical fields, including magnetic fields, ultrasound, and infrared radiation [22–24,31,33–36]. A promising strategy is the usage of tumor microenvironment's features including reduced pH of the tumor milieu (pH in the range from 6.3 to 7) if compare with pH in normal tissues (7.35-7.45). In this regard, the development of pH-responsive delivery systems that release cargo in response to slightly acidic pH opens up new venues for the treatment of poorly accessible tumors [37,38].

pH is a rigid biological constant in the human body. However, pH in soft tissues may differ from that in blood plasma depending on the metabolic activity of cells and surrounding conditions, which makes the usage of pH-sensitive systems for the targeted drug delivery possible. It is known that tumor cells are characterized by increased metabolic activity, which ensures a high proliferation rate. The energy needs of tumor cells are provided mainly by anaerobic glucose metabolism, especially in conditions of blood supply and oxygen deprivation, which leads to the accumulation of products of incomplete glucose oxidation [39]. As a result of the active metabolism of cancer cells, the tumor microenvironment has a higher acidity and reduced pH compared to normal tissues, that makes pH-responsive biomaterials highly important for targeted drug delivery to malignant neoplasms [40].

The use of pH as an endogenous trigger for the release of active components by stimulus-responsive carriers has a number of advantages, including wide applicability and the absence of the demand for external triggers. At the same time, authors indicate the low accuracy of DDS delivery and drug release in non-targeted sites of the body as disadvantages of pH as triggering stimuli, which

 doi:10.20944/preprints202305.0289.v1

is due to the possibility of shifts in acid–base homeostasis in tissues as a result of a wide range of physiological and pathological (inflammatory changes) reasons [41]. Synthesis strategies and classification of DDS capable of pH-responsive cargo release have been extensively reviewed elsewhere [42–45]. Here, we consider in detail the current paradigm and fundamentals of the idea of pH-responsive delivery systems, drug bioavailability issues in the body, and ways for overcoming them, the role of drug carriers in these processes, and the functions they have to implement to provide a therapeutic effect, introduce metrics for evaluation.

2. Principles of pH-responsive drug delivery

In the last few decades, the paradigm of drug carriers' usage to overcome the non-specific distribution of therapeutic agents in the body, including chemotherapeutic substances that exert severe toxic stress on healthy tissues, has been actively developed. To increase the accumulation of DDSs carrying therapeutic agents in tumor interstitium, differences between normal and cancer tissues properties are used. Structural features of tumors, such as hypervascularization, vascular pathologies, and impaired functionality of lymphatic drainage, can be utilized to differentiate tumors from healthy tissues and selectively accumulate drug carriers. In particular, tumor surrounding vessels are characterized by defects in the endothelial layer, represented by wide fenestrations (up to several microns) and other features that lead to an increase in the permeability of the vascular walls, which makes the effective extravasation of nanosized carriers from the bloodstream to tumor interstitium possible [46–48]. Methods of selective therapy via the systemic administration of therapeutic agents based on increased permeability of the tumor vessels' wall, known under the general name of the EPR effect ("enhanced permeability and retention"), have become widespread and have inspired the creation of a large number of vehicles proposed for the delivery of chemotherapeutic agents[49,50]. In summary, the EPR effect is based on the extravasation of nanoparticles through endothelial fenestra, and their retention in the interstitial volume of the tumor due to dysfunctional lymphatic drainage.

2.1. Design of drug carriers for pH-responsive delivery

Encapsulation of therapeutic compounds in micro-, submicro-, and nano-sized carriers has proven to be a promising approach to improve the therapeutic index of anticancer pharmaceuticals [51]. This approach has changed the paradigm of cancer treatment, setting off impressive developments over the past four decades. Modern carriers can serve for multiple issues including the protection of a therapeutic cargo from degradation in an aggressive extracellular environment, its delivery to the tumor, prevention of chemotherapeutic drug penetration into healthy tissue, and regulation over its release into tumor tissue. The last characteristic is one of the most important for DDSs applied for cancer therapy since the success of the targeted therapy via drug-loaded carriers directly depends on their capability to release the cargo precisely in the desired area, specifically after their extravasation into the tumor. In this regard, both active and passive methods of release are investigated. One of the most common factors used for passive cargo release is pH difference. Current approaches for targeted therapy in oncology mostly employ precise molecular targets such as specific receptors [52,53], microRNAs [54,55], or the ubiquitin–proteasome pathway [56,57]. However, the acidic pH in extracellular tumor tissues is a common phenotype across a wide range of cancer types that makes it a promising target for delivery systems [58]. Today, the dominant concept in pH-responsive drug delivery systems is to provide cargo release at the acidic pH of tumor parenchyma. The scientific community suggests different pH values that should trigger cargo release to provide effective therapy, but an average value of 5.7 can be estimated over the literature as it will be shown below.

There are a few strategies applied for pH-responsive drug delivery including degradation strategy, gatekeeper strategy, and bond cleavage strategy [59–61]. The first one is the widest employed strategy which supposes the degradation of drug carriers in response to an acidic microenvironment. A wide variety of materials and mechanisms are shown to induce the breaking down of drug carriers under an acidic tumor microenvironment resulting in site-specific drug release

[62]. Meanwhile, mostly polymeric carriers undergo swelling in dependence on microenvironment pH leading to changes in their porosity and chemical bounds [63,64]. The gatekeeper strategy employs an on-demand approach via core-shell structured carriers. Such systems mainly consist of mesoporous materials as a core for drug encapsulation and pH-responsive coating on the surface acting as a «gatekeeper» to provide controlled release [65,66]. These systems are mainly designed to prevent drug release in blood at normal physiological pH levels and provide drug release in an acidic environment. The bond cleavage strategy considers the development of chemically bound drug vehicles, which undergo hydrolysis of acid-labile bonds between drug and polymer, or within the polymer leading to the release of the free drug [67]. Besides the capability of DDSs to accurately unleash the drug in the tumor interstitium, the systemically administrated system required to provide a range of other features such as ability to be delivered with blood flow to the neoplasm. In general, favored drug carrier size is under 200 nm to provide higher specific surface areas, appropriate circulation time, penetration into tissues, and internalisation potential [68–70]. On the one hand, drug delivery systems should avoid extravasation by reticulo-endothelial system (RES) and kidney. The other important requirement is negative surface charge to avoid interaction with negatively charged cells in the blood flow [71]. Basically, any class of nanomaterials, both organic and inorganic, can be modified with a pH-responsive release mechanism. Organic materials for pH-responsive targeted delivery systems include polymeric nanoparticles: polymersomes, dendrimers, nanospheres, hydrogels, and polymeric micelles, and lipid nanoparticles, including liposomes, solid lipid nanoparticles (SLNs), and nanoemulsions. Organic nanoparticles are well suited for drug delivery because they are biodegradable, water-soluble, biocompatible, and biomimetic. Their surfaces can be easily modified for additional targeting, allowing them to deliver drugs, proteins, and genetic material directly into the tumor cell. At the same time, an increased risk of particle aggregation leading to their increased toxicity can be mentioned as disadvantages of organic nanoparticles [72,73]. Inorganic nanoparticles for pH-responsive targeted drug delivery include quantum dots, gold nanoparticles, silica nanoparticles, and magnetic nanoparticles. Most inorganic particles have good biocompatibility and stability and fill those application niches that require properties that are unattainable for organic materials. Limitations on the usage of some types of inorganic particles may be due to low solubility and toxicity, especially when heavy metals are included in their composition. In this regard, a wide range of papers considers hybrid carriers such as metal-organic frameworks (MOF) which combine properties of organic and inorganic materials. In the course of a meta-analysis of studies on the use of pH-responsive targeted delivery systems, it was found that 45.8% of studies used polymers to design nanoparticles, 10% - lipids, 12.5% - mesoporous silica, 6.7% - metals [74]. . However, current challenges push researchers to create hybrid carriers that combine properties of different materials, and DDS's developed over the last 5 years are mostly multicomponent capsules or particles comprising inorganic compounds and specific polymers to endow the system with multifunctionality.

Below different types of drug carriers will be considered in detail, to reveal the beneficial features such as drug loading capacity, drug release rates, functionality etc.

2.2. Intratumoral delivery strategy

It is assumed that the EPR effect promotes the entrapment of drug carriers in the vessels surrounding the tumor, due to their disturbed structure, followed by penetration into the tumor parenchyma. The acidic environment of the tumor "switches" the carrier properties leading to the cargo release. The pH of extracellular fluid (pHe) in healthy tissues is tightly regulated between 7.35 and 7.45 in order to sustain normal physiology and cellular metabolism. Normal physiological pH is a strict constant, but numerous studies show that tumor extracellular pH is acidic. Reduced extracellular pH values are a complex effect and are caused by a number of reasons, including poor blood supply leading to chronic hypoxia of tumor tissues and high levels of lactic acid due to the metabolization of glucose within the tumor into lactic acid instead of CO_2 (so-called The Warburg Effect) [75]. The probable reason for this process is the increased production of the enzyme carbonic anhydrase IX, which catalyses the reversible interconversion of CO_2 into HCO_3^- and H+. It should be

 doi:10.20944/preprints202305.0289.v1

noted that carbonic anhydrase IX overexpression is more intensive in the core sites producing the internal pH of the cells (pHi) at the core less acidic, but making the peripheral pHe of the tumor more acidic [76,77]. Numerical modeling of the data based on spheroid studies revealed that carbonic anhydrase IX maintains a sharp outward-directed CO_2 gradient, accelerating the CO_2 excretion, and acidification of extracellular pH as well as increasing pHi. These factors not only lead to an acidic pH in the tumor but also make the acidic environment a condition for the progression of the tumor [58]. The pH values in different types of tumors range between 6.3 and 7.0, which reflect the dysregulation of the acid-base homeostatic mechanisms operating within solid tumors. Numerous literature data on the extracellular pH of the tumor tissues and the corresponding normal tissues have been summarized by *G. Hao et al*. and represented in **Figure 1**. Selected results are received with pH-sensitive electrodes as the most common method for intratumoral pH measurements [78]. As shown in **Figure 1**, the pHe of tumor extracellular space is only 0.3–0.7 pH unit lower than that of corresponding normal tissues. For example, the average pHe uterine tumor tissues have an average pHe of 6.92 while the average pHe in a normal uterus is 7.64 [79]. Similarly, the average pHe in malignant melanoma tissues is 6.96 which is 0.43 lower than that in normal skin tissues (7.39) [80]. Vulvar tumors have an average pHe of 7.26 while the average pHe in normal vulvar tissues is 7.96 [79]. Similar pH differences have also been observed in other tissues, such as brain [81] and lung [82], breast [83], and skeletal muscle [84]. There are only a few types of cancer that have been shown to exhibit lower extracellular pH values, in particular astrocytomas and squamous cell carcinoma with pH values <6.0.

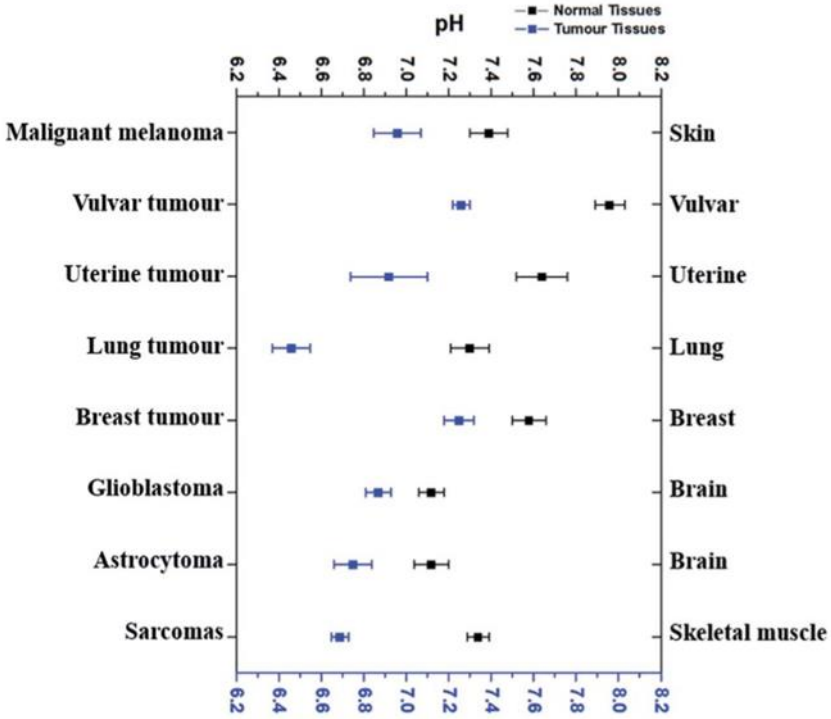

Figure 1. Extracellular pH values of tumor tissues in comparison to pH in the corresponding healthy tissues. Reprinted with permission from [78]. Copyright 2018, Royal Society of Chemistry.

Thus, the average gap between healthy tissues and the acidic extracellular environment in tumors is 0.3–0.7. This fact presents a challenging task for chemists since switching a carrier's state on such a short pH difference is difficult. An analysis of the literature data shows that the absolute majority of authors demonstrate pH-responsiveness towards pH values in the range of 5 to 6 with an average value of 5.7. However, as it is shown above these values of pHe are hardly reachable in the extracellular space of real tumors.

Moreover, these values a highly variable, and in general larger tumors tend to be more acidic, mostly at the late stages of the cancer progression [85]. Moreover, the pH values are unevenly distributed over the tumor with a downward gradient from the periphery to the center. This makes

pH-responsive drug delivery systems hardly applicable in the early stages of cancer progression or in small metastatic tumors, which is crucial for successful therapy.

2.3. Intracellular delivery strategy

Interestingly, overexpression of carbonic anhydrase IX not only leads to acidification of extracellular pH but also induces a slight shift of cancer intracellular pH rather neutral or slightly alkaline region, while the pH of normal cells is also slightly acidic (7.2). Cancer cells have a higher pHi (pHi >7.4) than normal cells (pHi ~7.2), leading to a reversed pH gradient across cancer cell membranes [78,86]. Nevertheless, the pH within endosomes and lysosomes of cancer cells is in the range of 4.5-6, which is more suitable for inducing pH-responsive release. Internalization of particles by cells occurs through endocytosis that supposes the formation of vesicles (endosomes). After the formation of an early endosome with an average pH of about 6.3, it passes into a late endosome with a pH of about 5.5 and then fuses with lysosomes (pH below 5), followed by degradation of the trapped particles by the action of enzymes. This process is a natural defense mechanism of a cell against extraneous substances (**Figure 2**).

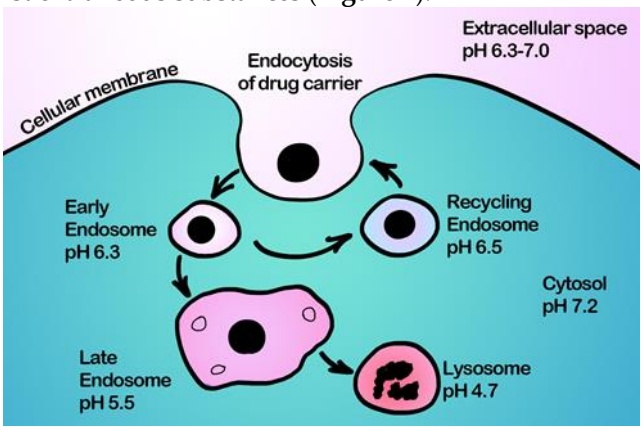

Figure 2. Illustration of pH at different stages of endocytosis

A large number of researchers suggest releasing directly into endosomes or lysosomes of cancer cells in response to low pH as an effective method of therapy [87–90]. However, the penetration mechanism of the drug through the endosome membrane as well as its' stability to the action of enzymes within the endosomes should be carefully considered. Such a strategy can be applied to low molecular weight chemotherapeutic and immunotherapeutic agents, while the delivery of high molecular weight compounds that are sensitive to the action of enzymes and unable to pass through the membrane requires the so-called endosomal escape from endosomes, which is a specific and complex task and requires the inclusion of endosome-disrupting agents into DDS. Otherwise, a large fraction of endocytosed therapeutic agents become trafficked to the degradative lysosomal compartment with subsequent damage to the encapsulated cargo [91,92]. In this regard, the endosomal escape process is preferable before the endosomal degradation of the drug carrier to perform the therapeutic effect of the encapsulated therapeutics. [91–93]. Currently, endosomal escape is one of the strongest barriers that limit the application of DDS's carrying biological therapeutic agents with intracellular targets (such as DNA, RNA, and proteins). In this case, pH-responsiveness should provide and enhance the pH-driven escape of the DDS from the endosome into the cytoplasm to improve the efficiency of drug delivery of these DDS's after endocytosis and to exert effects of cargo in other cellular compartments [94–96]. While natural objects, such as viruses and pathogenic bacteria have mechanisms for endosomal escape [97,98] it is still difficult for synthetic systems to deliver macromolecules into Cytosol and different compartments of a cell [99,100]. Most drug carriers employ cationic materials that passively provide swelling and subsequent rupture of endosome membrane with low efficiency [101,102]. Moreover, the issue of internalization of carriers by cancer cells in tumors is acute along with the following endosomal escape process to provide release of the therapeutics into the cell. Multiple literature data shows that only a small percentage (0.7-0.9) of the

 doi:10.20944/preprints202305.0289.v1

systemically administered carrier reaches the tumor, passing through the EPR effect into tumor parenchyma followed by internalization by cancer cells [46,103], and less than 0.0014% of administrated drug carriers are internalised by the cells [104]. Moreover, the features necessary for the effective uptake of drug carriers by tumor cells impede features for long-time circulation. Positively charged particles more easily interact with cells and become endocytosed because the cellular membrane is negatively charged, but on the other hand, it leads to faster cleaning of the particles by RES after administration [105]. To resolve this dilemma, drug carriers capable of changing their charge have been developed. Such carriers are negatively charged in blood circulation but the acidic microenvironment in tumors reverses particles to a positive charge which shows enhanced cellular uptake [71]. This effect is obtained by application of biomaterials which induce conformational changes in these carriers through various mechanisms such as protonation, charge reversal or cleavage of a chemical bond, leading to enhanced interaction of carriers with cell and promoting cell uptake [42].

2.4. Peculiarities of DDS administration

It is believed that the selective passive delivery of nanoparticles to tumors occurs due to the EPR [106], which is the key process in many cancer research and clinical trials. However, clinical trials have shown poor results in the survival of cancer patients [107], which pushes researchers to look for alternatives to EPR-mediated delivery of chemotherapeutic compounds [48].

Current data on long-term studies show that targeted drug delivery only allows slightly increase the accumulation of drugs in the target organ or tumor, while most of the drug is distributed throughout the body, accumulating mainly in the macrophage cells of the liver and spleen, leading to a strong toxicological effect and reduced therapy efficiency [103].

These facts lead to the need to develop new ways to improve the efficiency and bioavailability of drugs to reduce side effects. Multiple data on the short circulation time in the blood of typical nano- and micro-sized carriers as a result of sequestration into the mononuclear phagocytic system lead to the need for a complex approach to localizing the therapeutic effect, which will include not only targeting of carriers but also the use of methods to reduce the impact on critical organs such as blockage of the liver. Although a few ‘stealth’ systems demonstrated considerable success in stability and prolongation of circulation in the blood flow, such carriers exhibit poor cellular uptake and slow drug release from endosomes [108,109], that reduces drug bioavailability and compromises drug efficacy [110,111]. A few approaches, such as protonation and detachment of stealth-agents from particles have been suggested to achieve the synergistic benefits of long circulation, enhanced intracellular delivery, and cytoplasmic drug release [112–115]. These aspects make it possible to reveal the weak sides of the pH-responsive drug delivery concept. The EPR effect allows only a slight increase in the accumulation of particles in the target tissues of the tumor, while the liver still takes the main "strike", and the vast majority of the introduced particles end up in the mononuclear phagocytic system. Active transcytosis of carriers through the endothelial layer of capillaries ensures their effective delivery and retention in the interstitial volume but does not provide effective diffusion into the tumor parenchyma [116]. Moreover, not all tumor vessels are leaky enough to provide traffic of nanoparticles due to their structural heterogeneity [117], resulting in the EPR variety over different cancer types [48,107]. At the same time, a number of studies have shown that the EPR effect is characteristic of rodents, and in humans, it is much less pronounced, which was confirmed by clinical studies [48,118,119], which has shown low efficiency in passive targeting of chemotherapeutic agents through the EPR effect. Although the model is consistent, the described approach allows us to reach efficiency improvement only by fractions of a percent. Thus, about 0.7% of the systemically administered dose of the encapsulated form of the therapeutic agent reaches the target malignant tissue [46].

A further increase in the effect of the drug carriers' use was achieved by surface modification of carriers with various gels and polymers, for example, polyethylene glycol to increase the circulation time of carriers in the bloodstream and, accordingly, increase the accumulation in tumor vascular

abnormalities. However, the advisability of such surface modification must be carefully estimated, since surface modification of carriers results in difficult binding to target tumor cell receptors.

To solve this and other problems, a range of innovative approaches in the manner of personalized medicine concept are proposed, using such objects as own macrophages and vesicles consisting of the cytoplasmic membrane of tumor cells for multifunctional therapy and drug delivery with increased selectivity and increased circulation time in the blood [120–122]. A noticeable effect is achieved by the modification of carriers with ligands that have specific reactions with receptors specific to a particular site of the body [49,50,123]. This approach has demonstrated high efficiency of targeting using a wide range of carriers to tumor-affected sites of the body, including such as liposomes [124,125], micelles [126–128] and inorganic nanoparticles [129–134]. Such approaches are called "active" and allow to slight increase in the percentage of carrier accumulation in the target tumor compared to passive delivery up to 0.9%. The literature data indicate not only an increase in the efficiency of therapeutic compounds via drug carriers but also the possibility of overcoming the drug resistance of tumors [131]. Although the application of multifunctional carriers demonstrates an increase in the therapeutic index of antitumor pharmaceuticals and their bioavailability, these approaches are not a panacea and the best results can be achieved with an integrated approach that employs both passive and active targeting of carriers in combination with methods to reduce their effect on healthy body tissues. However, drug carrier and drug delivery formulations approved by the ministries of health of different countries show very modest survival results in clinical trials [107]. Today EPR approaches are aimed at increasing the ability of carriers to diffuse into the tumor extracellular matrix. Thus, the decomposition of nanosized carriers into fragments with a characteristic size of less than 10 nm in response to the impact of the tumor microenvironment increases diffusion in the tumor and provides access to tumor target cells, although this does not fully solve the mentioned problems of the method [135].

The problems of ERP-based DDS's push researchers to develop new drug delivery approaches, which are less dependent on the tumour biology [136]. Recently, an alternative concept of drug delivery based on the flash release of encapsulated cargo in the vessels surrounding the tumor has been proposed [137,138]. In this case, it is proposed to use carriers with reverse pH-responsiveness, capable of release at physiological pH (7.4) and "closing" at a lower pH. This concept eliminates a number of the problems described above, such as the poor outcome of the EPR effect in humans.

The application of carriers with a controlled release profile does not solve the aforementioned disadvantage of systemically administered encapsulated drugs, which is their rapid sequestration into the mononuclear phagocytic system. Moreover, macrophage cells also have a reduced pH of the intracellular space (pH of about 4 in some cases) which leads to a rapid release of the therapeutic agent from pH-responsive tumor-targeted carriers. As a result of the sequestration of carriers into the mononuclear phagocytic system, the time of their circulation in the bloodstream is significantly reduced by up to 1 minute, which obstructs the process of carriers' accumulation in the tumor [138]. Moreover, the total percentage of drug carriers trapped in the liver in some cases reaches 70% of the dose introduced into the bloodstream, which leads to strong toxicological stress. For example, gold nanoparticles have been shown to remain in liver macrophages for up to 12 months after administration [139]. The process of accumulation of carriers in the tumor tissue and the sequestration of carriers into the mononuclear phagocytic system is determined by a number of parameters, including the diameter of the particles, their shape, charge, and the nature of the surface[46], which pushes researchers to search for the optimal carrier for a particular task.

2.5. Outlook

Thus, the EPR effect nowadays seems to be a great problem for pH-responsive DDSs as penetration of carriers into the tumor parenchyma is a key process. Carriers capable of long-term release seem to be preferential considering obstructed penetration into tumor tissues, and most researchers focused on getting results within days. Tremendous efforts have been made to improve the accumulation and diffusion of carriers into the tumor as well as alternative approaches to avoid this problem have been developed such as flash release in vessels around the tumor. Furthermore,

the search for pH-responsive materials capable of release at pH values in the range of 6.2 - 6.8 is still a challenging task as the majority of authors demonstrate release at pH below 6. However, real tumors usually are not that acidic with pH values to be distributed unevenly throughout the tumor extracellular tissues. Delivery into endosomes and lysosomes of cancer cells is more effective in terms of pH responsiveness, however, it produces new requirements for the functionality of the particles. Features essential for the effective uptake of drug carriers by cancer cells impede features for long-time circulation. In this way, a carrier is required to provide a cascade of functions after being extravasated into the tumor such as reversion of the charge, uptake, release, and endosomal escape. Below we will consider current progress in the development of carriers for solving these problems both *in vitro* and *in vivo*.

3. Analysis of drug carriers' features

3.1. 1 Drug loading efficiency of different pH-responsive DDSs

One of the most important characteristics of drug delivery systems (DDS) is the amount of an active substance that can be loaded into them, and pH-responsive carriers are not an exception. A high loading capacity is required for the drug vehicle to induce a desired therapeutic effect in the organism. Also, it is worth noting that the presence of DDS itself in the body can be the reason for different metabolic issues. Thus the achievement of the maximal ratio of the loaded drug to the carriers' mass is preferable to minimize possible adverse effects caused by DDS application. Multiple studies have demonstrated the dependence of this characteristic on intermolecular interactions between drug molecules and carrier materials [140], and DDSs' structure (surface area, pores size, and internal volume) [141]. Depending on the DDS's type the carrier-cargo binding can be determined by different kinds of interaction including hydrophobic, electrostatic, covalent, hydrogen bonding, π-π stacking, and van der Waals force [140,142–144]. Since these forces depend on the charges of carrier and active substance, to one extent or another, it is important to consider the efficiency of the DDS loading process in terms of their electrostatic complementarity. Surface area, pores' size, and internal volume are also crucial parameters since they determine the loading capacity of a carrier and the interaction of a carrier with proteins, cells, and tissues. Furthermore, the ration between the mass of a carrier and the mass of the loaded drug is one of the most important characteristics of the DDS [140,145].

Usually, the Drug Loading Capacity (DLC) and the Drug Entrapment Efficiency (DEE) of carriers are used as the main features for the quantitative evaluation of drug loading efficiency [146–149]. DLC is the ratio of the weight of an active substance incorporated into the DDS to the weight of the substance-loaded DDS and can be presented as follow:

$$DLC = \frac{Wt\ of\ substance\ incorporated\ into\ DDS}{\text{Wt of loaded DDS}} \times 100\% \quad (1)$$

where *Wt of loaded DDS* is the sum of the DDS weight plus the weight of the incorporated substance. In its turn, DEE presents the ratio of the weight of an active ingredient incorporated into the DDS to the total weight of the active substance used for the loading of DDS, and it can be presented as follow:

$$DEE = \frac{Wt\ of\ substance\ incorporated\ into\ DDS}{\text{Wt of substance used for DDS loading}} \times 100\% \quad (2)$$

The comparison of different DDS in terms of loading efficiency is a complicated issue and requires detailed consideration. Since the DLC depends on both active substance and DDS properties, it is essential to compare the DLC of different carriers for the same substance.

For the last five years, an abundant number of articles dedicated to pH-sensitive DDS implied for cancer treatment have been published. The list of medications successfully loaded into metal-organic frameworks- and metal oxide-based DDSs include more than 10 items listed in **Table 1**. Based

on the data published over the last five years, we can conclude that Doxorubicin (DOX), Fluorouracil (5-Fu), and Curcumin (CUR) (**Figure 3**) are currently the most frequently used model substances for the evaluation of the pH-sensitive DDSs' efficiency due to their physical, chemical, and pharmaceutical properties. So, DOX is a convenient model drug because of its anticancer effect against a broad range of malignant cell lines [150], which simplifies the evaluation of the DDSs' efficiency and its fluorescent properties [151–153], which enables the investigation of the behavior of the drug inside the cell without additional labeling. 5-Fu as well as DOX is also one of the frequently administered chemotherapeutic agents due to its broad anticancer activity against tumors of the gastrointestinal tract, pancreas, ovary, head, liver, neck, breast, and brain [154]. Moreover, the development of an effective vehicle for 5-Fu delivery is a prioritized issue because of its high systemic toxicity [155], low bioavailability, and short plasma half-life [154]. CUR is considered as a naturally derived polyphenol that possesses a wide range of bioactive properties including anti-cancer and anti-inflammatory ones [149]. Besides, CUR is a coloring agent which makes it easy to control metabolic issues [156]. Also, CUR is a hydrophobic substance which makes researchers look for efficient ways to deliver CUR within the body [157,158]. Hereinafter we will compare the different configurations of drug vehicles in terms of the loading efficiency of the abovementioned drugs.

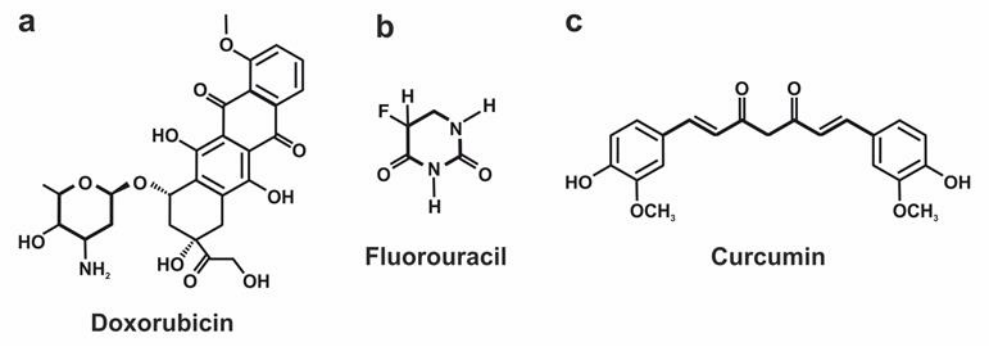

Figure 3. Stereochemical structure of the considering molecules.

Doxorubicin loading efficiency

DOX is a positively charged molecule at neutral and acidic conditions [159,160] with an average mass of around 543.5 Da and a maximal molecule diameter of around 1.5 nm [161]. The chemical structure of DOX molecules (**Figure 3a**) enables linking them with the carrier surface in both ways covalently [142,143] and through the hydrogen bonding [162,163]. Currently, MOFs are the most popular metal-comprising DDSs applied for pH-responsive DOX administration because of their DLC order of magnitude greater than for MeO NPs (**Table 1**). Comparative analysis has shown that Dextran modified ZIF-8 [162], UIO-66-NH2 with grown Prussian blue crystals on its surface [163], and hydrothermally reduced NH2-MIL-88B(Fe) (Fe-MOF) modified by polyelectrolyte multilayer [164] are characterized by the highest loading efficiency of DOX.

ZIF-8 is nanocrystals consisting of Zn^{2+} and 2-methylimidazole ions that possessed a relatively large pores size (3.4 - 18 Å) [165–167], surface area (1244 - 1630 m^2/g) [132,162,166,167], and pore volume (0.88 cm^3/g) [132] resulting in substantial loading capacity, and positive surface charge ranging from +12 mV to +29 mV [132,166,168–170]. As can be seen from **Table 1** DOX loading capacity of ZIF-8-based carriers highly depends on their final configuration and can vary from 10 to 63%. *Yongming Chen and co-authors* developed the DOX@ZIF-8/Dex configuration comprising ZIF-8 covered with dextran-linked imidazole to improve its colloidal dispersity in aqueous media [162]. The drug loading in this core-shell structure was performed through the hydrogen bonding of DOX with imidazole molecules and this configuration provided DLC of 63% for DOX which is the outstanding result among all considered ZIF-8-based vehicles.

UIO-66-NH2/PB/DOX is characterized by close to DOX@ZIF-8/Dex DOX loading capacity value (67.4%) despite its more than two times lower surface area (570 - 876 m^2/g) and pore volume (0.379

cm³/g) [163,171]. However, according to Ref. [171] UiO-66-NH2 crystals' pore diameter is around 19 nm which is 10-fold greater than for the abovementioned ZIF-8-based vehicle. Also, the significant DOX loading capacity of UIO-66-NH2 can be explained by the carrier's negative charge (−4.91 mV) [172] which in combination with the positive charge of DOX molecule results in high DLC. So, Jing Wang's research group has found that drug molecules mainly link with the carrier surface via hydrogen bonding between DOX's hydroxyl group and the carboxyl group of UIO-66-NH2/PB [163].

The most outstanding DOX loading capacity (88.4%) have been demonstrated by DDS based on modified NH2-MIL-88B(Fe). Fe-MOF is the needle-shaped nanoparticles with a relatively low surface area (592.2 m²/g) if compare with ZIF-8 carriers, and a large pore size (5.4 nm) [164].

The most outstanding DOX loading capacity (88.4%) has been demonstrated by DDS based on modified NH_2-MIL-88B(Fe) [164]. The authors explained such a high DLC of DDS by its large cavity and specific surface area. However, it is worth noting that Fe-MOF is the needle-shaped nanoparticle with a relatively low surface area (592.2 m²/g) if compared with ZIF-8 carriers. The pore size of Fe-MOF is 5.4 nm that is larger than for ZIF-8-based DDSs but lower than for UiO-66-NH2 ones, which both are inferior compared to Fe-MOF in DLC. ζ potential of Fe-MOF, also, does not shed light on the mechanism of high DLC. So, the authors noted that the ζ potential of the empty carrier is +26.9 mV and slightly decreases after its loading with positively charged DOX up to +19.8. In the context of the previously published work [10.1021/acsami.7b07981], which is mentioned as a Ref. for the method of MOF synthesis, these positive ζ potential values can be considered as a misprint, since MOFs-progenitors described in Ref. [173] possessed a strongly negative charge (less than −20). Also, the sorption of polymers on the MOF surface after loading with DOX can facilitate high DLC preventing premature cargo leakage.

Therefore, we can assume that the combination of strongly negative surface charge of the carrier implied for the DOX transportation with large pore size is the most suitable for DDS. Also, we can assume that the sorption of polymer molecules on the MOF surface can prevent undesirable premature leakage of drugs thereby increasing its DLC.

Table 1. Drug Loading Capacity (DLC) and Drug Entrapment Efficiency (DEE) criteria of different DDSs. * - Lipoic acid-curcumin, ** - 10-Hydroxycamptothecin (HCPT)

Active substance	DDS type	DDS configuration	Surface area (m^2/g)	Pore volume (cm^3/g)	Pore size (nm)	DDS's ζ potential (mV)	DLC (%)	DEE (%)	Ref.
	MOF (ZIF-)	**HMS@ZIF**	**788**	**0.65**	**-**	**-**	**-**	**-**	
		DOX/HMS	483	0.42	-	-	34	-	[174]
		DOX/HMS@ZIF	1152	-		+31.2	28	-	
		DOX/HMS@ZIF-50	120	-	-	+30.1	44	-	
		BSA/DOX@ZIF	-	-	-	+26.7	10	-	[152]
		DOX@ZIF-8	-	-	-	+27	10	-	[133]
		DOX@ZIF-8@AS1411	-	-	-	−8	-	-	[133]
		ZIF-8	**1465.9**	**-**	**0.6**	**+28.9**	**-**	**-**	

	8)	ZIF-8@DOX	-	-	-	−33.7	43.3	-	
		ZIF-8@DOX@Silica	-	-	-	−32.6	42.7	-	
		ZIF-8@DOX@Organosilica	-	-	-	−34.3	41.2	-	[166]
		ZIF-8	**1244**	**-**	**1.8**	**-**	**-**	**-**	
		DOX@ZIF-8/Dex	1078	-	1.8	-	63	-	[162]
		H-ZIF-8/PDA-CD JNPs	**-**	**-**	**-**	**−19.5**	**-**	**-**	[175]
		HCPT@DOX@H-ZIF-8/PDA-CD JNPs	-	-	-	-	42	-	
	MOF (ZIF-90)	**UC@mSiO2-RB@ZIF**	**556.2**	**0.68**	**-**	**-**	**-**	**-**	
		UC@mSiO2-RB@ZIFO2-DOX-PEGFA	-	-	-	-	6	-	[142]
	MOF	**UCMOFs**	**-**	**-**	**-**	**+19.1**	**-**	**-**	
		UCMOFs@Dox@5-Fu	-	-	-	+16.3	16.4	-	[143]
	MOF (UIO-66)	**UIO-66-NH2**	**569.595**	-	-	-	-	-	
		UIO-66-NH_2/PB/DOX	-	-	-	-	67.4	-	[163]
		Fe_3O_4@UIO-66-NH_2/Graphdiyne	**-**	**-**	**-**	**−23.2**	**-**	**-**	[159]
		Fe_3O_4@UIO-66-NH_2/Graphdiyne/DOX			-	+5.07	43.8	-	
	MOF (Cu (II)-porphyrin)	**Cu(II)-porphyrin/Graphene oxide**	**352**	**0.32**	**4.9**	**−19.8**	**-**	**-**	[176]
		Cu(II)-porphyrin/Graphene oxide-DOX	-	-	-	−2.15	45.7	-	
	γ-cyclodextrin-based MOF (CD-	DOX/γ-CD-MOF	-	-	-	-	-	45	
		DOX/GQDs@γ-CD-MOF	-	-	-	-	-	51.6	[177]
		DOX	-	-	-	-	-	89.1	

Doxorubicin (DOX)	MOF)	/AS1411@PEGMA@GQDs@ γ-CD-MOF							
	MOF (NH2-MIL-88B)	NH_2-MIL-88B	-	-	-	+57	-	-	[178]
		DOX@NH_2-MIL-88B	-	-	-	-	7.4	-	
		DOX@NH_2-MIL-88B-On-NH_2-MIL-88B	-	-	-	+86	14.4	-	
	MOF (NH2-MIL-88B (Fe))	**Fe-MOF**	**592.2**	**-**	**5.4**	**+26.9**	**-**	**-**	[164]
		DOX@FeMOF@PSS@MV-PAH@PSS	-	-	-	−13.5	88.4	-	
	MOF (MIL-101)	**MIL-101**	**4500**	**-**	**2.9 - 3.4**	**-**	**-**	**-**	[137]
		MIL-101@DOX	-	-	-	-	36.2 ± 1.4	-	
	MOF (Prussian blue)	NiCo-PBA@DOX	-	-	-	-	-	19.6	[134]
		NiCo-NiCo-PBA@Tb^{3+}@ DOX	-	-	-	-	-	16.9	
		NiCo-NiCo-PBA@Tb^{3+}@PEGMA@DOX	-	-	-	-	-	72.2	
		NiCo-PBA@Tb^{3+}@PEGMA@AS1411@DOX	-	-	-	-	-	60.3	
	MOF	**Bio-MOFs**	**935**	**0.37**	**3.47**	**-**	**-**	**-**	[148]
		DOX /Bio-MOFs	-	-	-	-	39	76	
		CS/BioMOF	**438**	**0.25**	**3.12**	**+2.4**	**-**	**-**	
		DOX / CS/BioMOF	-	-	-	-	48.1	92.5	
	MeO NPs	MnO_2NPs@Keratin@DOX	-	-	-	-	8.7	-	[179]
		CS/Zn-MOF@GO	**2.22**	**0.51**	**35.17**	**-**	**-**	**-**	

	MOF	5-Fu@CS/Zn-MOF@GO	-	-	-	-	45	-	[154]
	MOF	**UCMOFs**	**-**	**-**	**-**	**+19.1**	**-**	**-**	[143]
		UCMOFs@Dox@5-Fu	-	-	-	+16.3	24.7	-	
	MOF (UIO-66)	**UiO-67-CDC**	**818.3**	**0.91**	**-**	**+0.229**	**-**	**-**	[180]
		5-Fu@UiO-67-CDC	-	-	-	-	22.5	-	
		UiO-67-CDC-$(CH_3)_2$	**354.3**	**0.73**	**-**	**+22.017**		**-**	
		5-Fu@UiO-67-CDC-$(CH_3)_2$	-	-	-	−0.106	56.5	-	
Fluorouracil (5-Fu)	MOF	**$[Zn_3(BTC)_2(Me)(H_2O)_2](MeOH)_{13}$**	**1426**	**-**	**0.59**	**-**	**-**	**-**	[181]
		5-Fu/$[Zn_3(BTC)_2(Me)(H_2O)_2](MeOH)_{13}$	-	-	-	-	34.32	-	
	MOF (ZIF-L)	**ZIF-L**	**-**	**-**	**-**	**+3.8**	**-**	**-**	[182]
		CUR@ZIF-L	-	-	-	+4.1	-	98.21	
	MeO NPs	**N-succinyl-CS-ZnO**	**-**	**-**	**-**	**−26.1 ± 1.35**	**-**	**-**	[144]
		CUR-CS-ZnO	-	-	-	−16 ± 1.1	13	69.6	
		ZnO-PBA	**-**	**-**	**-**	**−4.7 ± 0.31**	**-**	**-**	[149]
		ZnO-PBA@CUR	-	-	-	−16.4 ± 0.30	35	27	
Curcumin (CUR)		**Fe_3O_4@Au-GSH**	**-**	**-**	**-**	**−5**	**-**	**-**	[183]
		Fe_3O_4@Au-LA-CUR/GSH*	-	-	-	−16	-	70	
		MIL-101(Fe)-Suc-CPT	1254	0.16	3.6	+6.4	17.6	-	[184]
		MIL-101(Fe)-Click-CPT	143	0.03	3.4	+3.4	18	-	

Camptothecin (CPT)	MOF (MIL)	MIL-100(Fe)-Suc-CPT	71	0.07	3.5	–27	1.3	-	
		MIL-100(Fe)-Click-CPT	70	0.09	3.6	–45.8	9.2	-	
	MOF	HCPT@DOX@H-ZIF-8/PDA-CD JNPs **	-	-	-	-	9.8	-	[175]
Dihydroartemisinin (DHA)	MOF (ZIF-8)	**ZIF-8**	**-**	**-**	**-**	**+14.9**	**-**	**-**	[168]
		DHA@ZIF-8	-	-	-	+15.3	14.9	77.2	
		Fe/ZIF-8/DHA	-	-	-	– 7.4	42.2 ± 3.3	96.2 ± 3.6	[121]
Quercetin (Q)	MeO NPs	**PBA-ZnO**	**-**	**-**	**-**	**–1.8 ± 0.12**	**-**	**-**	[38]
		PBA-ZnO-Q	-	-	-	−10.2 ± 0.36	29.83	46.69	
		ZnO-Q	-	-	-	-	17.4	-	[185]
Sonosensitizers Chlorin e6 (Ce6)	MOF	Cu-MOF/Ce6	-	-	-	-	8.7	-	[186]
	MOF (ZIF-8)	**ZIF-8**	**-**	**-**	**-**	**+17**	**-**	**-**	[170]
		Ce6-DNAzyme@ZIF-8	-	-	-	–22	10	-	
Alpha tocopheryl succinate (α-TOS)	MOF (ZIF-8)	**ZIF-8**	**1485**	**0.88**	**-**	+22.1	-	-	[132]
		α-TOS@ZIF-8	703	0.25	-	+20.2	43.03	-	]
As(III)-drugs	MOF	**Zn-MOF-74**	**1187**	**-**	**-**	**-**	**-**	**-**	[187]
		As2O3@Zn-MOF-74	452	-	-	-	11.6	-	
Chloroquine diphosphate (CQ)	MOF (ZIF-8)	**ZIF-8**				**+12.1**	**-**	**-**	[169]
		CQ@ZIF-8	756	-	-	+9.5	18	-	

Rose Bengal (RB)	MOF (ZIF-90)	**UC@mSiO2-RB@ZIF**	**556.2**	**0.68**	**-**	**-**	**-**	**-**	[142]
		UC@mSiO2-RB@ZIFO2-DOX-PEGFA	-	-	-	-	5.6	-	
Piperlongumine (PL)	MOF	**Fe-TPA**	**-**	**-**	**-**	**+45 ± 2.8**	**-**	**-**	[188]
		Tf-Lipo-Fe-TPA@PL	-	-	-	−10.2 ± 0.6	12.3 ± 4.33	78.7 ± 2.98	
Methyl gallate (MG)	MOF (ZIF-L)	MG@ZIF-L	-	-	-	–21	18.05	90.26	[189]
Imatinib	MeO NPs	Fe_3O_4@CS/Imatinib	-	-	-	-	52	61	[147]

Fluorouracil loading efficiency

5-Fu is a small (3×6 Å) [180] negatively charged [190] molecule with an average mass of around 130 Da (**Figure 3b**). Similarly, to DOX, different types of MOF-based DDSs were proposed in the superior majority of studies devoted to the pH-responsive vehicles for targeted 5-Fu delivery (**Table 1**). Among them, from the viewpoint of 5-Fu loading efficiency, we can emphasize two different configurations of zinc-based [154,181], and one modification of zirconium-based MOFs [180]. So, Zn^{II}-based MOF ($[Zn_3(BTC)_2(Me)(H_2O)_2](MeOH)_{13}$) is nano-sized porous spherical crystals comprising Zn^{2+} nudes linked by 1,3,5 - benzenetricarboxylic acid (H_3BTC) and melamine (Me) as organic ligands [181]. This MOF possesses a comparatively large surface area of 1426 cm2/g along with ZIF-8-based DDS and a small pore size of around 5.9 Å. Such configuration of DDS enables achieving a substantial 5-Fu loading capacity (34.32%) (**Table 1**). Jiying Wang and co-authors based on the Grand Canonical Monte Carlo simulation concluded that the 5-Fu molecule links with MOF via hydrogen bond interactions between fluorine and oxygen atoms of 5-Fu and hydrogen atoms of amino and hydroxy groups of MOF. The other DDS characterized by considerable DLC of 5-Fu is CS/Zn-MOF@GO hybrid which is a microspherical porous core-shell structure with a rough surface comprising the core made from Zn-MOF-covered graphene oxide nanosheets and a chitosan shell [154]. The authors reported the extremely small surface area (2.2 cm^2/g) which is almost three orders of magnitude lower than the surface area of Zn-based MOFs but the equivalent pore volume (0.51 cm^3/g) which can be explained by the extremely large pore size of CS/Zn-MOF@GO hybrid structures (average pore size of 35.17 nm) (**Table 1**). Despite the small surface area available for drug binding, the 5-Fu loading capacity of CS/Zn-MOF@GO is also high (around 45%). Authors explain this fact by a number of factors including drug molecules trapping inside the internal volume of Zn-MOF, hydrogen bonding, π-π stacking, and coordination bond interactions between 5-Fu and Zn-MOF@GO hybrid.

The most promising DDS in terms of 5-Fu loading efficiency is carbazolyl functionalized Zr-based MOF postsynaptically modified via N-quaternization (UiO-67-CDC-$(CH_3)_2$) [180]. The authors considered two configurations of Zr-MOF: UiO-67-CDC and UiO-67-CDC-$(CH_3)_2$ and found that the surface area and pore volume of MOF decreased after N-quaternization from 818.3 cm^2/g to 354.3 cm^2/g and from 0.91 cm^3/g to 0.73 cm^3/g respectively (**Table 1**). At the same time, this modification provided a significant rise in ζ potential of MOF from +0.229 mV to +22.017 mV and its 5-Fu loading capacity from 22.5% to 56.5%. En-Qing Gao and co-authors explain this high DLC by the high affinity between the anionic drug and the cationic MOF and the small size of a drug molecule.

Based on the above mentioned data we can conclude that ζ-potential is a much more essential characteristic for DDS developing for 5-Fu administration than surface area, pore volume, and size. As we can see the small size of the drug molecule does not demand the large internal volume from DDS to successfully load it, and the carrier's surface charge occupates the foreground of this issue.

Curcumin loading efficiency

Curcumin (CUR) is a polar hydrophobic molecule possessing a commensurable size compared with DOX (**Figure 3c**) at a remarkably smaller mass (368.4 Da). The negative charge is displaced to the central part of the molecule while aromatic rings are charged positively [191]. By contrast, DOX and 5-Fu, metal oxide-based nanoparticles are mainly used as carriers for CUR delivery (**Table 1**). In terms of CUR loading capacity, we can emphasize two configurations of ZnO nanoparticles including ones functionalized by N-succinyl chitosan [144] and by phenylboronic acid [149] . M. Reza Khorramizadeh with colleagues proposed to cover ZnO particles with a chitosan layer and then modify its molecules by succinic anhydride to form N-succinyl CS-ZnO particles [144]. CUR molecules in this system covalently bond with N-succinyl CS-ZnO particles via the conjunction of hydroxylic groups of CUR and carboxylic groups of the succinic-modified chitosan molecule. This approach ensures a CUR loading capacity of around 13%. However, the authors mentioned that the particles loading with CUR significantly decrease their electronegativity from −26.1 ± 1.35 mV to −16 ± 1.1 mV which resulted in the enhancement of their agglomeration and consequently decrease the stability in water media.

The modification of ZnO NPs with phenylboronic acid (PBA) provides more two-fold larger drug loading capacity for CUR [149] than NPs modified with N-succinyl chitosan [144]. So, the system proposed by Parames C. Sil's team demonstrates a DLC of 35%. The PBA adsorption on the surface of amine-functionalized ZnO NPs was provided by their covalent bound, and CUR loading, in its turn, was ensured by the formation of the chelate ring with ZnO. Also, the authors pointed to the superiority of the chelate binding of CUR with the carrier over the covalent one since it provides better sensitivity of DDS towards the changes in the milieu pH.

Since the curcumin molecule includes positively and negatively charged fragments and different functional groups available for bond formation including ketone, hydroxy, and methoxy ones, currently, the optimal way for curcumin binding with metal comprising DDSs resulting in high DLC has not been established. This, in combination with the promising anti-cancer and anti-inflammatory properties of curcumin, inspires scientists over the globe to search for new ways to effective delivery this bioactive molecule via different drug delivery systems.

3.2 pH-responsive release of the active substance from DDSs

The other crucial characteristic of pH-sensitive DDS is the rate of pH-responsive drug release. Currently, there are two opposite concepts to pH-driven drug delivery. The first is the conventional one implying the cargo release at slightly acidic pH level which is based on the differences in the intracellular (pH_i) and extracellular (pH_e) pH of normal and tumor tissues respectively [192]. Mainly tumor acidity is caused by the high metabolic (glycolysis rate) and proliferative activity of cancer cells at the oxygen deprivation conditions (hypoxia) resulting in the switching of cancer cells' metabolism to anaerobic glycolysis and accumulation of acidic metabolites in tumor interstitium [193,194]. The second one implies the cargo release at pH values close to neutral and has been developed recently [137]. This concept is based on the quick drug release in the endothelium (FlaRE) and implies the accumulation of DDS in capillaries of the perivascular leaky regions of the tumor, sharp vehicles degradation at neutral pH values providing sharp local bust in active substance concentration, and following drug diffusion according to the concentration gradients across the endothelial wall into the tumor interstitium [137]. Since these concepts place opposite demands on drug delivery systems they should be considered separately.

3.2.1 Acidic pH-triggered drug release

The application of the systemically administered DDS with drug release triggered by acidic pH supposes their long-term circulation in the vasculature system [103,195] and passive [196,197] or active [198–200] accumulation in the tumor region with the following drug release at tumor acidy conditions that result in a local raise of a drug concentration up to values providing an effective tumor treatment [201]. At the same time, the release of cargo from the carriers adversely accumulated in healthy tissues should be maximally prolonged and minimized to maintain the drug concentration below a toxic level, provide its gradual clearance and consequently decrease systemic side effects. Therefore, the "ideal" drug delivery system in the frame of this concept must completely unleash all cargo at an acidic pH and reliably retain it for a long time at physiological pH level.

According to multiple studies reviewed in Ref. [202], the pH in normal human tissue varies from 7.3 to 8.03 with an average value of around 7.4 while the tumor's pH values lie in the range of 5.44-7.96 with a mean value of 7.0. Therefore, since the difference in the average normal and tumor tissues' pH is around 0.4, the span between pH values at which the DDS retains cargo and releases it completely should be as small as possible. The other thesis pointing to the advantage of DDS with a narrow interval between retaining and releasing pH values is that the pH of tumor tissue gradually changes from the neutral value at the periphery to acidy at the central hypoxic zone. At the same time, the tumor's vascularization also decreases afferently (**Figure 4a**) [203]. Therefore, the probability of such DDS delivery with the blood flow to the poorly vascularized central zone with the lowest pH level is extremely low, and it means that the release should occur at a pH slightly lower than the normal one. In spite of mentioned above, authors mainly compare drug release at pH values close to the average in normal tissues (7.4) and much lower (5.0) than previously described as an average tumors' pH (7.0) to show the high efficiency of the pH-triggered drug release. Thus, hereinafter, we will consider and compare DDSs for which the cargo release at pH 5.0 and pH 7.4 was described to extend the data selection but also emphasize the promising carriers demonstrating substantial pH responsiveness at values close to the average tumors ones.

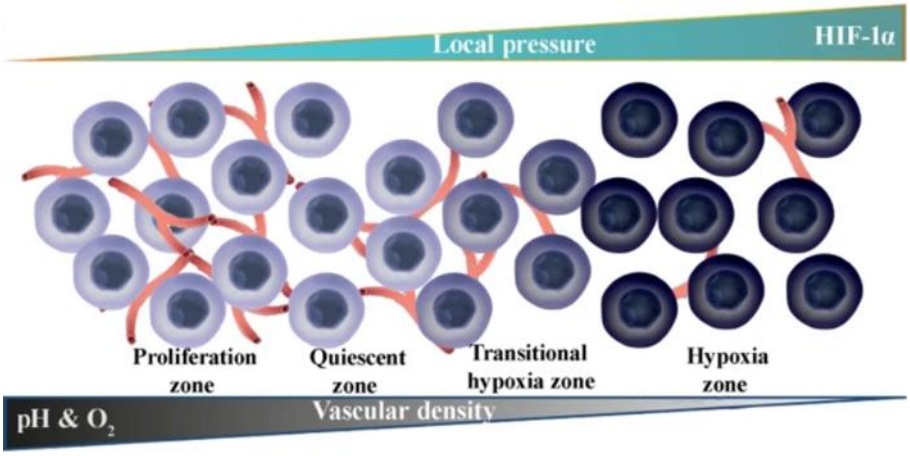

Figure 4. Illustration of tumor tissues. Reprinted with permission from [203]. Copyright 2021, Springer Nature.

For the last five years, more than 50 articles dedicated to the development of DDS with low pH-triggered drug release have been published and it still stays a frontier of experimental pharmacology. Thus, comparing carriers' efficiency is crucial for determining the further direction of the technology development. To compare DDS efficiency, the formulation of evaluation criteria is necessary. According to mentioned above profile of the "ideal" DDS with low pH-triggered drug release, two evaluation criteria (Drug Release Efficiency and Drug Retains Efficiency) can be formulated.

The Release Efficiency implies how good the DDS is at cargo releasing in a tumor and it retaining in normal tissues. It can be evaluated through the attitude of the released amount of drug at the tumors' pH(R_{pH_t}) to the amount of drug unleashed at normal tissues' pH(R_{pH_n}) after a certain period (**Figure 5**) and represented as follow:

 doi:10.20944/preprints202305.0289.v1

$$E_{rel} = \frac{pH(R_{pH_t})}{pH(R_{pH_n})} \quad (3)$$

where E_{rel} is the Release Efficiency of pH-sensitive DDS (r.u.), $pH(R_{pH_n})$ is the cargo release in % at pH 7.4 and $pH(R_{pH_t})$ is the cargo release in % at pH 5.0. However, the time period during which the DDS has to completely unleash active substances is still under debate. In some cases, the quick release of cargo during the first hours in an acidy tumor's conditions is determined as the most suitable strategy, since the sharp increase in the active substance concentration in the target area is required for effective therapy (**Figure 5, left part**). For example, the application of the DOX-loaded ZIF-90-based system for oxygen-enhanced photodynamic therapy implies the fast release of O_2 in the tumor microenvironment [142]. Alternatively, a sustainable drug release from DDS (**Figure 5, right part**) can increase the effectiveness of conventional chemotherapy since the maintenance of the drug therapeutic dose in the tumor area for a long time effectively suppresses cancer cell proliferation and consequently tumor growth [203]. However, it is important to emphasize that in case of prolonged drug release, its concentration in the tumor area should be maintained above the toxic level to provide a therapeutic effect. Thus, drug delivery systems developed in the frame of these strategies also should be considered separately.

The cargo Retains Efficiency implies how good the DDS is at retaining active substances in normal tissues for a long period of time. It can be estimated as an attitude of the incubation time of DDS at 7.4 pH to the amount of drug released at such conditions in this time point (Figure 2) and represented as follow:

$$E_{Ret} = \frac{t}{R_t} \quad (4)$$

where E_{Ret} is the cargo Retains Rfficiency by pH-sensitive DDS at 7.4 pH (r.u.), t is the incubation time of DDS at 7.4 pH (24h), R_t is the cargo release in % in t time point

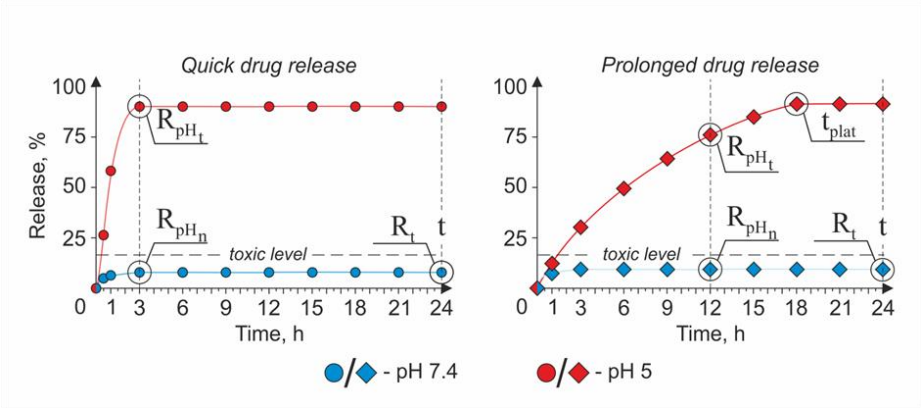

Figure 5. Profiles of the cargo release from DDS in the frames of quick (left part) and prolonged (right part) drug release strategies.

As was mentioned before, the physical and chemical properties of an active substance and a DDS mainly determine the carrier's loading capacity. At the same time, the drug release rate also highly depends on both cargo and carrier properties. Therefore, further, we compared the drug release rate of different DDS loaded with the same active substance.

3.2.1.1 The strategy of a quick drug release

The profile of the cargo release from DDS created in the frame of the quick drug release strategy approximately has the following view presented in **Figure 5** (left part). A perfect candidate for a role of a DDS in the frame of this concept should possess high values of the E_{rel} and E_{Ret} criteria. The quick rise (within the first three hours) in active substance concentration in the tumor interstitium

allows for achieving the following therapeutic goals: **i)** provide a sufficient amount of oxygen for the generation of reactive oxygen species (ROS) in a hypoxic tumor environment during enhanced photodynamic therapy (PDT) [142]; **ii)** provide a fast drug concentration boost inside the cancer cells [143,166,178].

Promising vehicles from this point of view are some particles of the MOFs class. In general, MOFs are inorganic-organic hybrid materials composed of metal ions linked by organic ligands [204]. This class of DDS is characterized by high porosity, large porous size, and surface area resulting in high payload capacity, biocompatibility and biodegradability, water solubility, and simplicity of the carrier's functionalization process. Also, several members of this class including Zeolitic Imidazolate Frameworks (ZIF-n family), Materials of Institute Lavoisier (MIL-n family), University of Oslo (UiO-n family), Dresden University of Technology (DUT-n family), etc. are characterized by pH-responsive drug release that makes them perfect candidates for targeted cancer treatment [205].

Jun Lin and coauthors proposed ZIF-90 based multilayer pH-responsive composite UC@mSiO$_2$-RB@ZIF-O$_2$-DOX-PEGFA (URODF) for oxygen-enhanced PDT accompanied by classical chemotherapy [142]. The URODF has the following core-shell structure: the core presented by NaYF$_4$:Yb/Er@NaYbF$_4$:Nd@NaGdF$_4$ upconversion nanoparticle (UCNP), the first layer of the shell is made from mesoporous silica (mSiO$_2$) loaded with Rose Bengal (RB), and the second one from ZIF-90. Also, to improve carriers' biocompatibility, provide active tumor-targeting, and achieve additional chemotherapy effects, authors modified the ZIF-90 surface with folic acid-conjugated polyethylene glycol (PEGFA) and doxorubicin (DOX) via covalent binding. The URODF usage for anticancer treatment implies their intravenous injection, active accumulation in the tumor interstitium, and the irradiation of the tumor region by the near-infrared (NIR) light source with 808 nm wavelength. In some detail, URODF delivered to the tumor's acidic microenvironment by the circulatory system releases oxygen and DOX due to ZIF-90 shell decomposition providing O$_2$ for PDT in oxygen-deprived conditions and boost in chemotherapeutic agent concentration. At the same time, the NIR-excited green emission of the UCNP core induces the RB activation resulting in the local escalation of the ROS concentration. Thus the anticancer effect of this composite depends on the release of two different substances: O$_2$ and DOX. The authors have shown that the main part of loaded oxygen is released for the first 90 seconds of MOFs incubation at pH 5.5 which is incomparably faster than the DOX release ratio. In its turn, the DOX release was found around 73% after three hours in acidic conditions and 5% in neutral one. Based on it we can conclude that the E_{rel} of DOX is 14.6. The E_{Ret} cannot be estimated for URODF, since the maximal time point at which the DOX release was considered is 17.5 h.

The other DDS developed in the frame of this strategy is the dual-drug MOF loaded with DOX and 5-FU proposed by Lining Sun's group (UCMOFs@D@5) [143]. As a Jun Lin designed MOF [142], the UCMOFs@D@5 possesses a core-shell structure the core of which is also presented by UCNP (NaYF$_4$:Yb/Er@NaGdF$_4$) and the shell by ZIF. The mechanisms of drug loading were different for DOX and 5-Fu: DOX molecules were covalently conjugated with the MOF's surface, whereas 5-Fu molecules were loaded into MOF's pores via electrostatic adsorption that resulted in differences in drugs release rate. Authors have noted a slower drug release for 5-Fu (~48% after 3h at pH 5.0) compared with DOX (~72% after 3h at pH 5.0), which according to Ref. [206]is caused by the high force of bonding between the base site of 5-FU and the Lewis acid site of metal. The release of 5-Fu and DOX after the same incubation period at pH 7.4 was ~4% and ~9% respectively, which allows us to determine E_{rel} for 5-Fu as 12 and DOX as 9. E_{Ret} after 24h of incubation were 4 for 5-Fu and 2.4 for DOX.

Hai-Liang Zhu and co-workers also contributed to this field of experimental pharmacology through the development of conventional pH-responsive dual pH- and redox-responsible MOFs for targeted DOX delivery [166]. The redox potential of the media was chosen as co-stimuli triggering the drug release to provide targeted intracellular delivery of the drug since the Glutathione (GSH) concentrations in the extracellular and intracellular media are around 2−20 μM and 1−10 mM respectively, which significantly impact their redox potential providing conditions for triggered drug release. In their article, the authors compared the drug release rate from pH-sensitive DOX-

containing ZIF-8 crystals (ZD) and dual-sensitive organosilica-coated ZD (ZDOS) at different pH and DDT concentrations. Based on the DOX release data, ZDOS was characterized by sustainable cargo release and should be considered as a system for a prolonged drug release strategy meanwhile ZD in opposite sharply released almost all cargo for the first hours of incubation at low pH. The DOX release from ZD after 3-h of incubation at acidic conditions was around 87% while at neutral one just 14%. However, the prolonged incubation of ZD for 24h at pH 7.4 revealed the leakage of a significant moiety of the loaded DOX (around 41%), which indicates the low stability of ZIF-8-based carriers at physiological pH. Thus E_{rel} of ZD is 6.2 and E_{Ret} is 0.58.

Xianying Cao's group proposed the other type of particles classified as MOF for the quick responsive pH-triggered drug delivery - MIL-n family [10.1021/acs.inorgchem.1c03855]. The authors suggested mono and dual-responsible drug delivery systems consisting of one (DM) and two (DMM) layers of NH2-MIL-88B respectively for the intracellular DOX delivery. As in the case of ZDOS proposed by *Hai-Liang Zhu*, the co-stimuli inducing the drug release from DDM is the media's redox potential. The main goal achieved by Cao's team through the growth of the second layer of MOF on the first one was the reduction of premature cargo leakage from DDS, thus the DDM should be considered in the frame of the prolonged drug release strategy. Meanwhile, DM's drug release profile has demonstrated the unleashing of a significant amount (around 85%) of cargo for the first three hours of incubation at low pH. However, the undesirable leakage of the active substance at neutral pH was also high (around 41%), therefore E_{rel} of DM can be determined as 2. E_{Ret} cannot be estimated for DM since the drug release was evaluated only during the first 18 hours.

DDSs based on metal oxide NPs can also be effectively applied as a drug vehicle characterized by the low pH-triggered release. M. Reza Khorramizadeh's research group suggested ZnO NPs functionalized by N-succinyl chitosan to improve the targeting and bioavailability of a such bioactive compound as CUR [144]. The loading of CUR was provided by its covalent binding with CS molecules adsorbed on the ZnO NPs surface. According to the presented data, CUR-loaded ZnO NPs demonstrated the rapid release of an active substance for the first hour with the following slowing down caused by the fast desorption of weakly bound CUR molecules from the surface of the particle. CUR release after three hours of incubation in acidic conditions (pH 5.2) was around 67% and at neutral pH around 28% which allows us to estimate E_{rel} to be equal to 2.4.

Table 2. E_{rel} and E_{Ret} of different DDS created in the frame of the quick drug release strategy. * - relise value was estimated at pH 5.5, ** - pH 5.2

Active substance	DDS type	DDS configuration	E_{Rel} (a.u.)	E_{Ret} (a.u.)	DLC (%)	Ref.
Doxorubicin (DOX)	MOF (MIL)	DOX@ NH_2-MIL-88B	2	-	7.4	[178]
	MOF (ZIF-90)	UC@mSiO_2-RB@ZIF-O_2-DOX-PEGFA	14.6*	-	6	[142]]
	MOF (ZIF-8)	DOX@ZIF-8	6.2	0.58	43.3	[166]
	MOF (ZIF)	UCMOFs@D@5	9	2.4	16.4	[143]
Fluorouracil (5-Fu)	MOF (ZIF)	UCMOFs@D@5	12	4	24.7	[143]
Curcumin (CUR)	MeO NPs	CUR-CS-ZnO	2.4**	-	13	[144]

Based on these data we can conclude that DDSs based on Zeolitic Imidazolate Frameworks developed in the frame of this concept are characterized by the best combination of E_{rel} and E_{Ret}

(**Table 2**). It is because of the pH instability of the ZIF-based platforms mainly caused by protonated imidazole in the ligand [207]. However, it is worth noting that DDSs possessing promising properties in the frame of this strategy are characterized by low DLC if compare with other pH-responsive vehicles (**Table 1**). At the same time, vehicles with substantial DLC suffer from drug leakage at neutral conditions [166] which do not fit into the concept of the "ideal" drug delivery systems. Therefore, the prioritized issue in the frame of the quick drug release strategy is the increasing DLC of developing systems

3.2.1.2 The strategy of a prolonged drug release

The prolonged drug release strategy implies the retention of a therapeutic dosage of an active substance in the desired area for a long period due to sustainable drug release. It means that the period between the time point when the release curve crosses the drug's toxicity threshold and the point of maximal drug release should be as long as possible (**Figure 5, right part**). Thus, for E_{Ret} evaluation, we considered $pH(R_{pH_t})$ and $pH(R_{pH_e})$ after 12h of incubation and also gave consideration to the time point at which the drug release curve had reached the plateau (t_{plat}).

Doxorubicin loaded DDSs

From the standpoint of the prolonged drug release strategy, two configurations of ZIF-based systems and one NH2-MIL-88B(Fe) stand out among others loaded with DOX considered in this article. One of them is the DOX-loaded ZIF-8 carrier the surface of which is functionalized by AS1411 aptamer to ensure cancer cell targeting and reduce off-target toxicity of the drug [133]. The ZIF-based configuration proposed by *Xiaogang Qu's* team demonstrated prominent results. So, DOX@ZIF-8@AS1411 released more than half (~68.5%) of loaded DOX after 12h of incubation at acidic conditions while the drug leakage at neutral pH was negligible (~2%), which enable to determine the E_{rel} equal to 34.2 (**Table 3**). The drug release after 24h of incubation at neutral conditions also was around 2% which demonstrated the reliability of this configuration for long-term storage of DOX. However, the DLC of DOX@ZIF-8 lying in the base of the proposed DDS was only 10% which is insufficient if compare with other ZIF-base configurations (**Table 1**). The t_{plat} of drug release was reached approximately after 20h at pH 5, which despite the low loading efficiency makes this system a promising candidate in the frame of considering strategy.

Almost the same values of E_{rel} (36.5 a.u.) and E_{ret} (12 a.u.) pertained to the other MOF-based composition (DOX@FeMOF@PSS@MV-PAH@PSS) described in Ref. [10.1039/D0NJ05105E]. According to the presented data NH2-MIL-88B(Fe)-based system released around 73% of cargo after 12h at pH 5 against less than 5% at neutral one. At the same time, this system is characterized by a much higher DLC (around 88.4%) and a more distant t_{plat} time point (24h) compared with DOX@ZIF-8@AS1411 [133] which makes it more suitable for sustainable DOX delivery. Detailed consideration of this configuration and mechanisms of DOX loading is presented **in section 2.1, subsection Doxorubicin loading efficiency.**

The highest value of E_{rel} criteria was described for the mesoporous silica@zeolitic imidazolate framework (HMS@ZIF) [174]. *Rui Cao and co-authors* proposed the core-shell-like structure where the particle of hollow mesoporous silica (HMS) serves as a core loaded with DOX and the shell is formed by sorption of ZIF nanoparticles on the HMS surface. Due to the high porosity, (788 m^2/g surface area and 0.65 cm^3/g pore volume), HMS particles ensure sufficient DOX loading capacity (34%) and authors suppose the recrystallization of DOX inside the HMS's cavities because of ultra-high drug concentration. The pH-responsiveness of DDS was provided via the sorption of the ZIF-consisting shell playing the role of the sealing agent. The authors noted the enlargement of the DDS surface area up to 1152 m^2/g after the shell sorption, explained by the porosity of the ZIF-shell itself but the final DLC of DOX/HMS@ZIF decreased to 28% because of the augment of DDS' mass. The proposed configuration allowed *Rui Cao's* group to achieve high reliability in low pH-triggered drug delivery. So, around 79% of the drug was released after 12h at pH 5 while less than 3% at pH 7.4. This E_{rel} can be estimated as 52.6% which is an outstanding result for considered pH-sensitive DDS loaded

with DOX (**Table 3**). However, the relatively fast release of cargo during the first 10h in acidic conditions is a weakness from the standpoint of sustainable drug delivery. The dug E_{rel} and E_{Ret} of carriers implicit for prolonged drug release mainly decrease at the enlargement of DLC as in the case of DDSs considered in the frame of quick drug release strategy (**Table 3**)[162,163,176]. It is probably caused by the inability of carriers effectively link the redundant drug molecules resulting in cargo leakage at pH values close to the physiological ones. The exception is described above DOX@FeMOF@PSS@MV-PAH@PSS configuration possessing high DOX loading capacity and providing prolonged drug release for 24h at low pH accompanied with negligible drug leakage at neutral one.

Table 3. E_{rel}, E_{Ret}, t_{plat} of different DDS created in the frame of the prolonged drug release strategy. *- relise value was estimated at pH 5.5

Active substance	DDS type	DDS configuration	E_{Rel} (a.u.)	t_{plat} (h)	E_{Ret} (a.u.)	DLC (%)	Ref.
Doxorubicin (DOX)	MOFs (ZIF-8)	DOX/HMS@ZIF	52.6	10	-	28	[174]
		BSA/DOX@ZIF	6.7	11	-	10	[152]
		DOX@ZIF-8@AS1411	34.2	20	12	-	[133]
		AuNCs@MOF-DOX	2.8	20	1	-	[208]
		ZIF-8@DOX@Organosilica	2.3	24	0.9	41.2	[166]
		ZIF-8@DOX	3.6	~72	1.3	-	[209]
		DOX@ZIF-8	3.3	50	1.3	-	[162]
		DOX@ZIF-8/Dex	2.8	68	1.7	63	
		H-ZIF-8/PDA-CD JNPs	3.2	30	1.1	-	[175]
		H−ZIF−8/PDA−CD JNPs + laser (808 nm, 1 W cm−2, 5 min)	2.7	-	-	-	
	MOFs (Cu-TCPP MOF)	Cu-TCPP-DOX	1.57	>60	0.75	-	[176]
	MOFs (graphene oxide/Cu (II)-porphyrin)	CuG1-DOX	2.8	60	1	45.7	
	MOFs (Fe-MOF)	DOX@FeMOF@PSS@MV-PAH@PSS	36.5	~24	12	88.4	[164]
		DOX/γ-CD-MOF	2.1	1	2.4	-	
		DOX/GQDs@γ-CD-MOF	9.5	72	8	-	

	MOFs (γ-cyclodextrin-based MOF)	DOX/AS1411@PEGMA@GQDs @ γ-CD-MOF	4.8	96	2.4	-	[177]
	MOFs (UIO-66)	UIO-66-NH_2/PB/DOX	15.6	36	6	67.4	[163]
		Fe_3O_4@UIO-66-NH_2/Graphdiyne/DOX	1.3	24	0.7	43.8	[159] [
	MOFs (MIL-88B)	DOX@ NH_2-MIL-88B-On-NH_2-MIL-88B	1.8	10	-	14.4	[178]
	MeO NPs	MnO_2 NPs@Keratin@DOX	1.4	24	0.7	8.7	[179]
Fluorouracil (5-Fu)	MOF	5-Fu@ $[Zn_3(BTC)_2(Me)(H_2O)_2](MeOH)_{13}$	2.8	~48	1.3	34.32	[181]
	MOF	5-Fu@CS/Zn-MOF@GO	1.8	24	1.2	45	[154]
	MOF (ZIF-8)	5-FU@ZIF-8@Lf-TC	3.15	24	0.9	24.9 ± 1.4	[146]
Curcumin (CUR)	MeO NPs	CUR-CS-ZnO	2.25	10	-	13	[144]
		ZnO-PBA@CUR	31	36	4.8	35	[149]
		Fe_3O_4@Au- LA-CUR	4.6*	6	1.3	-	[183]

Fluorouracil loaded DDSs

All considered configurations of MOF-based DSS for prolonged 5-Fu delivery are characterized by poor retention and consequently release efficiency (**Table 3**). So, previously considered in section 1.1 5-Fu@$[Zn_3(BTC)_2(Me)(H_2O)_2](MeOH)_{13}$ [181] and 5-Fu@CS/Zn-MOF@GO [154]possess relatively low E_{rel} equal to 2.8 and 1.8 a.u. and E_{Ret} equal to 1.3 and 1.2 a.u. respectively. The ZIF-8-based carrier proposed *by Srinivas Mutalik and co-authors* [146] also demonstrates negligible retain and release efficiency compared with DOX-loaded systems considered in the previous **subsection**. The 5-Fu@ZIF-8@Lf-TC configuration is the core-shell structure comprising the core presented by titanocene-loaded lactoferrin (Lf-TC) NP and shell consisting of ZIF-8. The authors did not reveal the mechanism of 5-Fu binding with DDS, however, they pointed out that the 5-Fu loading was performed during the step of ZIF-8 shell formation. The comparative analysis of the considering DDSs reveals the decrease in drug release efficiency, representing the attitude of the amount of cargo released at acidic conditions to the amount unleashed at neutral one, at the increase of the 5-Fu loading capacity. One of the reasons for this is the cargo's leakage gain at pH 7.4 probably caused by the weak binding of a substantial amount of drug with DDS's surface via hydrogen bonding and π-π stacking interaction and the oversaturation of DDS's structures available for such interaction by molecules of the active substance.

 doi:10.20944/preprints202305.0289.v1

Curcumin loaded DDSs

Among the DDS loaded with CUR, ZnO-PBA@CUR [149] configuration previously considered in section 1.1 possesses the most prospective characteristics. The chelate binding of drug molecules with ZnO-PBA NPs provides significant DLC (~35%) as well as substantial cargo release at pH 5 and its reliable storage at pH 7.4 (E_{rel} = 31, E_{Ret} = 4.8) (**Table 3**). The covalent binding of CUR with DDS in case CUR-CS-ZnO [144] does not ensure such a prominent DLC and sustainable low pH-triggered drug release and inferiors in efficiency to the previously described platform (**Table 3**).

3.2.2 Normal pH-triggered drug release

The pH-sensitive DDSs characterized by the release of cargo at the neutral pH have only recently attracted the attention of the scientific community, and currently, just a few articles devoted to this type of carrier have been published. This strategy, as it was mentioned above, is based on the concept implying fast accumulation of systemically administrated carriers in the microcapillaries supplying a solid tumor and rapid drug release at physiological pH values resulting in sharp elevation of active substance concentration in the target region and its diffusion into the tumor interstitium. Within this concept employed carriers must exhibit fast release of cargo in the physiological pH values (7.4) and high doses should be reached within 3 hours, but the better result probably would be reached at faster release. The particle size in this case is not that crucial since this concept does not imply the EPR effect and carriers are only supposed to be trapped by defects in vessels around the tumor. Firstly, this concept was proposed by *A.V. Zvyagin's* group in Ref. [137]. In their manuscript, the authors demonstrated in silico the effectiveness of the proposed approach compared with the prolonged drug release strategy and corroborate these results with *in vitro* and *in vivo* studies. As a DDS in the frame of this concept, authors suggested MIL-101 (Fe) metal-organic frameworks (MIL-101 NPs) comprising iron-based building units linked by terephthalic acid derivatives which are characterized by outstandingly large surface area (4500 m^2/g) and narrow pore size distribution (29–34 Å) (**Table 1**). This configuration provided the sufficient DLC of a wide range of model substances including DOX (36.2 ± 1.4%), and Rhodamine 123 (42 ± 3%), and their fast release in PBS within the first 30 min (72.1% and 54.7% respectively).

The other MOF-based DDS demonstrating alike pH-sensitive drug release pattern is UiO-67-CDC-$(CH_3)_2$, the chemical structure peculiarities of which were previously considered in **section 2.1** [180]. Since *En-Qing Gao and co-authors* had published their work one year earlier than the FlaRE approach was proposed, the authors do not highlight the applicability of their DDS within the frame of this strategy, however, they note the applicability of the developed carrier for a drug release in a blood pH conditions. Deferred from MIL-101 NPs, 5-Fu loaded DDS demonstrated a slower drug release rate and reach the release plateau approximately after 6h of incubation at pH 7.4 (around 80% of loaded cargo). UiO-67-based DDS was found to be stable at highly acidic conditions (pH 3), however, the increase in pH value up to 5 resulted in a drastic increase in drug leakage (~48% of cargo after 6h of incubation) which is more than 50% of the amount released at neutral conditions and indicate the low stability of DDS. The authors explain this peculiar behavior of DDS within the framework of the natural bond orbit theory (NBO), which leads to a stronger bond between O–H derived from PBS solution and Zr(IV) in comparison to the carboxyl O atom bond making Zr-MOF decompose under neutral conditions.

4 *In vitro* studies of pH-responsive DDSs

4.1 Cytotoxicity of DDSs

Since the application area of pH-responsive DDS is the targeted tumor treatment, the evaluation of desirable toxicity on tumor cells and off-target toxicity on the normal one is the most important characteristic of this kind of carrier which can be estimated *in vitro*. As in the case of two previously considered parameters, it is crucial to compare the cytotoxicity of different vehicles loaded with the same active substance because of the diverse mechanisms of action of different drugs. Also,

equivalently important to take into account the differences in structure and metabolic activities of different cell cultures [210] and diversity in mechanisms of kits' action for cell viability assessment [211,212], thus it is eligible to compare different DDSs on similar cell models tested via the same kit.

The common *in vitro* practice to standardize cytotoxicity results is the estimation/calculation of the half-maximal inhibitory concentration (IC_{50}) which indicates how much the testing substance is needed to inhibit estimating biological process by half [213]. Herein IC_{50} values are also used to compare the targeted toxicity of different drug-loaded carriers and applied the linear interpolation method broadly used for its calculation. At the same time, since DDS itself can be a reason for different metabolic issues it is important to consider the desirable cytotoxicity of drug-comprising carriers through a lens of the toxicity of empty DDS. It is worth noting that the best practice for *in vitro* cytotoxicity studies include the evaluation of target toxicity on the model cancer cell line and off-target toxicity on the normal one. However, because this process is laborious and expensive, usually the toxicity studies are performed on one predominantly cancer cell line (**Table 4**). According to the International Standard ISO 10993-5:2009, the conventional threshold level of cell viability value for safe substances is 70% [214]. So, the "ideal" drug delivery system should fit the following parameters: **i)** drug-loaded carriers should induce cancer cell suppression at the administration of the minimal possible amount of drug; **ii)** the equivalent amount of empty carriers should not decrease the cell viability by more than 30% compared to the control. Also, the DDS efficiency can be illustrated via the ratio of the efficiency of growth suppression of cancer cells by the capsulated form of the drug vs the free form. For this, here we introduce the coefficient describing the efficiency of cancer cells' suppression (ECCS), which presents the ratio of cell viability value at the free drug concentration equivalent to the IC_{50} of capsulated form to viability at IC_{50} of the capsulated form (**Table 4**).

Table 4. IC_{50} of drug-loaded DDSs presented as a concentration of capsulated substance (μg/mL) and an efficiency of cancer cells supression (ECCS) of different DDSs. * - Lipoic acid-curcumin.

Active substance	Test type	Cell line	DDS type	DDS configuration	24h		48h		72h		Ref.
					IC_{50}	ECCS	IC_{50}	ECCS	IC_{50}	ECCS	
				DOX/HMS@ZIF	~0.12	1.64	-	-	-	-	[174]
			MOFs (ZIF-8)	BSA/DOX@ZIF	~0.04	1.48	-	-	~0.037	1.42	[152]
			MOF (NH2-MIL-88B (Fe))	DOX@FeMOF	<2.5	-	-	-	-	-	[164]
				DOX@FeMOF@PSS@MV-PAH@PSS	<2.5	-	-	-	-	-	
		MCF-7	MOFs (γ-cyclodextrin-based MOF)	γ-CD-MOF	>90	-	-	-	-	-	[177]
				GQDs@γ-CD-MOF	~34.7	-	-	-	-	-	
				DOX/AS1411@PEGMA@GQDs@γ-CD-MOF	~15.76	-	-	-	-	-	
			MOF	DOX/CS/BioMOF	~2.45	1.3	-	-	-	-	[148]

			MOF (Cu (II)-porphyrin)	Cu(II)-porphyrin /Graphene oxide-DOX	~4	1.38	-	-	-	-	[176]
Doxorubicin (DOX)	**MTT**	HeLa	MOFs (ZIF-8)	DOX@ZIF-8	~3	1.74	-	-	-	-	[133]
				DOX@ZIF-8@AS1411	~1.64	1.82	-	-	-	-	
				ZIF-8@DOX@Organosilica	~0.34	1.18	-	-	-	-	[166]
			MOF (ZIF-90)	UC@mSiO$_2$@ZIF-DOX-PEGFA	>100	-	-	-	-	-	[142]
				UC@mSiO$_2$-RB@ZIF-DOX-PEGFA + 808 nm laser irradiation	~36.7	1.6	-	-	-	-	
				UC@mSiO$_2$-RB@ZIFO$_2$-DOX-PEGFA + 808 nm laser irradiation	~15.5	2	-	-	-	-	
			MOFs (UIO-66)	Fe$_3$O$_4$@UIO-66-NH$_2$/Graphdiyne/DOX	~20	0.62	~9.2	0.77	-	-	[159]
			MOF (Cu (II)-porphyrin)	Cu(II)-porphyrin /Graphene oxide-DOX	~14	1.16	-	-	-	-	[176]
		4T1	MOFs (ZIF-8)	AuNCs@MOF-DOX	~9.25	0.9	-	-	-	-	[208]
				AuNCs@MOF-DOX + 670 nm laser irradiation	~6	1.29	-	-	-	-	
			MOF (ZIF-90)	UC@mSiO$_2$@ZIF-DOX-PEGFA	>100	-	-	-	-	-	[142]
				UC@mSiO$_2$-RB@ZIF-DOX-PEGFA + 808 nm laser irradiation	~56.6	1.54	-	-	-	-	

			UC@mSiO$_2$-RB@ZIFO$_2$-DOX-PEGFA + 808 nm laser irradiation	~29.6	1.58	-	-	-	-	
		MOF (Prussian blue)	NiCo-PBA@DOX	>140	-	-	-	-	-	[134]
			NiCo-PBA@Tb^{3+}@DOX	>140	-	-	-	-	-	
			NiCo-PBA@Tb^{3+}@PEGMA@DOX	~6.4	1.52	-	-	-	-	
			NiCo-PBA@Tb^{3+}@PEGMA@AS1411@DOX	~5.8	1.56	-	-	-	-	
	A549	MOF (NH2-MIL-88B (Fe))	DOX@FeMOF	<2.5	-	-	-	-	-	[164]
			DOX@FeMOF@PSS@MV-PAH@PSS	<2.5	-	-	-	-	-	
	HUVEC	MOF (Cu (II)-porphyrin)	Cu(II)-porphyrin /Graphene oxide-DOX	>139.2	-	-	-	-	-	[176]
	NIH-3T3			>139.2	-	-	-	-	-	
WST-8 / CCK-8	MCF-7	MOF (ZIF-8)	DOX@ZIF-8/Dex	>10	-	-	-	-	-	[162]
	MCF-7/ADR			27.7	1.4	-	-	-	-	
	HeLa			>10	-	-	-	-	-	
		MOF	UCMOFs@Dox	~1.57	1	-	-	-	-	[143]
	4T1	MOF (NH2-MIL-88B)	DOX@NH$_2$-MIL-88B	~3.5	-	-	-	-	-	[178]
			DOX@NH$_2$-MIL-88B-On-NH$_2$-MIL-88B	~2.8	-	-	-	-	-	
	A549	MOF	5-Fu/[Zn$_3$(BTC)$_2$(Me)(H$_2$O)$_2$](MeOH)$_{13}$	~45.76	-	-	-	-	-	[181]
	HEK 293			>171.6	-	-	-	-	-	

Fluorouracil (5-Fu)	MTT	MDA-MB 231	MOF	5-Fu@CS/Zn-MOF@GO	-	-	-	-	~31.25	0.73	[154]
	WST-8 / CCK-8	HeLa	MOF	UCMOFs@5-Fu	>83	-	-	-	-	-	[143]
Curcumin (CUR)	MTT	MCF-7	MeO NPs	ZnO-PBA@CUR	-	-	~9.58	1.45	-	-	[149]
		MCF-10a			-	-	>40	-	-	-	
		MDA-MB- 231		CUR-CS-ZnO	-	-	~40	~0	-	-	[144]
		HEK 293			-	-	>100	-	-	-	
		Astrocytes		Fe_3O_4@Au-LA-CUR/GSH*	-	-	~97	0.64	-	-	[183]
		U87MG			-	-	~67.5	0.2	-	-	
	WST-8 / CCK-8	A549	MOF (ZIF-L)	CUR@ZIF-L	~2.2	1.88	-	-	-	-	[182]
Camptothecin (CPT)	MTT	HeLa	MOF (ZIF-8)	CPT@ZIF-8@RGD	~3.3	1.87	-	-	-	-	[215]
			MOF (MIL)	MIL-101(Fe)-Suc-CPT	0.078 ± 0.016	-	-	-	-	-	[184]
				MIL-101(Fe)-Click-CPT	0.063 ± 0.015	-	-	-	-	-	
		3T3		MIL-101(Fe)-Suc-CPT	3.794 ± 0.459	-	-	-	-	-	
				MIL-101(Fe)-Click-CPT	6.393 ± 0.773	-	-	-	-	-	
		SH-SY5Y		MIL-101(Fe)-Suc-CPT	0.040 ± $3.2\ 10^{-3}$	-	-	-	-	-	
				MIL-101(Fe)-Click-CPT	0.029 ± $2.5\ 10^{-3}$	-	-	-	-	-	
Quercetin (Q)	MTT	MCF-7	MeO NPs	PBA-ZnO-Q	-	-	~7.36	1.3	-	-	[38]
		3T3-L1		ZnO-Q	-	-	-	-	<1	-	[185]
					-	-	-	-	>1	-	

As can be seen from **Table 4**, there are a significant number of different combinations of the model cell lines and tests assessing their viability. So, currently, the high throughput screening method utilizing tetrazolium-based dyes is the good standard for drug/DDS cytotoxicity evaluation

 doi:10.20944/preprints202305.0289.v1

and applies in the majority of studies. MTT (3-(4,5-dimethylthiazol-2-yl)-2,5-diphenyltetrazolium bromide), WST-8 (2-(2-methoxy-4-nitrophenyl)-3-(4-nitrophenyl)-5-(2,4-disulfophenyl)-2Htetrazolium, monosodium salt), and Cell Counting Kit-8 (CCK-8) comprising WST-8 are the most widely used kits for this purpose (**Table 4**). Despite both MTT and WST-8 are tetrazolium salts and their principle of action is based on the same basis [216], the comparative analysis of data obtained via these kits is not eligible, since these dyes possess different water solubility that significantly affects the results of cell viability evaluation [217–219]. The application of both dyes as well as many other tetrazoliums- and resazurin-based reagents imply their incubation with cells accompanied by dyes conversion into colored or fluorescent products under the action of viable cells' enzymes with the following detection using the plate reader. Dead cells, in its turn, are unable to perform such a transformation, which ensures a reliable way for cell metabolic activity evaluation and based on it indirect cell viability assessment [220]. In the case of tetrazolium salts application, the formazans are detectable products characterized by pronounced absorbance at 570 nm for MTT and 460 nm for WST-8. However, it is worth noting that formazan products of MTT tetrazolium are insoluble in water and require solubilization before measurement while products of metabolism of WST-8 are well soluble in growth media that substantially increase test sensitivity and reliability [217–219]. Thus the conclusions derived from the comparison of data from cytotoxicity tests on the same cell model obtained by different test systems can be imprecise or even wrong. The other obstacle mitigating the volume of data that is eligible for comparative analysis is the different periods of co-incubation of DDS with cell lines. As we can see from **Table 4**, the efficiency of the metabolic activity suppression in cancer cells by drug-loaded DDS is predominantly estimated after 24h of their co-incubation. However, in some cases, the metabolic issues are assessed after 48h [38,144,149,183] and 72h [154,185] of incubation as for the majority of metal oxide-based DDS mentioned in this review, consequently truncating the range of DDS eligible for the comparative analysis.

Next, to evaluate and compare efficiencies of different DDS's, IC_{50} is considered as a function of DLC and release rate. In this regard, systems investigated with comparable cell lines, viability test methods, and drugs have been analyzed. Here, we chose three groups of papers that investigate the efficiency of MOF-based DDSs using DOX as a drug and MTT test to evaluate cell viability using MCF-7 (1), HeLa (2), and 4T1.

DOX-MTT-MCF-7

Thus, different MOF systems functionalized with both organic and inorganic components to provide responsiveness towards the pH of the microenvironment were analyzed in terms of their drug delivery properties and cytotoxicity *in vitro*. Meta-analysis of the data clearly shows higher release rate provides higher cytotoxic efficiency. *Jia et al.* developed DOX/HMS@ZIF submicron particles capable of releasing ~90% of encapsulated DOX within 10 h that resulted in superior IC_{50} of 0.12 μm/mL [174]. Similarly, Z. Liang reported hybrid BSA/DOX@ZIF particles with a high release rate (~80% for 10 h) that resulted in great IC_{50} of 0.04 μm/mL [152]. Probably, smaller size promoted cytotoxicity of the system in comparison to DOX/HMS@ZIF particles (~100 nm versus 600 nm) which significantly affects the internalization process. A few papers show hybrid MOF particles with modest release rates (around 65% within 24 h) that resulted in reduced IC_{50} <2.5 μm/mL [148,164] and IC_{50} <4 μm/mL [176]. Accordingly, slow release rates result in poor cytotoxicity of the system. *Q.Jia* reported a detailed study of hybrid γ-cyclodextrin-based MOF carriers which exhibit slow rates of release (maximum of ~80% for 60 h) and corresponding IC_{50} values in the range of 15.76 - 90 μm/mL in dependence on the composition [177].

DOX-MTT-HeLa

Corresponding results are obtained using HeLa cell lines. Thus Ren et al. demonstrated MOF coated by biodegradable organosilica to exhibit pH-responsiveness and an excellent release rate of ~65% for 10 h which allowed high cytotoxicity of the system and IC_{50} of 0.34 μm/mL [166]. Another study showed MOF-based carriers DOX@ZIF-8@AS1411 to exhibit a modest release rate of 50% for 24 h and corresponding low cytotoxicity of released DOX with IC_{50} values of 1.64-3μm/mL [133].

Newly developed graphene oxide/Cu (II)-porphyrin MOF nanocomposite also showed a modest release rate (~45-65% for 24 h) with poor IC_{50} of 14 μm/mL [176]. Perfect release rate was shown by Xie et al. using UC@mSiO$_2$-RB@ZIF-O$_2$-DOX-PEGFA nanoparticles, however, poor DLC of 6% resulted in the low cytotoxic effect of DOX and IC_{50} values in the range of 15.5-100 μm/mL in dependence on the structure of the particles [142]. This pattern was also confirmed by Xue et al. using novel Fe$_3$O$_4$@UIO-66-NH$_2$/graphdiyne MOF-based particles for encapsulation of DOX. Fe$_3$O$_4$@UIO-66-NH$_2$/graphdiyne particles were shown to provide prolonged release over 36 h (48%) that resulted in reduced cytotoxicity and IC_{50} of 20 μm/mL [159].

DOX-MTT-4T1

Meta-analysis of drug carriers investigated using 4T1 cell line has demonstrated the same pattern. Jia et al. have shown DOX release dependence from NiCo-PBA@DOX particles on additional modification with Tb^{3+} and poly(ethylene glycol)methacrylate and the corresponding increase in cytotoxicity and IC_{50} values with an increased release rate from ~6 μm/mL when 44% of DOX released for 10 h to 140 μm/mL when <20% of DOX released for 24 h [134]. Nanoparticles of AuNCs@MOF-DOX structure were found to possess high release rates of 67% for 15 h and consistently showed high cytotoxic effect and IC_{50} values of 6-9.25, however, the cytotoxic effect was compromised by low DLC of the particles [208]. A low cytotoxic effect (IC_{50} = 29.6-100 μm/mL) was also been shown using UC@mSiO$_2$-RB@ZIF-O2-DOX-PEGFA and 4T1 cell line because of low DLC (6%) despite a high release rate of these particles[142].

This data evidence that drug loading capacity and release rate of the carriers are crucial parameters for DDS. Studies made using different cell lines demonstrate that prolonged drug release is not preferable under in vitro conditions and the higher release rates as well as higher DLC demonstrate increased cytotoxicity. It means not only the total dose of the drug plays a role but concentration that can be reached within a cell. Obviously, the characterization of the DDS efficiency in terms of drug delivery is an extremely complex process and it is not limited by IC_{50} values in vitro, however, these relations should be taken into account. Highly important to analyze carriers' features in terms of internalization ability together with the ability to circulate in the blood flow without fast infiltration. Another important task is to evaluate the gap in release between acidic and physiological conditions to reveal possible outcomes. Although the long-term release is not preferable in vitro, it is not necessary means that in vivo studies would confirm this point as the time period between injection and uptake can be considerable.

4.2. Internalization of pH-responsive DDSs

Internalization via endocytosis of cells is a key process because it provides intracellular release in endosomes which is an important approach due to a range of factors such as pH below 5.5 as it was described above. In general, small carriers with a size <200 nm enter the cell through endocytosis with high efficiency in dependence on their size, shape, and surface charge[221–223]. However, required long-time circulation drives researchers to modify drug carriers with additional components such as PEG and provide a negative charge to avoid infiltration which impedes features necessary for effective internalization[108,109,224]. In this regard, different techniques allowing the change in carriers' structure and features in response to acidic pH have been developed to achieve synergistic effects of long circulation without obstructed cell uptake. For example, conformational changes, protonation, and PEG detachment in response to slightly acidic pH were shown to promote cell uptake [108,225–229] Protonation supposes the application of ionizable chemical groups as a component of drug carriers. At physiological pH, these groups are deprotonated/deionized but an acidic microenvironment induces protonation or charge reversal resulting in structural transformation or disassembly of the carriers [113,114]. Current data demonstrate pH-responsive systems based on the protonation mechanism to be able of enhanced cellular uptake into cancer cells. Additional applications of specific ligands, antibodies, etc. have been shown to promote the internalization of drug carriers into cancer cells [105,230–233].

Considering the necessity of the following endosomal escape mechanism, it means that today simple internalization process is not of interest. Cascaded-responsive DDS that combine multiple functions within the system are demanded [234]. It means that the characterization of the system should satisfy at least a few requirements such as high loading capacity, long-term circulation, diffusion into tumor interstitium, effective internalization, and sufficient drug release accompanied by highly specific behavior. [42,115]

5. *In vivo* studies of pH-responsive DDSs

The use of pH as an endogenous trigger for the release of active components by stimulus-responsive carriers has a number of advantages, including wide applicability and the absence of the need for external triggers. At the same time, the authors indicate the low accuracy of delivery and release in non-targeted sites of the body to the disadvantages of using pH as a trigger, which is due to the possibility of shifts in acid-base homeostasis in tissues as a result of a wide range of physiological and pathological (inflammatory changes) causes [41]. A meta-analysis of studies over the past 5 years shows that the use of pH-responsive drug carriers for targeted delivery enhances the antitumor effect under experimental conditions on various models of malignant neoplasms, which is characterized by an increase in tumor regression compared to the control and indicates an increase in accumulation of drugs in target tumor [74]. The heterogeneity and abnormal permeability of the vasculature in tumors are important factors that contribute to the accumulation of nanoparticles in them, which, in combination with a pH-responsive release mechanism, provide conditions for the preferential release of cargo in acidic tumor tissues. However, according to the results of a meta-analysis, on average, only 0.7% of injected nanoparticles reach tumors [46], which can significantly reduce the efficiency and selectivity of delivery by pH-responsive DDS's and makes the selection of nanomaterials for designing such systems crucial for successful therapy. Drug carriers for pH-responsive targeted delivery systems should have a number of features that ensure their stability in the bloodstream, penetration through histohematological barriers, effective EPR effect, and absorption of carriers by tumor cells [51]. As it was described above, different materials ranging from inorganic composites to polymeric particles have been shown to exhibit pH-triggered release and used as a material for DDS's. Both natural and artificial polymers have been employed as pH-responsive materials for designing DDS's. In general, such systems are biocompatible and able to encapsulate a wide range of compounds.

Many polymers enable the fabrication of pH-responsive carriers so that external pH would induce structural and conformational changes in a carrier leading to the release of encapsulated cargo. For example, estrone-modified glycol-chitosan pH-responsive nanoparticles (GCNP-ES) were studied in vivo for targeted delivery of paclitaxel (PTX) to MCF-7 breast tumor xenograft model in mice. Application of PTX/GCNP-ES demonstrated an increase in accumulation of the active component in the tumor tissues, which led to a higher index of tumor growth inhibition - up to 81.4%, in comparison to PTX/GCNP (69.4%) and PTX solution (48.8 %). In addition, in vivo studies of PTX/GCNP-ES have not revealed histological or hematological toxicity [235]. An increase in accumulation of doxorubicin-triphenylphosphine in tumors has been shown in vivo by the application of pH-responsive nanoparticles consisting of a drug-loaded polylactic and glycolic acid core covalently "wrapped" in a cross-linked bovine serum albumin shell. The shell was suggested to minimize interaction with serum proteins that inhibit target recognition, and with macrophages that absorb carriers. The shell of the carriers was additionally functionalized with a pH-sensitive ATRAM peptide in order to promote the internalization of the carriers by cancer cells in the acidic tumor microenvironment. The introduction of these particles was shown to significantly reduce the volume of the 4T1 mammary tumor in mice [236]. Another example of DOX delivery was demonstrated by Shiyong Song et al., with polymeric microcarriers comprising pH-sensitive nanogel based on hyaluronic acid. Intravenous injection of the pH-responsive nanogel to animals with H22 tumor xenografts, a 10-fold decrease in tumor volume was observed on the 15th day of treatment, which is associated with prolonged circulation, selective accumulation of the nanogel, and pH-responsive release of doxorubicin in the tumor focus. Moreover, histological analysis revealed significant areas

 doi:10.20944/preprints202305.0289.v1

of tumor tissue necrosis. At the same time, doxorubicin-loaded pH-responsive nanogels showed no systemic toxicity [237].

In order to overcome the limitations of reduced EPR effect, polymer carriers capable of changing their conformation and structure within the body at different stages of the delivery have been developed. Athymic nude mice with tumors of the human pancreas BxPC-3, human lung cancer resistant to cisplatin A549R, and metastatic breast cancer 4T1 were employed to demonstrate the efficiency of iCluster nanoparticles system for the targeted delivery of cisplatin. iCluster is a cluster system of nanoparticles capable of decomposition into smaller parts as it overcomes biological barriers in the tumor environment. The initial size of ~100 nm favors stable circulation of the carriers in the bloodstream and accumulation in the tumor, due to the increased permeability of its vessels. Acidic pH in tumor tissues triggers local cleavage of the system into much smaller (~5 nm) dendrimers, which improve tissue penetration and thus deliver more cisplatin to malignant cells. In vivo studies have shown administration of the free drug to inhibit BxPC-3 tumor growth by 10%, while the iCluster system inhibited growth by 95%[238].

At the same time, literature data show a practical application of polymer carriers as a targeted delivery system for chemotherapeutic drugs to be difficult due to low stability in the bloodstream and targeting inefficiency, which obstruct the expected increase in therapeutic effect compared to free drugs. A decrease in the stability of carriers in the bloodstream and reduced efficiency of targeted accumulation were suggested to be a result of the interaction of the carrier's surface with serum proteins, which affects target recognition ability and leads to nonspecific distribution in the body [239]. One of the most common methods for improving micelle stability and drug retention is increasing the hydrophobic properties of the loaded drug and its mixing properties with the carrier's material using a variety of physical and chemical strategies. However, these complex modifications of the system structure often lead to aggregation of the loaded drugs during the self-assembly process, resulting in reduced therapeutic efficacy of the system[240].

Targeted delivery systems based on liposomes loaded with anticancer drugs, including doxorubicin, daunorubicin, and vincristine, are currently under clinical trials [241]. Lipid-based carriers have also been modified with pH-responsive components and shown to provide targeted drug delivery to tumor cells. Permeability of the liposomal membrane occurs in response to a change in pH in the tumor environment by means of protonation/deprotonation of functional groups, leading to morphological changes in lipid bilayers and ensuring the release of the drug. In particular, the efficiency of pH-responsive liposomes modified with EphA 10 in the delivery of triphenylphosphine docetaxel was demonstrated, which was accompanied by significant antiproliferative, antiangiogenic, and proapoptotic effects in MCF-7 tumors in mice [242]. The main factor limiting the application of lipid carriers, including pH-responsive liposomes, is their rapid absorption by phagocytes of the reticuloendothelial system, which leads to a very short circulation time. To increase the circulation time of liposomes, pegylated phospholipids (PEG lipids) are introduced into their membranes, which prevent the phagocytosis of such particles, but at the same time reduce the stability and pH-responsiveness of the carriers [243]. Comparison of doxorubicin delivery efficiency by pegylated and non-pegylated pH-responsive liposomes in BALB/c mice with a 4T1 mammary tumor revealed that the presence of PEG in the carrier reduces the antitumor activity [244]. To reduce the systemic toxicity of docetaxel (DTX) and increase its therapeutic potential, pegylated pH-responsive liposomes functionalized with anti-VEGF antibodies (VEGF-PEG-pH-Lipo-DTX) have been developed. However, the conjugation of antibodies to the PEGylated surface of liposomes reduced their circulation time. VEGF-PEG-pH-Lipo-DTX was eliminated from the bloodstream faster than PEG-pH-Lipo-DTX due to the mononuclear phagocytes system [245]. Attempts have been made to increase the affinity of the tumor to pH-responsive liposomes using the TAT (transactivator of transcription)-peptide. However, in vivo studies showed TAT to reduce the therapeutic efficacy of the drug due to inefficient accumulation in the tumor and a higher rate of release into the bloodstream [246]. Wang et al. have demonstrated inhibition of GL261 glioma induced by systemic administration of paclitaxel (PTX)-loaded polymersomes (PL) to animals in the ventral striatum. The results of PTX@PS treatment showed over 99% inhibition of glioma growth in

vivo due to the sustained release of PTX without the occurrence of drug resistance. The authors showed that an acidic microenvironment (similar to the tumor microenvironment) induces the release of up to 79.79% of paclitaxel from the synthesized nanosystem within 19 days [247]. André Luis Branco de Barros et al. showed high antitumor efficacy of pH-responsive liposomes (SpHL) loaded with doxorubicin and coated with folic acid to enhance selective accumulation in tumor sites. Intravenous administration of the SpHL-DOX-Fol hybrid liposomes to mice with breast cancer (4T1) resulted in a 68% inhibition of tumor growth and a sharp decrease in lung metastasis. Moreover, histological analysis of tumors after SpHL-DOX-Fol treatment showed more extensive areas of necrosis compared to treatment with free doxorubicin or with particles uncoated with folic acid [248]. Jong Oh Kim et al. developed biocompatible pH-responsive liposomes modified with anti-CD25 antibodies and conjugated to T-regulatory cells to enhance stability, sustained circulation, and localized release of interleukin-2(IL), anti-ligand-1 (PD-L1), and imiquimod (IQ), increasing their ability to provide antitumor immunotherapy. Intravenous administration of these carriers to mice with B16/BL6 melanoma resulted in a 5-fold decrease in tumor volume with a high content of apoptosis and necrosis. Notably, the engineered liposomes were specifically transported into the B16/BL6 tumor microenvironment and exhibited long retention times (up to 72 hours)[249]. Guangya Xiang et al. showed the antitumor efficacy of pH-responsive liposomes loaded with doxorubicin and imatinibine and targeted to cell folate receptors. After intravenous administration of liposomes to animals with MCF-7/ADR xenograft tumors, effective tumor inhibition was observed with minimal toxicity to healthy organs. Moreover, liposomes provided the excellent long-term circulating ability and sensitivity to the acidic environment of the tumor, promoting the release of anticancer drugs [250]. Xiuli Zhao et al. reported the antitumor efficacy of pH-responsive liposomes loaded with doxorubicin and small interfering RNA (siRNA). Intravenous administration of the liposomes to animals with breast cancer (MCF-7) showed high antitumor activity (the inhibition rate was 35.8%), which was probably due to the fact that the liposome-based drug delivery system could effectively deliver the therapeutic agent to tumor tissue. An additional coating of liposomes with p olyethylene glycol increased the rate of tumor inhibition to 50.13% primarily by increasing the circulation time of liposomes in the bloodstream [251].

Mesoporous silica particles should be highlighted as one of the most promising inorganic drug carriers. Mesoporous silica is safe for systemic administration via intravenous injections in concentrations up to 40 mg/kg and does not cause acute or chronic toxicity. Besides mesoporous silica particles are biodegradable and are completely eliminated from the body. Interestingly, the bioavailability of mesoporous silica particles does not depend on the route of administration but depends on the particle size. Increasing the particle size from ~32 to ~142 nm leads to a monotonic decrease in systemic bioavailability, regardless of the route of administration, with a corresponding accumulation in the liver and spleen [252]. In recent years, a system of pH-responsive and visualizable drug carriers based on mesoporous silica particles and sodium alginate doped with gadolinium (Gd) has been developed. These particles had a spherical shape with an average size of about 83.2 ± 8.7 nm. The results of the in vivo safety assessment and hemolysis analysis confirmed the high biocompatibility of the system. During experiments on mice using MRI, the accumulation of particles in the 4T1 tumor was demonstrated, which allowed the authors to consider a synthesized hybrid nanosystem as a promising system for pH-responsive drug delivery and MRI imaging for cancer diagnosis and treatment [253]. Mesoporous silica particles and hybrids based on them have been extensively studied in vivo. Polyacrylic acid (PAA) and pH-responsive lipid (PSL) coated silica particles have been developed for synergistic delivery and dual pH-responsive sequential release of arsenic trioxide (ATO) and paclitaxel (PTX). Additional modification of silica particles with the F56 peptide provided an increase in the specificity of delivery to tumor cells. In vivo testing of these particles in mice with tumors derived from MCF-7 demonstrated the co-delivery of ATO and PTX using MSN coated with LP and PSL significantly increased antitumor activity. Additional modification of the particles with F56 enabled increased selectivity accompanied by a better inhibitory effect on tumor growth [254].

Metal nanoparticles are the fourth most frequently used material for designing pH-responsive DDS's in the last 5 years [74]. Studies have shown that metal oxide nanoparticles (such as zinc oxide) exhibit high cancer cell selectivity, drug retention, and controlled release. Many types of metal oxide nanoparticles show low toxicity and good biocompatibility. For example, ZnO nanoparticles rapidly degrade to Zn2+ ions at a pH below 5.5. However, as we described above, pH values lower than 6.2 are not found in real tumors (except for the 2 types of tumors that exhibit lower pH values in some cases) and the only way is delivery into endosomes and lysosomes. Nevertheless, zinc oxide nanoparticles exhibit a cytotoxic effect on tumor cells through mitochondrial dysfunction, the release of reactive oxygen species, lipid peroxidation, DNA damage, and finally apoptosis. In addition, ease of detection due to intrinsic fluorescence, simple synthesis methods, and low cost make zinc oxide particles suitable as nanocarriers for cancer treatment. Such nanocarriers can easily extravasate and accumulate in the tumor focus due to damaged vessels and immature lymphatic vessels of the tumor tissue.

In the last 5 years, researchers tend to use hybrid nanoparticles combined with organic materials to endow the system with multifunctionality. For example, Parames C. Sil et al. synthesized phenylboronic acid (PBA) conjugated zinc oxide nanoparticles (PBA-ZnO) loaded with quercetin (a bioflavonoid widely found in plants). The presence of PBA fragments on the surface of the nanoparticles facilitated the targeted delivery of quercetin to cancer cells. Moreover, quercetin-loaded PBA-ZnO nanoparticles (PBA-ZnO-Q) demonstrated pH-responsive drug release within the tumor via ZnO dissociation. In vivo studies showed an intravenous injection of PBA-ZnO-Q into animals to induce apoptotic death of human breast cancer cells (MCF-7) by increasing oxidative stress and damage to mitochondria [38]. The cytotoxic potential of the nanohybrid is explained by the authors as a combinatorial cytotoxic effect of quercetin and ZnO on cancer cells. A similar DDS was employed to deliver curcumin, which has strong anti-inflammatory, anti-cancer, and anti-angiogenic properties. Intravenous administration of ZnO-PBA-Curcumin in vivo effectively reduced tumor growth in mice with Ehrlich ascitic carcinoma due to increased selective accumulation of curcumin. A decrease in tumor cell multinucleation was observed in response to ZnO-PBA-Curcumin treatment. Moreover, the biosafety study of hybrid nanoparticles did not reveal signs of hepato- and renal toxicity. Guang Yang et al. demonstrated keratin to be an efficient platform for the synthesis of metal oxide nanosystems, including manganese dioxide nanoparticles and gadolinium oxide nanoparticles characterized with excellent colloidal stability and biocompatibility. Nanoparticles synthesized using keratin were shown to exhibit a pH-responsive release of doxorubicin, primarily due to the cleavage of disulfide crosslinks between keratin chains in the acidic tumor microenvironment. In vivo biodistribution experiments have shown that the hybrid nanoparticles after 7 days of intravenous administration to animals with 4T1 tumors demonstrate accumulation in the liver and almost complete elimination from the body 15 days after injection. Also, these particles enable excellent contrast signals in the tumor in vivo for MRI imaging. Moreover, systemic administration of these particles does not induce damage in healthy intact tissues and organs indicating good biocompatibility of the nanosystem [179]. Active targeting was demonstrated by gold nanoparticles coated with a naturally derived pH-responsive short tripeptide sequence (Lys-Phe-Gly or KFG) have recently been developed to deliver doxorubicin. This targeted DDS for doxorubicin has demonstrated a significant reduction in cell proliferation and tumor growth of BT-474 in mice [255]. However, inorganic nanoparticles can induce metabolic problems, for example, gold nanoparticles have been shown to remain in liver macrophages for up to 12 months after administration [139]. Such long-term outcomes should be carefully considered to select the right carrier for a particular task.

A wide range of MOF's modifications has been developed and demonstrated successful results during in vivo testing. Zhang et al. investigated the therapeutic efficacy of zeolite imidazolate backbone (ZIF-8) nanocarriers for the delivery of doxorubicin (DOX) and acetazolamide (ACE). After a single intratumoral injection, the nanocomposite showed excellent antitumor efficacy against hepatocellular carcinoma in vivo. Under the influence of ultrasound, (DOX+ACE)@ZIF-8 tended to accumulate directly at the site of the tumor and invade tumor cells through endocytosis pathways, and the pH-sensitive release of doxorubicin and acetazolamide was associated with disruption of the

 doi:10.20944/preprints202305.0289.v1

coordination of zinc ions and ZIF-8 imidazole rings. (DOX+ACE)@ZIF-8 showed minimal damage to healthy tissues and adverse hematological effects, demonstrating high biocompatibility [88]. Jing Wang et al. reported nanocomposites based on a porous organic framework functionalized with 8-hydroxyquinoline and the drug 5-fluorouracil (5-FU@COF-HQ). B16 melanoma mice treated with 5-FU@COF-HQ by intratumoral injection had extensive areas of necrosis or apoptosis compared to control groups, indicating that 5-FU@COF-HQ entered the cancer cells (by endocytosis) and had an inhibitory ability against tumor cells. The system showed a pH-dependent release of 5-fluorouracil in response to the acidic environment of the endosomes due to the presence of a large number of conjugated nitrogen atoms, including quinoline groups and C=N in the organic framework. 5-FU@COF-HQ demonstrated low toxicity and good biocompatibility of COF-HQ in vivo. However, it should be taken into account that these examples employ intratumoral injections for the administration of the particles into the body which strictly limits the application of these formulations. In the other case, authors demonstrate ZIF-8 based carriers to penetrate into tumor tissues of mice through the EPR effect. Wenhe Zhu et al. demonstrated the excellent therapeutic efficacy of MOF particles (ZIF-8) loaded with dihydroartemisin (DHA) to produce a DHA@ZIF-8-NPs nanocomposite. The authors showed that the H22 tumor inhibition coefficient in the group of mice with intravenous DHA@ZIF-8-NPs was higher (76.7%) than in the group with free DHA (49.2%). Moreover, significant cellular necrosis was found in the tumor after treatment with DHA@ZIF-8-NPs. This effective therapeutic effect is mainly due to the EPR effect, the pH-dependent release of dihydroartemisin in response to the acidic tumor microenvironment, and the good protection of the loaded drug in the blood due to ZIF-8 [168]. Jing Wang et al. demonstrated the therapeutic effect of hybrid MOF's (UIO-66-NH2) modified with Prussian blue (Prussian Blue, PB) and loaded with doxorubicin (UIO-66-NH2/PB-DOX) after intravenous administration to animals with cervical carcinoma. DOX release was shown in response to tumor extracellular pH, UIO-66-NH2/PB-DOX significantly inhibited tumor growth, which also appeared to be associated with the synergistic effects of chemotherapy and chemodynamic therapy [163]. Shuxian Meng et al. showed the antitumor efficacy of a multifunctional three-dimensional DDS (magnet@FUGY/DOX) based on the hybridization of a MOF and graphdiin (FUGY), which provides efficient drug release at pH 5.0. The doxorubicin was loaded into FUGY and served as both an anti-cancer drug to treat the tumor and a fluorescent probe for detection of FUGY accumulation site. Magnet@FUGY/DOX after intravenous administration to animals demonstrated significant antitumor efficacy against HeLa tumor with a tumor inhibition ratio of 77.8%. Fluorescence imaging results have shown that magnet@FUGY/DOX can increase tumor uptake of drugs for targeted cancer therapy [159]. Wang et al. reported on combined gene and photodynamic therapy for breast cancer (MCF-7) using ZIF-8 modified with deoxyribozymes known as powerful gene therapy therapeutic agents and the photosensitizer chlorin-Ce6. ZIF-8 nanoparticles degraded in response to acidic extracellular pH with the simultaneous release of deoxyribozymes and chlorin-Ce6. Intravenous administration of the nanocomplex to animals showed their excellent ability to accumulate at the site of the tumor due to the EPR effect. Simultaneous delivery of functional DNA and the Ce6 photosensitizer to the tumor site resulted in deoxyribozymes-mediated inhibition of the transcription factor EGR-1 along with photogenerated cellular apoptosis[170].

Besides the hybrid nature of these carriers, researchers often create additional surface coating to provide the functionality of the particles such as improved selectivity of accumulation in tumors or improved endocytosis process. In this way, nanoparticles comprising a zeolite-imidazole framework (ZIF) loaded with apilimod (Ap) were coated with a solid lipid shell SLN with an embedded pH-responsive linker (L) based on oleylamine (OA) modified with 3-(bromomethyl)-4-methyl-2,5-furandione (MMfu) and polyethylene glycol. Acidic tumor microenvironment causes hydrophilic polyethylene glycol and MMfu removal, leading to hydrophobic OA to be "opened", which increases the uptake of the carriers by cancer cells and accumulation in the tumor. The ZIF@SLN#L nanoparticles induce the production of reactive oxygen species within cancer cells. Ap released from Ap-ZIF@SLN#L also promotes the intracellular generation of reactive oxygen species and lactate dehydrogenase. In vivo experiments using mice with pancreatic tumors demonstrated Ap-

ZIF@SLN#L system significantly reduced the tumor volume and increased the survival rate of animals. In vivo tests using mice with pancreatic tumors showed DDS based on the Ap-ZIF@SLN#L system to reduce the tumor volume and increase the survival rate of animals. At the same time, the authors note that after the administration of the developed particles in animals, there were no histopathological changes in the main target organs (heart, liver, spleen, lungs, kidneys), as well as a normal level of transaminase activity in the blood serum, which characterizes the absence of significant toxic effects [256]. Piaoping Yang et al. developed a nanoplatform based on a zeolite imidazolate framework-8 (ZIF-8) (defined as α-TOS@ZIF-8) loaded with unstable and hydrophobic D-α-tocopherol succinate (α-TOS). The nanocomposite was coated with a hyaluronic acid shell to form the HA/α-TOS@ZIF-8 nanoplatform. In vivo experiments in mice with cervical tumor (U14) demonstrated tumor reduction on the 14th day of the experiment after intravenous administration of HA/α-TOS@ZIF-8. The study confirmed the tumor-specific release of D-α-tocopherol succinate as a result of the destruction of hyaluronic acid in the tumor microenvironment, which led to the degradation of ZIF-8 in the acidic tumor microenvironment with the release of loaded α-TOS. Thus, the HA/α-TOS@ZIF-8 nanoplatform was developed as a tumor-specific drug delivery system, which increased the efficiency of the treatment [132]. Zhang et al. showed effective inhibition of subcutaneous HeLa tumor xenograft after intravenous injection of a pH-responsive CAMEL-R nanocomplex synthesized on the basis of MOFs coated with a HeLa cancer cell membrane for targeted delivery of small interfering RNA (siRNA). The introduction of CAMEL-R demonstrated the inhibition of tumor volume 15 times more effective than the control injection of saline[122]. Tan et al. synthesized nanocomposites (Dox/Cel/MOF@Gel) based on MOF coated with a pH-responsive hydrogel and loaded with doxorubicin and celecoxib (Cel). Intratumoral injection of these nanocomposites demonstrated high efficacy in SCC-9 tumor inhibition in vivo, inducing tumor apoptosis and regulating tumor angiogenesis, due to the synergistic action of DOX and Cel. The efficiency of tumor inhibition after administration of DOX/Cel/MOF@Gel was 4 and 7 times higher compared with the administration of free doxorubicin and celecoxibine, respectively. Such treatment has been found to result in a significant reduction in systemic toxicity and no apparent damage to intact organs [257].

Promising results have been made using additional functionalization of MOF's with inorganic components. Zhang X. et al. reported hypoxia-responsive copper MOF particles (Cu-MOF NPs), which are copper clusters linked by organic ligands loaded with the sonosensitizer chlorin e6 (Ce6). After intravenous injection into the caudal artery, Cu-MOF-Ce6 nanoparticles effectively accumulated deep in the microenvironment of the breast tumor (MCF-7) due to the EPR effect, and tumor hypoxia triggered the degradation of nanoparticles, followed by the release of Cu^{2+} and chlorin e6. Internalized Cu^{2+} reacted with tumor histamine, depleting the latter and reducing Cu^{2+} to Cu^{+}, which subsequently reacted with endogenous H_2O_2 to form cytotoxic hydroxyl radicals (OH). In addition, ultrasonic irradiation (2 W/cm^2) of Cu-MOF-Ce5 showed the best ability to suppress tumor growth in mammary gland [186]. Zeng L. et al. demonstrated the therapeutic efficacy of doxorubicin (DOX) encapsulated in ZIF-8 particles with built-in gold solasters (AuNCs@MOF-DOX nanocomposites) via intravenous administration to laboratory mice in vivo. The acidic microenvironment of a breast tumor led to the degradation of the pH-responsive ZIF-8, which accelerated the release of AuNC and DOX in tumor cells and increased the effectiveness of PDT/chemotherapy [208]. Hai-Liang Zhu et al. synthesized spherical ZIF-8 particles loaded with doxorubicin (DOX) and coated with a biodegradable organic silica shell containing many disulfide bonds acting as a "gatekeeper" that can close or open the silica shell door under the influence of external stimuli. The authors demonstrated efficient accumulation of ZIF-8@DOX@organo-silica nanocomposites in HeLa tumors after intravenous administration to animals and the best therapeutic efficacy (with an inhibition rate of 89.4%). Moreover, necrosis and pathological changes were observed in the tumor zone, which confirmed the excellent therapeutic efficacy of the drug delivery system developed by the authors [166]. Miao Du et al. demonstrated the effective therapeutic ability of MOF particles based on γ-cyclodextrin (γ-CD-MOF) containing graphene quantum dots in the structure to impart fluorescence to the complex and modification with pH-sensitive poly(ethylene

glycol) dimethacrylate (PEGMA), promoting a stimulus-responsive controlled release of doxorubicin from nanocomposite. Aptamer AS1411 was chosen as a targeting agent for tumor cells. In vivo experiments in mice with MCF-7 tumor demonstrated tumor reduction on the 14th day of the experiment after intravenous administration with few side effects after treatment [177]. Quanyan Liu et al. reported biomimetic ZIF-8 nanoparticles doped with iron ions (Fe^{2+}) and loaded with dihydroartemisinin (DHA) exhibiting stimulus-responsive drug release in response to changes in tumor pH. In the acidic microenvironment of the tumor, dihydroartemisinin and ferrous ions supposed to release as a result of the degradation of the organometallic framework. Following intravenous administration of particles to laboratory animals, the combination of the antimalarial drug DHA and Fe^{2+} released from ZIF-8 nanoparticles resulted in a 90.8% reduction in tumor growth in the HepG2 human hepatocellular carcinoma model. Moreover, the nanocomplex showed no apparent hepatic or renal toxicity, indicating excellent biocompatibility [121].

Certain progress has been made in the development of nanomaterials based on calcium carbonate ($CaCO_3$) for the delivery of anticancer drugs. $CaCO_3$-based nanomaterials easily dissolve into Ca^{2+} and CO_2 upon contact with the acidic environment, which enables pH-responsive controlled drug release in the tumor. Usually, calcium carbonate is employed for drug delivery in the form of vaterite due mesoporous structure of the polymorph modification. However, the dissolution rate of calcium carbonate at pH above 6 and even at pH above 5 is low, which is problematic for a wide use of calcium carbonate in such systems. A probable way of $CaCO_3$ particle application is delivery into endosomes of target cells which can be obstructed by the large size of these particles (above 300 nm) and their surface chemistry. Nevertheless, Zhiyu Zhang et al. developed a pH-responsive nanosystem based on calcium carbonate particles conjugated to a methoxy-poly(ethyleneglycol)-block-poly(L-glutamic acid) (mPEG-b-PGA) linker for the delivery of doxorubicin and its controlled release in response to low pH in tumor cells. Intravenous administration of particles to animals with an orthotopic osteosarcoma model led to a slow decrease of DOX level in blood and a significant increase in systemic circulation time, which is probably due to the fact that mineralization of $CaCO_3$ increased the stability of nanoparticles and inhibited DOX leakage during circulation in vivo. CaNP/DOX carriers demonstrated the strongest inhibitory effect on the growth of K7 osteosarcoma as a result of excellent selective accumulation and release of doxorubicin in the acidic tumor microenvironment. The tumor suppression rate of free DOX and CaNP/DOX was 54.7% and 79.8%, respectively [258]. Alternatively, $CaCO_3$ can be employed as a pH-responsive coating which solves both the problem of $CaCO_3$ large size and the problem of low rate dissolution due to the low thickness of the layer. In this way, hybrid carriers consisted of manganese oxide (MnO_2) particles modified with a pH-sensitive layer of $CaCO_3$, small interfering RNA (targeted to the tumor cell receptor PD-L1) and loaded with the photosensitizer indocyanine green (ICG), which has a high potential in photodynamic and photothermal cancer therapy[259]. Systemic administration of these carriers to mice with a Lewis lung cancer model demonstrated an enhanced antitumor response under laser irradiation and a decrease in tumor volume by 9 times relative to control groups.

Thus, pH-responsive systems for targeted drug delivery are of high interest for the treatment of malignant neoplasms. For the design of such systems, nanoparticles based on polymers, MNS, lipids, and metals are most often used. At present, convincing results of in vivo approbation of pH-sensitive systems based on these classes of nanoparticles have been shown, which reflect an increase in the effectiveness of antitumor drugs upon targeted delivery. Each of the classes of compounds used to design pH-responsive targeted DDS's has advantages and limitations due to complex interactions with the body during systemic circulation, penetration through histohematological barriers, as well as specific reactions to the tumor microenvironment and absorption of nanoparticles by cells. The current trend towards more complex and hybrid systems allows for overcoming many barriers limiting our possibilities in cancer therapy. Although clinical tests are not so successful so far due to a range of problems such as poor EPR effect in humans and high activity of the phagocytic mononuclear system, new tremendous work done on the development of new complex systems which widely been tested in vivo on animals give us hope for better results in nearest future.

 doi:10.20944/preprints202305.0289.v1

5. Conclusions

pH-responsive drug delivery is a promising technology as it allows site-specific cargo release by endogenous trigger. Apart from the general advantages of DDSs such as reduction of side effects, delivery of unstable and hydrophobic compounds, etc., pH responsiveness as an endogenous release trigger is an exciting concept. However, there is still a wide range of challenges, the solution of which is currently in the progress. Although the initial concept of pH-responsive DDSs was consistent, the number of problems revealed over the years significantly shifted requirements to drug carriers for pH-responsive delivery. Basic requirements for the carriers include size in the range of 20-200 nm and a negative charge to reduce their interaction with cells during circulation in the blood flow. Based on analysis of MOF particles and 3 most popular model drugs it was shown that ζ-potential is a much more essential parameter of drug carriers in terms of loading capability than surface area, pore volume, and size. Therefore, the developed DDSs should be analyzed considering the particular drug to be delivered. Meta-analysis of different DDS studied in vitro revealed that a high drug release rate, as well as high drug loading capacity, are important to provide the appropriate cytotoxic effect. It means not only the total dose of the drug that is transferred into tumor tissues plays a role but concentration that can be reached within a cell.

The difference in pH between healthy tissues and tumors of about 0.3-0.7 appears to be insufficient to provide a switchable release for the 85% of carriers that rely on a release in response to pH below 6 or even below 5.5. Moreover, extracellular pH within tumors is heterogeneous which represents a difficult task for pH-mediated tumor targeting strategy. Achieving intracellular delivery to endosomes and lysosomes solves this problem, but produces new challenges since the traffic of systemically administrated carriers into endosomes of cancer cells is a multistage task. A particular problem concerns the slow diffusion of carriers from the blood into the parenchyma via the EPR effect in humans.

Intracellular delivery requires additional functionalization to control complex processes of targeted internalization, release, and subsequent endosome escape effect. At the same time, the DDS should provide prolonged circulation time in the blood flow to increase the probability of accumulation in the deceased site and reduce absorption by the mononuclear phagocytic system which impedes features required for effective uptake by cancer cells. This fact drives the researcher to develop even more complex drug carriers capable of changing their properties in the tumor microenvironment such as reversing their charge to improve uptake followed by controlled intracellular release and endosomal escape. Stealth coatings for longer circulation of drug carriers were shown to increase accumulation in target tumors after systemic administration, however, these coatings obstruct other functions of the carriers such as internalization and drug release.

Currently, a variety of barriers and drug bioavailability issues makes the dominant majority of authors rely on a long-term process and expect a release within at least 6 hours. In these regards, today researchers have to search for alternative approaches which will help to avoid problems with the EPR effect or provide effective internalization into cancer cells. Various approaches have been developed to avoid this problem, such as the disintegration of carriers into small components immediately upon entering the tumor or flash release in the vessels surrounding the tumor.

Despite significant success in animal models, results in clinical studies demonstrate poor viability. Although pH-responsive delivery undergoes a crisis of poor EPR effect in humans, the general trend towards increasing complexity of the carrier's structure to combine multiple functions to be performed in a cascade manner, as well as the development of alternative approaches, allows us to hope that new systems will demonstrate success in clinical trials.

Author Contributions: Conceptualization, R.A.V., A.V.E.; formal analysis R.A.V., A.N.I., E.V.L., K.A.T., N.Yu.S.; writing—original draft preparation R.A.V., A.N.I., E.V.L., A.V.E.; visualization, R.A.V., A.V.E.; supervision R.A.V., A.V.E.; funding acquisition A.V.E., All authors have read and agreed to the published version of the manuscript

Funding: The study was supported by the RUSSIAN SCIENTIFIC FOUNDATION grant No. 22-73-10032, https://rscf.ru/project/22-73-10032/

Acknowledgments:

The authors acknowledge Ms. Alexandra Lengert, without whom the article would have been submitted half a year earlier.

Conflicts of Interest: The authors declare no conflict of interest.

References

1. Gadducci, A.; Cosio, S. Neoadjuvant Chemotherapy in Locally Advanced Cervical Cancer: Review of the Literature and Perspectives of Clinical Research. *Anticancer Research* **2020**, *40*, 4819–4828, doi:10.21873/anticanres.14485.

2. Vernousfaderani, E.K.; Akhtari, N.; Rezaei, S.; Rezaee, Y.; Shiranirad, S.; Mashhadi, M.; Hashemi, A.; Khankandi, H.P.; Behzad, S. Resveratrol and Colorectal Cancer: A Molecular Approach to Clinical Researches. *Current Topics in Medicinal Chemistry* **2021**, *21*, 2634–2646, doi:10.2174/1568026621666211105093658.

3. Vogl, U.M.; Beer, T.M.; Davis, I.D.; Shore, N.D.; Sweeney, C.J.; Ost, P.; Attard, G.; Bossi, A.; de Bono, J.; Drake, C.G.; et al. Lack of consensus identifies important areas for future clinical research: Advanced Prostate Cancer Consensus Conference (APCCC) 2019 findings. *European Journal of Cancer* **2022**, *160*, 24–60, doi:10.1016/j.ejca.2021.09.036.

4. Hu, Y.; Sun, Y.; Wan, C.; Dai, X.; Wu, S.; Lo, P.-C.; Huang, J.; Lovell, J.F.; Jin, H.; Yang, K. Microparticles: biogenesis, characteristics and intervention therapy for cancers in preclinical and clinical research. *Journal of Nanobiotechnology* **2022**, *20*, 189, doi:10.1186/s12951-022-01358-0.

5. Sarmento-Ribeiro, A.B.; Scorilas, A.; Gonçalves, A.C.; Efferth, T.; Trougakos, I.P. The emergence of drug resistance to targeted cancer therapies: Clinical evidence. *Drug Resistance Updates* **2019**, *47*, 100646, doi:10.1016/j.drup.2019.100646.

6. Sharma, P.C.; Bansal, K.K.; Sharma, A.; Sharma, D.; Deep, A. Thiazole-containing compounds as therapeutic targets for cancer therapy. *European Journal of Medicinal Chemistry* **2020**, *188*, 112016, doi:10.1016/j.ejmech.2019.112016.

7. Zhang, Z.; Zhou, L.; Xie, N.; Nice, E.C.; Zhang, T.; Cui, Y.; Huang, C. Overcoming cancer therapeutic bottleneck by drug repurposing. *Signal Transduction and Targeted Therapy* **2020**, *5*, 113, doi:10.1038/s41392-020-00213-8.

8. Leinwand, J.; Miller, G. Regulation and modulation of antitumor immunity in pancreatic cancer. *Nature Immunology* **2020**, *21*, 1152–1159, doi:10.1038/s41590-020-0761-y.

9. Moreno Ayala, M.A.; Li, Z.; DuPage, M. Treg programming and therapeutic reprogramming in cancer. *Immunology* **2019**, *157*, 198–209, doi:10.1111/imm.13058.

10. Alvandi, N.; Rajabnejad, M.; Taghvaei, Z.; Esfandiari, N. New generation of viral nanoparticles for targeted drug delivery in cancer therapy. *Journal of Drug Targeting* **2022**, *30*, 151–165, doi:10.1080/1061186X.2021.1949600.

11. Ghosh, B.; Biswas, S. Polymeric micelles in cancer therapy: State of the art. *Journal of Controlled Release* **2021**, *332*, 127–147, doi:10.1016/j.jconrel.2021.02.016.

12. Yang, G.; Liu, Y.; Wang, H.; Wilson, R.; Hui, Y.; Yu, L.; Wibowo, D.; Zhang, C.; Whittaker, A.K.; Middelberg, A.P.J.; et al. Bioinspired Core–Shell Nanoparticles for Hydrophobic Drug Delivery. *Angewandte Chemie International Edition* **2019**, *58*, 14357–14364, doi:10.1002/anie.201908357.

13. Skotland, T.; Iversen, T.G.; Llorente, A.; Sandvig, K. Biodistribution, pharmacokinetics and excretion studies of intravenously injected nanoparticles and extracellular vesicles: Possibilities and challenges. *Advanced Drug Delivery Reviews* **2022**, *186*, 114326, doi:10.1016/j.addr.2022.114326.

14. Sindeeva, O.A.; Verkhovskii, R.A.; Abdurashitov, A.S.; Voronin, D. V; Gusliakova, O.I.; Kozlova, A.A.; Mayorova, O.A.; Ermakov, A. V; Lengert, E. V; Navolokin, N.A.; et al. Effect of Systemic Polyelectrolyte Microcapsule Administration on the Blood Flow Dynamics of Vital Organs. *ACS Biomaterials Science & Engineering* **2020**, doi:10.1021/acsbiomaterials.9b01669.

15. Fam, S.Y.; Chee, C.F.; Yong, C.Y.; Ho, K.L.; Mariatulqabtiah, A.R.; Tan, W.S. Stealth Coating of Nanoparticles in Drug-Delivery Systems. *Nanomaterials* **2020**, *10*, 787, doi:10.3390/nano10040787.

16. Verkhovskii, R.; Ermakov, A.; Sindeeva, O.; Prikhozhdenko, E.; Kozlova, A.; Grishin, O.; Makarkin, M.; Gorin, D.; Bratashov, D. Effect of Size on Magnetic Polyelectrolyte Microcapsules Behavior: Biodistribution, Circulation Time, Interactions with Blood Cells and Immune System. *Pharmaceutics* **2021**, *13*, 2147, doi:10.3390/pharmaceutics13122147.

17. D'Angelo, N.A.; Noronha, M.A.; Kurnik, I.S.; Câmara, M.C.C.; Vieira, J.M.; Abrunhosa, L.; Martins, J.T.; Alves, T.F.R.; Tundisi, L.L.; Ataide, J.A.; et al. Curcumin encapsulation in nanostructures for cancer therapy: A 10-year overview. *International Journal of Pharmaceutics* **2021**, *604*, 120534, doi:10.1016/j.ijpharm.2021.120534.

18. Valencia-Lazcano, A.A.; Hassan, D.; Pourmadadi, M.; Shamsabadipour, A.; Behzadmehr, R.; Rahdar, A.; Medina, D.I.; Díez-Pascual, A.M. 5-Fluorouracil nano-delivery systems as a cutting-edge for cancer therapy. *European Journal of Medicinal Chemistry* **2023**, *246*, 114995, doi:10.1016/j.ejmech.2022.114995.

19. Ibrahim, M.; Abuwatfa, W.H.; Awad, N.S.; Sabouni, R.; Husseini, G.A. Encapsulation, Release, and Cytotoxicity of Doxorubicin Loaded in Liposomes, Micelles, and Metal-Organic Frameworks: A Review. *Pharmaceutics* **2022**, *14*, 254, doi:10.3390/pharmaceutics14020254.

20. Moghassemi, S.; Dadashzadeh, A.; Azevedo, R.B.; Feron, O.; Amorim, C.A. Photodynamic cancer therapy using liposomes as an advanced vesicular photosensitizer delivery system. *Journal of Controlled Release* **2021**, *339*, 75–90, doi:10.1016/j.jconrel.2021.09.024.

21. Ermakov, A. V.; Verkhovskii, R.A.; Babushkina, I. V.; Trushina, D.B.; Inozemtseva, O.A.; Lukyanets, E.A.; Ulyanov, V.J.; Gorin, D.A.; Belyakov, S.; Antipina, M.N. In Vitro Bioeffects of Polyelectrolyte Multilayer Microcapsules Post-Loaded with Water-Soluble Cationic Photosensitizer. *Pharmaceutics* **2020**, *12*, 610, doi:10.3390/pharmaceutics12070610.

22. Li, F.; Qin, Y.; Lee, J.; Liao, H.; Wang, N.; Davis, T.P.; Qiao, R.; Ling, D. Stimuli-responsive nano-assemblies for remotely controlled drug delivery. *Journal of Controlled Release* **2020**, *322*, 566–592, doi:10.1016/j.jconrel.2020.03.051.

23. Li, L.; Yang, W.-W.; Xu, D.-G. Stimuli-responsive nanoscale drug delivery systems for cancer therapy. *Journal of Drug Targeting* **2019**, *27*, 423–433, doi:10.1080/1061186X.2018.1519029.

24. Andrade, F.; Roca-Melendres, M.M.; Durán-Lara, E.F.; Rafael, D.; Schwartz, S. Stimuli-Responsive Hydrogels for Cancer Treatment: The Role of pH, Light, Ionic Strength and Magnetic Field. *Cancers* **2021**, *13*, 1164, doi:10.3390/cancers13051164.

25. Khan, A.N.; Ermakov, A. V.; Saunders, T.; Giddens, H.; Gould, D.; Sukhorukov, G.; Hao, Y. Electrical Characterization of Micron-Sized Chambers Used as a Depot for Drug Delivery. *IEEE Sensors Journal* **2022**, *22*, 18162–18169, doi:10.1109/JSEN.2022.3194717.

26. Islam, R.; Maeda, H.; Fang, J. Factors affecting the dynamics and heterogeneity of the EPR effect: pathophysiological and pathoanatomic features, drug formulations and physicochemical factors. *Expert Opinion on Drug Delivery* **2022**, *19*, 199–212, doi:10.1080/17425247.2021.1874916.

27. Yoo, J.; Park, C.; Yi, G.; Lee, D.; Koo, H. Active Targeting Strategies Using Biological Ligands for Nanoparticle Drug Delivery Systems. *Cancers* **2019**, *11*, 640, doi:10.3390/cancers11050640.

28. Jiang, Z.; Guan, J.; Qian, J.; Zhan, C. Peptide ligand-mediated targeted drug delivery of nanomedicines. *Biomaterials Science* **2019**, *7*, 461–471, doi:10.1039/C8BM01340C.

29. Jin, Q.; Deng, Y.; Chen, X.; Ji, J. Rational Design of Cancer Nanomedicine for Simultaneous Stealth Surface and Enhanced Cellular Uptake. *ACS Nano* **2019**, acsnano.8b07746, doi:10.1021/acsnano.8b07746.

30. Liu, Y.-L.; Chen, D.; Shang, P.; Yin, D.-C. A review of magnet systems for targeted drug delivery. *Journal of Controlled Release* **2019**, *302*, 90–104, doi:10.1016/j.jconrel.2019.03.031.

31. Verkhovskii, R.; Ermakov, A.; Grishin, O.; Makarkin, M.A.; Kozhevnikov, I.; Makhortov, M.; Kozlova, A.; Salem, S.; Tuchin, V.; Bratashov, D. The Influence of Magnetic Composite Capsule Structure and Size on Their Trapping Efficiency in the Flow. *Molecules* **2022**, *27*, 6073, doi:10.3390/molecules27186073.

32. Manzoor, A.A.; Lindner, L.H.; Landon, C.D.; Park, J.-Y.; Simnick, A.J.; Dreher, M.R.; Das, S.; Hanna, G.; Park, W.; Chilkoti, A.; et al. Overcoming Limitations in Nanoparticle Drug Delivery: Triggered, Intravascular Release to Improve Drug Penetration into Tumors. *Cancer Research* **2012**, *72*, 5566–5575, doi:10.1158/0008-5472.CAN-12-1683.

33. Racca, L.; Cauda, V. Remotely Activated Nanoparticles for Anticancer Therapy. *Nano-Micro Letters* **2021**, *13*, 11, doi:10.1007/s40820-020-00537-8.

34. Mirvakili, S.M.; Langer, R. Wireless on-demand drug delivery. *Nature Electronics* **2021**, *4*, 464–477, doi:10.1038/s41928-021-00614-9.

35. Kaczmarek, K.; Hornowski, T.; Antal, I.; Timko, M.; Józefczak, A. Magneto-ultrasonic heating with

nanoparticles. *Journal of Magnetism and Magnetic Materials* **2019**, *474*, 400–405, doi:10.1016/j.jmmm.2018.11.062.

36. Gelmi, A.; Schutt, C.E. Stimuli-Responsive Biomaterials: Scaffolds for Stem Cell Control. *Advanced Healthcare Materials* **2021**, *10*, 2001125, doi:10.1002/adhm.202001125.

37. Tang, H.; Zhao, W.; Yu, J.; Li, Y.; Zhao, C. Recent Development of pH-Responsive Polymers for Cancer Nanomedicine. *Molecules* **2018**, *24*, 4, doi:10.3390/molecules24010004.

38. Sadhukhan, P.; Kundu, M.; Chatterjee, S.; Ghosh, N.; Manna, P.; Das, J.; Sil, P.C. Targeted delivery of quercetin via pH-responsive zinc oxide nanoparticles for breast cancer therapy. *Materials Science and Engineering: C* **2019**, *100*, 129–140, doi:10.1016/j.msec.2019.02.096.

39. Liberti, M. V.; Locasale, J.W. The Warburg Effect: How Does it Benefit Cancer Cells? *Trends in Biochemical Sciences* **2016**, *41*, 211–218, doi:10.1016/j.tibs.2015.12.001.

40. Zhuo, S.; Zhang, F.; Yu, J.; Zhang, X.; Yang, G.; Liu, X. pH-Sensitive Biomaterials for Drug Delivery. *Molecules* **2020**, *25*, 5649, doi:10.3390/molecules25235649.

41. AlSawaftah, N.M.; Awad, N.S.; Pitt, W.G.; Husseini, G.A. pH-Responsive Nanocarriers in Cancer Therapy. *Polymers* **2022**, *14*, 936, doi:10.3390/polym14050936.

42. Kanamala, M.; Wilson, W.R.; Yang, M.; Palmer, B.D.; Wu, Z. Mechanisms and biomaterials in pH-responsive tumour targeted drug delivery: A review. *Biomaterials* **2016**, *85*, 152–167, doi:10.1016/j.biomaterials.2016.01.061.

43. Zhu, Y.-J.; Chen, F. pH-Responsive Drug-Delivery Systems. *Chemistry - An Asian Journal* **2015**, *10*, 284–305, doi:10.1002/asia.201402715.

44. Mu, Y.; Gong, L.; Peng, T.; Yao, J.; Lin, Z. Advances in pH-responsive drug delivery systems. *OpenNano* **2021**, *5*, 100031, doi:10.1016/j.onano.2021.100031.

45. Li, Z.; Huang, J.; Wu, J. pH-Sensitive nanogels for drug delivery in cancer therapy. *Biomaterials Science* **2021**, *9*, 574–589, doi:10.1039/D0BM01729A.

46. Wilhelm, S.; Tavares, A.J.; Dai, Q.; Ohta, S.; Audet, J.; Dvorak, H.F.; Chan, W.C.W. Analysis of nanoparticle delivery to tumours. *Nature Reviews Materials* **2016**, *1*, 16014, doi:10.1038/natrevmats.2016.14.

47. Parra-Nieto, J.; del Cid, M.A.G.; Cárcer, I.A.; Baeza, A. Inorganic Porous Nanoparticles for Drug Delivery in Antitumoral Therapy. *Biotechnology Journal* **2021**, *16*, 2000150, doi:10.1002/biot.202000150.

48. Danhier, F. To exploit the tumor microenvironment: Since the EPR effect fails in the clinic, what is the future of nanomedicine? *Journal of Controlled Release* **2016**, *244*, 108–121, doi:10.1016/j.jconrel.2016.11.015.

49. Danhier, F.; Feron, O.; Préat, V. To exploit the tumor microenvironment: Passive and active tumor targeting of nanocarriers for anti-cancer drug delivery. *Journal of Controlled Release* **2010**, *148*, 135–146,

doi:10.1016/j.jconrel.2010.08.027.

50. Maso, K.; Grigoletto, A.; Vicent, M.J.; Pasut, G. Molecular platforms for targeted drug delivery. In; 2019; pp. 1–50.

51. Mitchell, M.J.; Billingsley, M.M.; Haley, R.M.; Wechsler, M.E.; Peppas, N.A.; Langer, R. Engineering precision nanoparticles for drug delivery. *Nature Reviews Drug Discovery* **2021**, *20*, 101–124, doi:10.1038/s41573-020-0090-8.

52. Gschwind, A.; Fischer, O.M.; Ullrich, A. The discovery of receptor tyrosine kinases: targets for cancer therapy. *Nature Reviews Cancer* **2004**, *4*, 361–370, doi:10.1038/nrc1360.

53. Krause, D.S.; Van Etten, R.A. Tyrosine Kinases as Targets for Cancer Therapy. *New England Journal of Medicine* **2005**, *353*, 172–187, doi:10.1056/NEJMra044389.

54. Muhammad, N.; Bhattacharya, S.; Steele, R.; Ray, R.B. Anti-miR-203 suppresses ER-positive breast cancer growth and stemness by targeting SOCS3. *Oncotarget* **2016**, *7*, 58595–58605, doi:10.18632/oncotarget.11193.

55. Rupaimoole, R.; Slack, F.J. MicroRNA therapeutics: towards a new era for the management of cancer and other diseases. *Nature Reviews Drug Discovery* **2017**, *16*, 203–222, doi:10.1038/nrd.2016.246.

56. Singh, S. V; Ajay, A.K.; Mohammad, N.; Malvi, P.; Chaube, B.; Meena, A.S.; Bhat, M.K. Proteasomal inhibition sensitizes cervical cancer cells to mitomycin C-induced bystander effect: the role of tumor microenvironment. *Cell Death & Disease* **2015**, *6*, e1934–e1934, doi:10.1038/cddis.2015.292.

57. Soave, C.L.; Guerin, T.; Liu, J.; Dou, Q.P. Targeting the ubiquitin-proteasome system for cancer treatment: discovering novel inhibitors from nature and drug repurposing. *Cancer and Metastasis Reviews* **2017**, *36*, 717–736, doi:10.1007/s10555-017-9705-x.

58. Lee, S.-H.; Griffiths, J.R. How and Why Are Cancers Acidic? Carbonic Anhydrase IX and the Homeostatic Control of Tumour Extracellular pH. *Cancers* **2020**, *12*, 1616, doi:10.3390/cancers12061616.

59. Tan, J.; Li, H.; Hu, X.; Abdullah, R.; Xie, S.; Zhang, L.; Zhao, M.; Luo, Q.; Li, Y.; Sun, Z.; et al. Size-Tunable Assemblies Based on Ferrocene-Containing DNA Polymers for Spatially Uniform Penetration. *Chem* **2019**, *5*, 1775–1792, doi:10.1016/j.chempr.2019.05.024.

60. Cabral, H.; Matsumoto, Y.; Mizuno, K.; Chen, Q.; Murakami, M.; Kimura, M.; Terada, Y.; Kano, M.R.; Miyazono, K.; Uesaka, M.; et al. Accumulation of sub-100 nm polymeric micelles in poorly permeable tumours depends on size. *Nature Nanotechnology* **2011**, *6*, 815–823, doi:10.1038/nnano.2011.166.

61. RUSU, V.; NG, C.; WILKE, M.; TIERSCH, B.; FRATZL, P.; PETER, M. Size-controlled hydroxyapatite nanoparticles as self-organized organic?inorganic composite materials. *Biomaterials* **2005**, *26*, 5414–5426, doi:10.1016/j.biomaterials.2005.01.051.

62. Abri Aghdam, M.; Bagheri, R.; Mosafer, J.; Baradaran, B.; Hashemzaei, M.; Baghbanzadeh, A.; de la Guardia, M.; Mokhtarzadeh, A. Recent advances on thermosensitive and pH-sensitive liposomes

employed in controlled release. *Journal of Controlled Release* **2019**, *315*, 1–22, doi:10.1016/j.jconrel.2019.09.018.

63. Han, Z.; Wang, P.; Mao, G.; Yin, T.; Zhong, D.; Yiming, B.; Hu, X.; Jia, Z.; Nian, G.; Qu, S.; et al. Dual pH-Responsive Hydrogel Actuator for Lipophilic Drug Delivery. *ACS Applied Materials & Interfaces* **2020**, *12*, 12010–12017, doi:10.1021/acsami.9b21713.

64. Yan, T.; He, J.; Liu, R.; Liu, Z.; Cheng, J. Chitosan capped pH-responsive hollow mesoporous silica nanoparticles for targeted chemo-photo combination therapy. *Carbohydrate Polymers* **2020**, *231*, 115706, doi:10.1016/j.carbpol.2019.115706.

65. Zeng, X.; Liu, G.; Tao, W.; Ma, Y.; Zhang, X.; He, F.; Pan, J.; Mei, L.; Pan, G. A Drug-Self-Gated Mesoporous Antitumor Nanoplatform Based on pH-Sensitive Dynamic Covalent Bond. *Advanced Functional Materials* **2017**, *27*, 1605985, doi:10.1002/adfm.201605985.

66. Wen, J.; Yang, K.; Liu, F.; Li, H.; Xu, Y.; Sun, S. Diverse gatekeepers for mesoporous silica nanoparticle based drug delivery systems. *Chemical Society Reviews* **2017**, *46*, 6024–6045, doi:10.1039/C7CS00219J.

67. Liu, Y.; Wang, W.; Yang, J.; Zhou, C.; Sun, J. pH-sensitive polymeric micelles triggered drug release for extracellular and intracellular drug targeting delivery. *Asian Journal of Pharmaceutical Sciences* **2013**, *8*, 159–167, doi:10.1016/j.ajps.2013.07.021.

68. Biswas, A.K.; Islam, M.R.; Choudhury, Z.S.; Mostafa, A.; Kadir, M.F. Nanotechnology based approaches in cancer therapeutics. *Advances in Natural Sciences: Nanoscience and Nanotechnology* **2014**, *5*, 043001, doi:10.1088/2043-6262/5/4/043001.

69. Wang, L.; Hu, C.; Shao, L. The antimicrobial activity of nanoparticles: present situation and prospects for the future. *International Journal of Nanomedicine* **2017**, *Volume 12*, 1227–1249, doi:10.2147/IJN.S121956.

70. Rodzinski, A.; Guduru, R.; Liang, P.; Hadjikhani, A.; Stewart, T.; Stimphil, E.; Runowicz, C.; Cote, R.; Altman, N.; Datar, R.; et al. Targeted and controlled anticancer drug delivery and release with magnetoelectric nanoparticles. *Scientific Reports* **2016**, *6*, 20867, doi:10.1038/srep20867.

71. Zhang, M.; Chen, X.; Li, C.; Shen, X. Charge-reversal nanocarriers: An emerging paradigm for smart cancer nanomedicine. *Journal of Controlled Release* **2020**, *319*, 46–62, doi:10.1016/j.jconrel.2019.12.024.

72. Albanese, A.; Chan, W.C.W. Effect of Gold Nanoparticle Aggregation on Cell Uptake and Toxicity. *ACS Nano* **2011**, *5*, 5478–5489, doi:10.1021/nn2007496.

73. Sharma, V.K. Aggregation and toxicity of titanium dioxide nanoparticles in aquatic environment—A Review. *Journal of Environmental Science and Health, Part A* **2009**, *44*, 1485–1495, doi:10.1080/10934520903263231.

74. Morarasu, S.; Morarasu, B.C.; Ghiarasim, R.; Coroaba, A.; Tiron, C.; Iliescu, R.; Dimofte, G.-M. Targeted Cancer Therapy via pH-Functionalized Nanoparticles: A Scoping Review of Methods and Outcomes. *Gels* **2022**, *8*, 232, doi:10.3390/gels8040232.

75. Kallinowski, F.; Vaupel, P. Factors governing hyperthermia-induced pH changes in Yoshida sarcomas. *International Journal of Hyperthermia* **1989**, *5*, 641–652, doi:10.3109/02656738909140487.

76. Swietach, P.; Patiar, S.; Supuran, C.T.; Harris, A.L.; Vaughan-Jones, R.D. The Role of Carbonic Anhydrase 9 in Regulating Extracellular and Intracellular pH in Three-dimensional Tumor Cell Growths. *Journal of Biological Chemistry* **2009**, *284*, 20299–20310, doi:10.1074/jbc.M109.006478.

77. Swietach, P.; Wigfield, S.; Cobden, P.; Supuran, C.T.; Harris, A.L.; Vaughan-Jones, R.D. Tumor-associated Carbonic Anhydrase 9 Spatially Coordinates Intracellular pH in Three-dimensional Multicellular Growths. *Journal of Biological Chemistry* **2008**, *283*, 20473–20483, doi:10.1074/jbc.M801330200.

78. Hao, G.; Xu, Z.P.; Li, L. Manipulating extracellular tumour pH: an effective target for cancer therapy. *RSC Advances* **2018**, *8*, 22182–22192, doi:10.1039/C8RA02095G.

79. Naeslund, J.; Swenson, K.-E. Investigations on the pH of Malignant Tumours in Mice and Humans after the Administration of Glucose. *Acta Obstetricia et Gynecologica Scandinavica* **1953**, *32*, 359–367, doi:10.3109/00016345309157588.

80. Ashby, B.S. pH STUDIES IN HUMAN MALIGNANT TUMOURS. *The Lancet* **1966**, *288*, 312–315, doi:10.1016/S0140-6736(66)92598-0.

81. Pampus, F. Die Wasserstoffionenkonzentration des Hirngewebes bei raumfordernden intracraniellen Prozessen. *Acta Neurochirurgica* **1963**, *11*, 305–318, doi:10.1007/BF01402010.

82. Mürdter, T.E.; Friedel, G.; Backman, J.T.; McClellan, M.; Schick, M.; Gerken, M.; Bosslet, K.; Fritz, P.; Toomes, H.; Kroemer, H.K.; et al. Dose Optimization of a Doxorubicin Prodrug (HMR 1826) in Isolated Perfused Human Lungs: Low Tumor pH Promotes Prodrug Activation by β-Glucuronidase. *Journal of Pharmacology and Experimental Therapeutics* **2002**, *301*, 223–228, doi:10.1124/jpet.301.1.223.

83. Van Den Berg, A.P.; Wike-Hooley, J.L.; Van Den Berg-Block, A.F.; Van Der Zee, J.; Reinhold, H.S. Tumour pH in human mammary carcinoma. *European Journal of Cancer and Clinical Oncology* **1982**, *18*, 457–462, doi:10.1016/0277-5379(82)90114-6.

84. Thistlethwaite, A.J.; Leeper, D.B.; Moylan, D.J.; Nerlinger, R.E. pH distribution in human tumors. *International Journal of Radiation Oncology*Biology*Physics* **1985**, *11*, 1647–1652, doi:10.1016/0360-3016(85)90217-2.

85. Wike-Hooley, J.L.; van den Berg, A.P.; van der Zee, J.; Reinhold, H.S. Human tumour pH and its variation. *European Journal of Cancer and Clinical Oncology* **1985**, *21*, 785–791, doi:10.1016/0277-5379(85)90216-0.

86. Webb, B.A.; Chimenti, M.; Jacobson, M.P.; Barber, D.L. Dysregulated pH: a perfect storm for cancer progression. *Nature Reviews Cancer* **2011**, *11*, 671–677, doi:10.1038/nrc3110.

87. Aoki, A.; Akaboshi, H.; Ogura, T.; Aikawa, T.; Kondo, T.; Tobori, N.; Yuasa, M. Preparation of pH-sensitive Anionic Liposomes Designed for Drug Delivery System (DDS) Application. *Journal of Oleo*

Science **2015**, *64*, 233–242, doi:10.5650/jos.ess14157.

88. Jing, Z.; Wang, X.; Li, N.; Sun, Z.; Zhang, D.; Zhou, L.; Yin, F.; Jia, Q.; Wang, M.; Chu, Y.; et al. Ultrasound-guided percutaneous metal-organic frameworks based codelivery system of doxorubicin/acetazolamide for hepatocellular carcinoma therapy. *Clinical and Translational Medicine* **2021**, *11*, doi:10.1002/ctm2.600.

89. Yuba, E.; Sugahara, Y.; Yoshizaki, Y.; Shimizu, T.; Kasai, M.; Udaka, K.; Kono, K. Carboxylated polyamidoamine dendron-bearing lipid-based assemblies for precise control of intracellular fate of cargo and induction of antigen-specific immune responses. *Biomaterials Science* **2021**, *9*, 3076–3089, doi:10.1039/D0BM01813A.

90. Kanamala, M.; Palmer, B.D.; Ghandehari, H.; Wilson, W.R.; Wu, Z. PEG-Benzaldehyde-Hydrazone-Lipid Based PEG-Sheddable pH-Sensitive Liposomes: Abilities for Endosomal Escape and Long Circulation. *Pharmaceutical Research* **2018**, *35*, 154, doi:10.1007/s11095-018-2429-y.

91. Rayamajhi, S.; Marchitto, J.; Nguyen, T.D.T.; Marasini, R.; Celia, C.; Aryal, S. pH-responsive cationic liposome for endosomal escape mediated drug delivery. *Colloids and Surfaces B: Biointerfaces* **2020**, *188*, 110804, doi:10.1016/j.colsurfb.2020.110804.

92. Kermaniyan, S.S.; Chen, M.; Zhang, C.; Smith, S.A.; Johnston, A.P.R.; Such, C.; Such, G.K. Understanding the Biological Interactions of pH-Swellable Nanoparticles. *Macromolecular Bioscience* **2022**, *22*, 2100445, doi:10.1002/mabi.202100445.

93. Ramírez-García, P.D.; Retamal, J.S.; Shenoy, P.; Imlach, W.; Sykes, M.; Truong, N.; Constandil, L.; Pelissier, T.; Nowell, C.J.; Khor, S.Y.; et al. A pH-responsive nanoparticle targets the neurokinin 1 receptor in endosomes to prevent chronic pain. *Nature Nanotechnology* **2019**, *14*, 1150–1159, doi:10.1038/s41565-019-0568-x.

94. Du Rietz, H.; Hedlund, H.; Wilhelmson, S.; Nordenfelt, P.; Wittrup, A. Imaging small molecule-induced endosomal escape of siRNA. *Nature Communications* **2020**, *11*, 1809, doi:10.1038/s41467-020-15300-1.

95. Kelly, I.B.; Fletcher, R.B.; McBride, J.R.; Weiss, S.M.; Duvall, C.L. Tuning Composition of Polymer and Porous Silicon Composite Nanoparticles for Early Endosome Escape of Anti-microRNA Peptide Nucleic Acids. *ACS Applied Materials & Interfaces* **2020**, *12*, 39602–39611, doi:10.1021/acsami.0c05827.

96. Ding, H.; Tan, P.; Fu, S.; Tian, X.; Zhang, H.; Ma, X.; Gu, Z.; Luo, K. Preparation and application of pH-responsive drug delivery systems. *Journal of Controlled Release* **2022**, *348*, 206–238, doi:10.1016/j.jconrel.2022.05.056.

97. Kay, M.A.; Glorioso, J.C.; Naldini, L. Viral vectors for gene therapy: the art of turning infectious agents into vehicles of therapeutics. *Nature Medicine* **2001**, *7*, 33–40, doi:10.1038/83324.

98. Lagache, T.; Danos, O.; Holcman, D. Modeling the Step of Endosomal Escape during Cell Infection by a Nonenveloped Virus. *Biophysical Journal* **2012**, *102*, 980–989, doi:10.1016/j.bpj.2011.12.037.

99. Stewart, M.P.; Lorenz, A.; Dahlman, J.; Sahay, G. Challenges in carrier-mediated intracellular delivery: moving beyond endosomal barriers. *WIREs Nanomedicine and Nanobiotechnology* **2016**, *8*, 465–478,

doi:10.1002/wnan.1377.

100. Lächelt, U.; Wagner, E. Nucleic Acid Therapeutics Using Polyplexes: A Journey of 50 Years (and Beyond). *Chemical Reviews* **2015**, *115*, 11043–11078, doi:10.1021/cr5006793.

101. Varkouhi, A.K.; Scholte, M.; Storm, G.; Haisma, H.J. Endosomal escape pathways for delivery of biologicals. *Journal of Controlled Release* **2011**, *151*, 220–228, doi:10.1016/j.jconrel.2010.11.004.

102. Ahmad, A.; Khan, J.M.; Haque, S. Strategies in the design of endosomolytic agents for facilitating endosomal escape in nanoparticles. *Biochimie* **2019**, *160*, 61–75, doi:10.1016/j.biochi.2019.02.012.

103. Jin, Y.; Wang, H.; Yi, K.; Lv, S.; Hu, H.; Li, M.; Tao, Y. Applications of Nanobiomaterials in the Therapy and Imaging of Acute Liver Failure. *Nano-Micro Letters* **2021**, *13*, 25, doi:10.1007/s40820-020-00550-x.

104. Dai, Q.; Wilhelm, S.; Ding, D.; Syed, A.M.; Sindhwani, S.; Zhang, Y.; Chen, Y.Y.; MacMillan, P.; Chan, W.C.W. Quantifying the Ligand-Coated Nanoparticle Delivery to Cancer Cells in Solid Tumors. *ACS Nano* **2018**, *12*, 8423–8435, doi:10.1021/acsnano.8b03900.

105. Deng, H.; Liu, J.; Zhao, X.; Zhang, Y.; Liu, J.; Xu, S.; Deng, L.; Dong, A.; Zhang, J. PEG- b -PCL Copolymer Micelles with the Ability of pH-Controlled Negative-to-Positive Charge Reversal for Intracellular Delivery of Doxorubicin. *Biomacromolecules* **2014**, *15*, 4281–4292, doi:10.1021/bm501290t.

106. Maeda, H.; Nakamura, H.; Fang, J. The EPR effect for macromolecular drug delivery to solid tumors: Improvement of tumor uptake, lowering of systemic toxicity, and distinct tumor imaging in vivo. *Advanced Drug Delivery Reviews* **2013**, *65*, 71–79, doi:10.1016/j.addr.2012.10.002.

107. Bertrand, N.; Wu, J.; Xu, X.; Kamaly, N.; Farokhzad, O.C. Cancer nanotechnology: The impact of passive and active targeting in the era of modern cancer biology. *Advanced Drug Delivery Reviews* **2014**, *66*, 2–25, doi:10.1016/j.addr.2013.11.009.

108. Hatakeyama, H.; Ito, E.; Akita, H.; Oishi, M.; Nagasaki, Y.; Futaki, S.; Harashima, H. A pH-sensitive fusogenic peptide facilitates endosomal escape and greatly enhances the gene silencing of siRNA-containing nanoparticles in vitro and in vivo. *Journal of Controlled Release* **2009**, *139*, 127–132, doi:10.1016/j.jconrel.2009.06.008.

109. Remaut, K.; Lucas, B.; Braeckmans, K.; Demeester, J.; De Smedt, S.C. Pegylation of liposomes favours the endosomal degradation of the delivered phosphodiester oligonucleotides. *Journal of Controlled Release* **2007**, *117*, 256–266, doi:10.1016/j.jconrel.2006.10.029.

110. Li, Y.; Liu, R.; Yang, J.; Shi, Y.; Ma, G.; Zhang, Z.; Zhang, X. Enhanced retention and anti-tumor efficacy of liposomes by changing their cellular uptake and pharmacokinetics behavior. *Biomaterials* **2015**, *41*, 1–14, doi:10.1016/j.biomaterials.2014.11.010.

111. Hatakeyama, H.; Akita, H.; Harashima, H. The Polyethyleneglycol Dilemma: Advantage and Disadvantage of PEGylation of Liposomes for Systemic Genes and Nucleic Acids Delivery to Tumors. *Biological and Pharmaceutical Bulletin* **2013**, *36*, 892–899, doi:10.1248/bpb.b13-00059.

112. Gao, Z.; Zhang, L.; Sun, Y. Nanotechnology applied to overcome tumor drug resistance. *Journal of Controlled Release* **2012**, *162*, 45–55, doi:10.1016/j.jconrel.2012.05.051.

113. Fleige, E.; Quadir, M.A.; Haag, R. Stimuli-responsive polymeric nanocarriers for the controlled transport of active compounds: Concepts and applications. *Advanced Drug Delivery Reviews* **2012**, *64*, 866–884, doi:10.1016/j.addr.2012.01.020.

114. Ganta, S.; Devalapally, H.; Shahiwala, A.; Amiji, M. A review of stimuli-responsive nanocarriers for drug and gene delivery. *Journal of Controlled Release* **2008**, *126*, 187–204, doi:10.1016/j.jconrel.2007.12.017.

115. Jing, X.; Hu, H.; Sun, Y.; Yu, B.; Cong, H.; Shen, Y. The Intracellular and Extracellular Microenvironment of Tumor Site: The Trigger of Stimuli-Responsive Drug Delivery Systems. *Small Methods* **2022**, *6*, 2101437, doi:10.1002/smtd.202101437.

116. Sindhwani, S.; Syed, A.M.; Ngai, J.; Kingston, B.R.; Maiorino, L.; Rothschild, J.; MacMillan, P.; Zhang, Y.; Rajesh, N.U.; Hoang, T.; et al. The entry of nanoparticles into solid tumours. *Nature Materials* **2020**, *19*, 566–575, doi:10.1038/s41563-019-0566-2.

117. Jain, R.K.; Stylianopoulos, T. Delivering nanomedicine to solid tumors. *Nature Reviews Clinical Oncology* **2010**, *7*, 653–664, doi:10.1038/nrclinonc.2010.139.

118. Nichols, J.W.; Bae, Y.H. EPR: Evidence and fallacy. *Journal of Controlled Release* **2014**, *190*, 451–464, doi:10.1016/j.jconrel.2014.03.057.

119. Rosenblum, D.; Joshi, N.; Tao, W.; Karp, J.M.; Peer, D. Progress and challenges towards targeted delivery of cancer therapeutics. *Nature Communications* **2018**, *9*, 1410, doi:10.1038/s41467-018-03705-y.

120. Xia, Y.; Rao, L.; Yao, H.; Wang, Z.; Ning, P.; Chen, X. Engineering Macrophages for Cancer Immunotherapy and Drug Delivery. *Advanced Materials* **2020**, *32*, 2002054, doi:10.1002/adma.202002054.

121. Xiao, Y.; Huang, W.; Zhu, D.; Wang, Q.; Chen, B.; Liu, Z.; Wang, Y.; Liu, Q. Cancer cell membrane-camouflaged MOF nanoparticles for a potent dihydroartemisinin-based hepatocellular carcinoma therapy. *RSC Advances* **2020**, *10*, 7194–7205, doi:10.1039/C9RA09233A.

122. Zhang, Y.; Yang, L.; Wang, H.; Huang, J.; Lin, Y.; Chen, S.; Guan, X.; Yi, M.; Li, S.; Zhang, L. Bioinspired metal–organic frameworks mediated efficient delivery of siRNA for cancer therapy. *Chemical Engineering Journal* **2021**, *426*, 131926, doi:10.1016/j.cej.2021.131926.

123. Pérez-Herrero, E.; Fernández-Medarde, A. Advanced targeted therapies in cancer: Drug nanocarriers, the future of chemotherapy. *European Journal of Pharmaceutics and Biopharmaceutics* **2015**, *93*, 52–79, doi:10.1016/j.ejpb.2015.03.018.

124. Suzuki, R.; Takizawa, T.; Kuwata, Y.; Mutoh, M.; Ishiguro, N.; Utoguchi, N.; Shinohara, A.; Eriguchi, M.; Yanagie, H.; Maruyama, K. Effective anti-tumor activity of oxaliplatin encapsulated in transferrin–PEG-liposome. *International Journal of Pharmaceutics* **2008**, *346*, 143–150, doi:10.1016/j.ijpharm.2007.06.010.

125. Mamot, C.; Drummond, D.C.; Noble, C.O.; Kallab, V.; Guo, Z.; Hong, K.; Kirpotin, D.B.; Park, J.W.

Epidermal Growth Factor Receptor–Targeted Immunoliposomes Significantly Enhance the Efficacy of Multiple Anticancer Drugs In vivo. *Cancer Research* **2005**, *65*, 11631–11638, doi:10.1158/0008-5472.CAN-05-1093.

126. Yoo, H.S.; Park, T.G. Folate receptor targeted biodegradable polymeric doxorubicin micelles. *Journal of Controlled Release* **2004**, *96*, 273–283, doi:10.1016/j.jconrel.2004.02.003.

127. Hu, Z.; Luo, F.; Pan, Y.; Hou, C.; Ren, L.; Chen, J.; Wang, J.; Zhang, Y. Arg-Gly-Asp (RGD) peptide conjugated poly(lactic acid)-poly(ethylene oxide) micelle for targeted drug delivery. *Journal of Biomedical Materials Research Part A* **2008**, *85A*, 797–807, doi:10.1002/jbm.a.31615.

128. Cheng, C.; Wei, H.; Zhu, J.-L.; Chang, C.; Cheng, H.; Li, C.; Cheng, S.-X.; Zhang, X.-Z.; Zhuo, R.-X. Functionalized Thermoresponsive Micelles Self-Assembled from Biotin-PEG- b -P(NIPAAm- co -HMAAm)- b -PMMA for Tumor Cell Target. *Bioconjugate Chemistry* **2008**, *19*, 1194–1201, doi:10.1021/bc8000062.

129. Rodrigues, C.F.; Alves, C.G.; Lima-Sousa, R.; Moreira, A.F.; de Melo-Diogo, D.; Correia, I.J. Inorganic-based drug delivery systems for cancer therapy. In *Advances and Avenues in the Development of Novel Carriers for Bioactives and Biological Agents*; Elsevier, 2020; pp. 283–316.

130. Danhier, F.; Vroman, B.; Lecouturier, N.; Crokart, N.; Pourcelle, V.; Freichels, H.; Jérôme, C.; Marchand-Brynaert, J.; Feron, O.; Préat, V. Targeting of tumor endothelium by RGD-grafted PLGA-nanoparticles loaded with Paclitaxel. *Journal of Controlled Release* **2009**, *140*, 166–173, doi:10.1016/j.jconrel.2009.08.011.

131. Jang, C.; Lee, J.H.; Sahu, A.; Tae, G. The synergistic effect of folate and RGD dual ligand of nanographene oxide on tumor targeting and photothermal therapy in vivo. *Nanoscale* **2015**, *7*, 18584–18594, doi:10.1039/C5NR05067G.

132. Sun, Q.; Bi, H.; Wang, Z.; Li, C.; Wang, X.; Xu, J.; Zhu, H.; Zhao, R.; He, F.; Gai, S.; et al. Hyaluronic acid-targeted and pH-responsive drug delivery system based on metal-organic frameworks for efficient antitumor therapy. *Biomaterials* **2019**, *223*, 119473, doi:10.1016/j.biomaterials.2019.119473.

133. Dong, K.; Wang, Z.; Zhang, Y.; Ren, J.; Qu, X. Metal–Organic Framework-Based Nanoplatform for Intracellular Environment-Responsive Endo/Lysosomal Escape and Enhanced Cancer Therapy. *ACS Applied Materials & Interfaces* **2018**, *10*, 31998–32005, doi:10.1021/acsami.8b11972.

134. Jia, Q.; Li, Z.; Guo, C.; Huang, X.; Kang, M.; Song, Y.; He, L.; Zhou, N.; Wang, M.; Zhang, Z.; et al. PEGMA-modified bimetallic NiCo Prussian blue analogue doped with Tb(III) ions: Efficiently pH-responsive and controlled release system for anticancer drug. *Chemical Engineering Journal* **2020**, *389*, 124468, doi:10.1016/j.cej.2020.124468.

135. Wong, C.; Stylianopoulos, T.; Cui, J.; Martin, J.; Chauhan, V.P.; Jiang, W.; Popović, Z.; Jain, R.K.; Bawendi, M.G.; Fukumura, D. Multistage nanoparticle delivery system for deep penetration into tumor tissue. *Proceedings of the National Academy of Sciences* **2011**, *108*, 2426–2431, doi:10.1073/pnas.1018382108.

136. Izci, M.; Maksoudian, C.; Manshian, B.B.; Soenen, S.J. The Use of Alternative Strategies for Enhanced

Nanoparticle Delivery to Solid Tumors. *Chemical Reviews* **2021**, *121*, 1746–1803, doi:10.1021/acs.chemrev.0c00779.

137. Zelepukin, I. V.; Griaznova, O.Y.; Shevchenko, K.G.; Ivanov, A. V.; Baidyuk, E. V.; Serejnikova, N.B.; Volovetskiy, A.B.; Deyev, S.M.; Zvyagin, A. V. Flash drug release from nanoparticles accumulated in the targeted blood vessels facilitates the tumour treatment. *Nature Communications* **2022**, *13*, 6910, doi:10.1038/s41467-022-34718-3.

138. Parakhonskiy, B. V.; Shilyagina, N.Y.; Gusliakova, O.I.; Volovetskiy, A.B.; Kostyuk, A.B.; Balalaeva, I. V.; Klapshina, L.G.; Lermontova, S.A.; Tolmachev, V.; Orlova, A.; et al. A method of drug delivery to tumors based on rapidly biodegradable drug-loaded containers. *Applied Materials Today* **2021**, *25*, 101199, doi:10.1016/j.apmt.2021.101199.

139. Su, J.L.; Wang, B.; Wilson, K.E.; Bayer, C.L.; Chen, Y.-S.; Kim, S.; Homan, K.A.; Emelianov, S.Y. Advances in clinical and biomedical applications of photoacoustic imaging. *Expert Opinion on Medical Diagnostics* **2010**, *4*, 497–510, doi:10.1517/17530059.2010.529127.

140. Li, Y.; Yang, L. Driving forces for drug loading in drug carriers. *Journal of Microencapsulation* **2015**, *32*, 255–272, doi:10.3109/02652048.2015.1010459.

141. Kowalczuk, A.; Trzcinska, R.; Trzebicka, B.; Müller, A.H.E.; Dworak, A.; Tsvetanov, C.B. Loading of polymer nanocarriers: Factors, mechanisms and applications. *Progress in Polymer Science* **2014**, *39*, 43–86, doi:10.1016/j.progpolymsci.2013.10.004.

142. Xie, Z.; Cai, X.; Sun, C.; Liang, S.; Shao, S.; Huang, S.; Cheng, Z.; Pang, M.; Xing, B.; Kheraif, A.A. Al; et al. O 2 -Loaded pH-Responsive Multifunctional Nanodrug Carrier for Overcoming Hypoxia and Highly Efficient Chemo-Photodynamic Cancer Therapy. *Chemistry of Materials* **2019**, *31*, 483–490, doi:10.1021/acs.chemmater.8b04321.

143. Ling, D.; Li, H.; Xi, W.; Wang, Z.; Bednarkiewicz, A.; Dibaba, S.T.; Shi, L.; Sun, L. Heterodimers made of metal–organic frameworks and upconversion nanoparticles for bioimaging and pH-responsive dual-drug delivery. *Journal of Materials Chemistry B* **2020**, *8*, 1316–1325, doi:10.1039/C9TB02753J.

144. Ghaffari, S.-B.; Sarrafzadeh, M.-H.; Salami, M.; Khorramizadeh, M.R. A pH-sensitive delivery system based on N-succinyl chitosan-ZnO nanoparticles for improving antibacterial and anticancer activities of curcumin. *International Journal of Biological Macromolecules* **2020**, *151*, 428–440, doi:10.1016/j.ijbiomac.2020.02.141.

145. Bavnhøj, C.G.; Knopp, M.M.; Madsen, C.M.; Löbmann, K. The role interplay between mesoporous silica pore volume and surface area and their effect on drug loading capacity. *International Journal of Pharmaceutics: X* **2019**, *1*, 100008, doi:10.1016/j.ijpx.2019.100008.

146. Pandey, A.; Kulkarni, S.; Vincent, A.P.; Nannuri, S.H.; George, S.D.; Mutalik, S. Hyaluronic acid-drug conjugate modified core-shell MOFs as pH responsive nanoplatform for multimodal therapy of glioblastoma. *International Journal of Pharmaceutics* **2020**, *588*, 119735, doi:10.1016/j.ijpharm.2020.119735.

147. Karimi Ghezeli, Z.; Hekmati, M.; Veisi, H. Synthesis of Imatinib-loaded chitosan-modified magnetic nanoparticles as an anti-cancer agent for pH responsive targeted drug delivery. *Applied Organometallic Chemistry* **2019**, *33*, e4833, doi:10.1002/aoc.4833.

148. Abazari, R.; Mahjoub, A.R.; Ataei, F.; Morsali, A.; Carpenter-Warren, C.L.; Mehdizadeh, K.; Slawin, A.M.Z. Chitosan Immobilization on Bio-MOF Nanostructures: A Biocompatible pH-Responsive Nanocarrier for Doxorubicin Release on MCF-7 Cell Lines of Human Breast Cancer. *Inorganic Chemistry* **2018**, *57*, 13364–13379, doi:10.1021/acs.inorgchem.8b01955.

149. Kundu, M.; Sadhukhan, P.; Ghosh, N.; Chatterjee, S.; Manna, P.; Das, J.; Sil, P.C. pH-responsive and targeted delivery of curcumin via phenylboronic acid-functionalized ZnO nanoparticles for breast cancer therapy. *Journal of Advanced Research* **2019**, *18*, 161–172, doi:10.1016/j.jare.2019.02.036.

150. Cortés-Funes, H.; Coronado, C. Role of anthracyclines in the era of targeted therapy. *Cardiovascular Toxicology* **2007**, *7*, 56–60, doi:10.1007/s12012-007-0015-3.

151. Kunene, S.C.; Lin, K.-S.; Weng, M.-T.; Carrera Espinoza, M.J.; Wu, C.-M. In vitro study of doxorubicin-loaded thermo- and pH-tunable carriers for targeted drug delivery to liver cancer cells. *Journal of Industrial and Engineering Chemistry* **2021**, *104*, 93–105, doi:10.1016/j.jiec.2021.08.012.

152. Liang, Z.; Yang, Z.; Yuan, H.; Wang, C.; Qi, J.; Liu, K.; Cao, R.; Zheng, H. A protein@metal–organic framework nanocomposite for pH-triggered anticancer drug delivery. *Dalton Transactions* **2018**, *47*, 10223–10228, doi:10.1039/C8DT01789A.

153. Schindler, C.; Collinson, A.; Matthews, C.; Pointon, A.; Jenkinson, L.; Minter, R.R.; Vaughan, T.J.; Tigue, N.J. Exosomal delivery of doxorubicin enables rapid cell entry and enhanced in vitro potency. *PLOS ONE* **2019**, *14*, e0214545, doi:10.1371/journal.pone.0214545.

154. Pooresmaeil, M.; Asl, E.A.; Namazi, H. A new pH-sensitive CS/Zn-MOF@GO ternary hybrid compound as a biofriendly and implantable platform for prolonged 5-Fluorouracil delivery to human breast cancer cells. *Journal of Alloys and Compounds* **2021**, *885*, 160992, doi:10.1016/j.jallcom.2021.160992.

155. Álvarez, P.; Marchal, J.A.; Boulaiz, H.; Carrillo, E.; Vélez, C.; Rodríguez-Serrano, F.; Melguizo, C.; Prados, J.; Madeddu, R.; Aranega, A. 5-Fluorouracil derivatives: a patent review. *Expert Opinion on Therapeutic Patents* **2012**, *22*, 107–123, doi:10.1517/13543776.2012.661413.

156. Raduly, F.; Raditoiu, V.; Raditoiu, A.; Purcar, V. Curcumin: Modern Applications for a Versatile Additive. *Coatings* **2021**, *11*, 519, doi:10.3390/coatings11050519.

157. Pan-On, S.; Dilokthornsakul, P.; Tiyaboonchai, W. Trends in advanced oral drug delivery system for curcumin: A systematic review. *Journal of Controlled Release* **2022**, *348*, 335–345, doi:10.1016/j.jconrel.2022.05.048.

158. Sethiya, A.; Agarwal, D.K.; Agarwal, S. Current Trends in Drug Delivery System of Curcumin and its Therapeutic Applications. *Mini-Reviews in Medicinal Chemistry* **2020**, *20*, 1190–1232, doi:10.2174/1389557520666200429103647.

159. Xue, Z.; Zhu, M.; Dong, Y.; Feng, T.; Chen, Z.; Feng, Y.; Shan, Z.; Xu, J.; Meng, S. An integrated targeting drug delivery system based on the hybridization of graphdiyne and MOFs for visualized cancer therapy. *Nanoscale* **2019**, *11*, 11709–11718, doi:10.1039/C9NR02017A.

160. Alimohammadi, E.; Maleki, R.; Akbarialiabad, H.; Dahri, M. Novel pH-responsive nanohybrid for simultaneous delivery of doxorubicin and paclitaxel: an in-silico insight. *BMC Chemistry* **2021**, *15*, 11, doi:10.1186/s13065-021-00735-4.

161. Bilalis, P.; Tziveleka, L.-A.; Varlas, S.; Iatrou, H. pH-Sensitive nanogates based on poly(<scp>l</scp> -histidine) for controlled drug release from mesoporous silica nanoparticles. *Polymer Chemistry* **2016**, *7*, 1475–1485, doi:10.1039/C5PY01841B.

162. Lai, X.; Liu, H.; Zheng, Y.; Wang, Z.; Chen, Y. Drug Loaded Nanoparticles of Metal-Organic Frameworks with High Colloidal Stability for Anticancer Application. *Journal of Biomedical Nanotechnology* **2019**, *15*, 1754–1763, doi:10.1166/jbn.2019.2807.

163. Gao, H.; Chi, B.; Tian, F.; Xu, M.; Xu, Z.; Li, L.; Wang, J. Prussian Blue modified Metal Organic Frameworks for imaging guided synergetic tumor therapy with hypoxia modulation. *Journal of Alloys and Compounds* **2021**, *853*, 157329, doi:10.1016/j.jallcom.2020.157329.

164. Wang, S.; Wu, H.; Sun, K.; Hu, J.; Chen, F.; Liu, W.; Chen, J.; Sun, B.; Hossain, A.M.S. A novel pH-responsive Fe-MOF system for enhanced cancer treatment mediated by the Fenton reaction. *New Journal of Chemistry* **2021**, *45*, 3271–3279, doi:10.1039/D0NJ05105E.

165. Zheng, H.; Zhang, Y.; Liu, L.; Wan, W.; Guo, P.; Nyström, A.M.; Zou, X. One-pot Synthesis of Metal–Organic Frameworks with Encapsulated Target Molecules and Their Applications for Controlled Drug Delivery. *Journal of the American Chemical Society* **2016**, *138*, 962–968, doi:10.1021/jacs.5b11720.

166. Ren, S.-Z.; Zhu, D.; Zhu, X.-H.; Wang, B.; Yang, Y.-S.; Sun, W.-X.; Wang, X.-M.; Lv, P.-C.; Wang, Z.-C.; Zhu, H.-L. Nanoscale Metal–Organic-Frameworks Coated by Biodegradable Organosilica for pH and Redox Dual Responsive Drug Release and High-Performance Anticancer Therapy. *ACS Applied Materials & Interfaces* **2019**, *11*, 20678–20688, doi:10.1021/acsami.9b04236.

167. Sun, C.-Y.; Qin, C.; Wang, X.-L.; Yang, G.-S.; Shao, K.-Z.; Lan, Y.-Q.; Su, Z.-M.; Huang, P.; Wang, C.-G.; Wang, E.-B. Zeolitic imidazolate framework-8 as efficient pH-sensitive drug delivery vehicle. *Dalton Transactions* **2012**, *41*, 6906, doi:10.1039/c2dt30357d.

168. Li, Y.; Song, Y.; Zhang, W.; Xu, J.; Hou, J.; Feng, X.; Zhu, W. MOF nanoparticles with encapsulated dihydroartemisinin as a controlled drug delivery system for enhanced cancer therapy and mechanism analysis. *Journal of Materials Chemistry B* **2020**, *8*, 7382–7389, doi:10.1039/D0TB01330G.

169. Shi, Z.; Chen, X.; Zhang, L.; Ding, S.; Wang, X.; Lei, Q.; Fang, W. FA-PEG decorated MOF nanoparticles as a targeted drug delivery system for controlled release of an autophagy inhibitor. *Biomaterials Science* **2018**, *6*, 2582–2590, doi:10.1039/C8BM00625C.

170. Wang, H.; Chen, Y.; Wang, H.; Liu, X.; Zhou, X.; Wang, F. DNAzyme-Loaded Metal–Organic

Frameworks (MOFs) for Self-Sufficient Gene Therapy. *Angewandte Chemie* **2019**, *131*, 7458–7462, doi:10.1002/ange.201902714.

171. Luu, C.L.; Nguyen, T.T. Van; Nguyen, T.; Hoang, T.C. Synthesis, characterization and adsorption ability of UiO-66-NH 2. *Advances in Natural Sciences: Nanoscience and Nanotechnology* **2015**, *6*, 025004, doi:10.1088/2043-6262/6/2/025004.

172. Chen, Q.; He, Q.; Lv, M.; Xu, Y.; Yang, H.; Liu, X.; Wei, F. Selective adsorption of cationic dyes by UiO-66-NH2. *Applied Surface Science* **2015**, *327*, 77–85, doi:10.1016/j.apsusc.2014.11.103.

173. Ranji-Burachaloo, H.; Karimi, F.; Xie, K.; Fu, Q.; Gurr, P.A.; Dunstan, D.E.; Qiao, G.G. MOF-Mediated Destruction of Cancer Using the Cell's Own Hydrogen Peroxide. *ACS Applied Materials & Interfaces* **2017**, *9*, 33599–33608, doi:10.1021/acsami.7b07981.

174. Jia, X.; Yang, Z.; Wang, Y.; Chen, Y.; Yuan, H.; Chen, H.; Xu, X.; Gao, X.; Liang, Z.; Sun, Y.; et al. Hollow Mesoporous Silica@Metal-Organic Framework and Applications for pH-Responsive Drug Delivery. *ChemMedChem* **2018**, *13*, 400–405, doi:10.1002/cmdc.201800019.

175. Li, S.; Zhang, L.; Liang, X.; Wang, T.; Chen, X.; Liu, C.; Li, L.; Wang, C. Tailored synthesis of hollow MOF/polydopamine Janus nanoparticles for synergistic multi-drug chemo-photothermal therapy. *Chemical Engineering Journal* **2019**, *378*, 122175, doi:10.1016/j.cej.2019.122175.

176. Gharehdaghi, Z.; Rahimi, R.; Naghib, S.M.; Molaabasi, F. Cu (II)-porphyrin metal–organic framework/graphene oxide: synthesis, characterization, and application as a pH-responsive drug carrier for breast cancer treatment. *JBIC Journal of Biological Inorganic Chemistry* **2021**, *26*, 689–704, doi:10.1007/s00775-021-01887-3.

177. Jia, Q.; Li, Z.; Guo, C.; Huang, X.; Song, Y.; Zhou, N.; Wang, M.; Zhang, Z.; He, L.; Du, M. A γ-cyclodextrin-based metal–organic framework embedded with graphene quantum dots and modified with PEGMA via SI-ATRP for anticancer drug delivery and therapy. *Nanoscale* **2019**, *11*, 20956–20967, doi:10.1039/C9NR06195A.

178. Ni, W.; Zhang, L.; Zhang, H.; Zhang, C.; Jiang, K.; Cao, X. Hierarchical MOF-on-MOF Architecture for pH/GSH-Controlled Drug Delivery and Fe-Based Chemodynamic Therapy. *Inorganic Chemistry* **2022**, *61*, 3281–3287, doi:10.1021/acs.inorgchem.1c03855.

179. Li, Y.; Song, K.; Cao, Y.; Peng, C.; Yang, G. Keratin-Templated Synthesis of Metallic Oxide Nanoparticles as MRI Contrast Agents and Drug Carriers. *ACS Applied Materials & Interfaces* **2018**, *10*, 26039–26045, doi:10.1021/acsami.8b08555.

180. Sun, X.-Y.; Zhang, H.-J.; Zhao, X.-Y.; Sun, Q.; Wang, Y.-Y.; Gao, E.-Q. Dual functions of pH-sensitive cation Zr-MOF for 5-Fu: large drug-loading capacity and high-sensitivity fluorescence detection. *Dalton Transactions* **2021**, *50*, 10524–10532, doi:10.1039/D1DT01772A.

181. Cai, Y.; Sheng, Z.; Wang, J. A Biocompatible Zinc(II)-based Metal-organic Framework for pH Responsive Drug Delivery and Anti-Lung Cancer Activity. *Zeitschrift für anorganische und allgemeine Chemie* **2018**,

644, 877–882, doi:10.1002/zaac.201800248.

182. Liu, Z.; Wu, Q.; He, J.; Vriesekoop, F.; Liang, H. Crystal-Seeded Growth of pH-Responsive Metal–Organic Frameworks for Enhancing Encapsulation, Stability, and Bioactivity of Hydrophobicity Compounds. *ACS Biomaterials Science & Engineering* **2019**, *5*, 6581–6589, doi:10.1021/acsbiomaterials.9b01070.

183. Ghorbani, M.; Bigdeli, B.; Jalili-baleh, L.; Baharifar, H.; Akrami, M.; Dehghani, S.; Goliaei, B.; Amani, A.; Lotfabadi, A.; Rashedi, H.; et al. Curcumin-lipoic acid conjugate as a promising anticancer agent on the surface of gold-iron oxide nanocomposites: A pH-sensitive targeted drug delivery system for brain cancer theranostics. *European Journal of Pharmaceutical Sciences* **2018**, *114*, 175–188, doi:10.1016/j.ejps.2017.12.008.

184. Cabrera-García, A.; Checa-Chavarria, E.; Rivero-Buceta, E.; Moreno, V.; Fernández, E.; Botella, P. Amino modified metal-organic frameworks as pH-responsive nanoplatforms for safe delivery of camptothecin. *Journal of Colloid and Interface Science* **2019**, *541*, 163–174, doi:10.1016/j.jcis.2019.01.042.

185. Sathishkumar, P.; Li, Z.; Govindan, R.; Jayakumar, R.; Wang, C.; Long Gu, F. Zinc oxide-quercetin nanocomposite as a smart nano-drug delivery system: Molecular-level interaction studies. *Applied Surface Science* **2021**, *536*, 147741, doi:10.1016/j.apsusc.2020.147741.

186. Zhang, K.; Meng, X.; Yang, Z.; Dong, H.; Zhang, X. Enhanced cancer therapy by hypoxia-responsive copper metal-organic frameworks nanosystem. *Biomaterials* **2020**, *258*, 120278, doi:10.1016/j.biomaterials.2020.120278.

187. Schnabel, J.; Ettlinger, R.; Bunzen, H. Zn-MOF-74 as pH-Responsive Drug-Delivery System of Arsenic Trioxide. *ChemNanoMat* **2020**, *6*, 1229–1236, doi:10.1002/cnma.202000221.

188. Xu, R.; Yang, J.; Qian, Y.; Deng, H.; Wang, Z.; Ma, S.; Wei, Y.; Yang, N.; Shen, Q. Ferroptosis/pyroptosis dual-inductive combinational anti-cancer therapy achieved by transferrin decorated nanoMOF. *Nanoscale Horizons* **2021**, *6*, 348–356, doi:10.1039/D0NH00674B.

189. R., P.; R., M.A.; R., A.; G., A.; N.M., P.; A., P.; N., S. Ecofriendly one pot fabrication of methyl gallate@ZIF-L nanoscale hybrid as pH responsive drug delivery system for lung cancer therapy. *Process Biochemistry* **2019**, *84*, 39–52, doi:10.1016/j.procbio.2019.06.015.

190. Wang, Y.; Li, P.; Kong, L. Chitosan-Modified PLGA Nanoparticles with Versatile Surface for Improved Drug Delivery. *AAPS PharmSciTech* **2013**, *14*, 585–592, doi:10.1208/s12249-013-9943-3.

191. Zsila, F.; Bikádi, Z.; Simonyi, M. Molecular basis of the Cotton effects induced by the binding of curcumin to human serum albumin. *Tetrahedron: Asymmetry* **2003**, *14*, 2433–2444, doi:10.1016/S0957-4166(03)00486-5.

192. Bami, M.S.; Raeisi Estabragh, M.A.; Khazaeli, P.; Ohadi, M.; Dehghannoudeh, G. pH-responsive drug delivery systems as intelligent carriers for targeted drug therapy: Brief history, properties, synthesis, mechanism and application. *Journal of Drug Delivery Science and Technology* **2022**, *70*, 102987,

doi:10.1016/j.jddst.2021.102987.

193. Stubbs, M.; McSheehy, P.M..; Griffiths, J.R.; Bashford, C.L. Causes and consequences of tumour acidity and implications for treatment. *Molecular Medicine Today* **2000**, *6*, 15–19, doi:10.1016/S1357-4310(99)01615-9.

194. Mura, S.; Nicolas, J.; Couvreur, P. Stimuli-responsive nanocarriers for drug delivery. *Nature Materials* **2013**, *12*, 991–1003, doi:10.1038/nmat3776.

195. Homayun, B.; Lin, X.; Choi, H.-J. Challenges and Recent Progress in Oral Drug Delivery Systems for Biopharmaceuticals. *Pharmaceutics* **2019**, *11*, 129, doi:10.3390/pharmaceutics11030129.

196. Das, R.P.; Gandhi, V. V.; Singh, B.G.; Kunwar, A. Passive and Active Drug Targeting: Role of Nanocarriers in Rational Design of Anticancer Formulations. *Current Pharmaceutical Design* **2019**, *25*, 3034–3056, doi:10.2174/1381612825666190830155319.

197. Attia, M.F.; Anton, N.; Wallyn, J.; Omran, Z.; Vandamme, T.F. An overview of active and passive targeting strategies to improve the nanocarriers efficiency to tumour sites. *Journal of Pharmacy and Pharmacology* **2019**, *71*, 1185–1198, doi:10.1111/jphp.13098.

198. Raj, S.; Khurana, S.; Choudhari, R.; Kesari, K.K.; Kamal, M.A.; Garg, N.; Ruokolainen, J.; Das, B.C.; Kumar, D. Specific targeting cancer cells with nanoparticles and drug delivery in cancer therapy. *Seminars in Cancer Biology* **2021**, *69*, 166–177, doi:10.1016/j.semcancer.2019.11.002.

199. Torchilin, V.P. Passive and Active Drug Targeting: Drug Delivery to Tumors as an Example. In; 2010; pp. 3–53.

200. Ali, E.S.; Sharker, S.M.; Islam, M.T.; Khan, I.N.; Shaw, S.; Rahman, M.A.; Uddin, S.J.; Shill, M.C.; Rehman, S.; Das, N.; et al. Targeting cancer cells with nanotherapeutics and nanodiagnostics: Current status and future perspectives. *Seminars in Cancer Biology* **2021**, *69*, 52–68, doi:10.1016/j.semcancer.2020.01.011.

201. He, X.; Li, J.; An, S.; Jiang, C. pH-sensitive drug-delivery systems for tumor targeting. *Therapeutic Delivery* **2013**, *4*, 1499–1510, doi:10.4155/tde.13.120.

202. Wike-Hooley, J.L.; Haveman, J.; Reinhold, H.S. The relevance of tumour pH to the treatment of malignant disease. *Radiotherapy and Oncology* **1984**, *2*, 343–366, doi:10.1016/S0167-8140(84)80077-8.

203. Soltani, M.; Souri, M.; Moradi Kashkooli, F. Effects of hypoxia and nanocarrier size on pH-responsive nano-delivery system to solid tumors. *Scientific Reports* **2021**, *11*, 19350, doi:10.1038/s41598-021-98638-w.

204. Li, J.-R.; Kuppler, R.J.; Zhou, H.-C. Selective gas adsorption and separation in metal–organic frameworks. *Chemical Society Reviews* **2009**, *38*, 1477, doi:10.1039/b802426j.

205. Wang, Y.; Yan, J.; Wen, N.; Xiong, H.; Cai, S.; He, Q.; Hu, Y.; Peng, D.; Liu, Z.; Liu, Y. Metal-organic frameworks for stimuli-responsive drug delivery. *Biomaterials* **2020**, *230*, 119619, doi:10.1016/j.biomaterials.2019.119619.

206. Zhang, F.-M.; Dong, H.; Zhang, X.; Sun, X.-J.; Liu, M.; Yang, D.-D.; Liu, X.; Wei, J.-Z. Postsynthetic Modification of ZIF-90 for Potential Targeted Codelivery of Two Anticancer Drugs. *ACS Applied Materials & Interfaces* **2017**, *9*, 27332–27337, doi:10.1021/acsami.7b08451.

207. Huang, A.; Dou, W.; Caro, J. Steam-Stable Zeolitic Imidazolate Framework ZIF-90 Membrane with Hydrogen Selectivity through Covalent Functionalization. *Journal of the American Chemical Society* **2010**, *132*, 15562–15564, doi:10.1021/ja108774v.

208. Zhang, L.; Gao, Y.; Sun, S.; Li, Z.; Wu, A.; Zeng, L. pH-Responsive metal–organic framework encapsulated gold nanoclusters with modulated release to enhance photodynamic therapy/chemotherapy in breast cancer. *Journal of Materials Chemistry B* **2020**, *8*, 1739–1747, doi:10.1039/C9TB02621E.

209. Lei, J.; Wang, H.; Zhu, D.; Wan, Y.; Yin, L. Combined effects of avasimibe immunotherapy, doxorubicin chemotherapy, and metal–organic frameworks nanoparticles on breast cancer. *Journal of Cellular Physiology* **2020**, *235*, 4814–4823, doi:10.1002/jcp.29358.

210. Lovitt, C.; Shelper, T.; Avery, V. Advanced Cell Culture Techniques for Cancer Drug Discovery. *Biology* **2014**, *3*, 345–367, doi:10.3390/biology3020345.

211. Präbst, K.; Engelhardt, H.; Ringgeler, S.; Hübner, H. Basic Colorimetric Proliferation Assays: MTT, WST, and Resazurin. In; 2017; pp. 1–17.

212. Ramirez, C.N.; Antczak, C.; Djaballah, H. Cell viability assessment: toward content-rich platforms. *Expert Opinion on Drug Discovery* **2010**, *5*, 223–233, doi:10.1517/17460441003596685.

213. Aykul, S.; Martinez-Hackert, E. Determination of half-maximal inhibitory concentration using biosensor-based protein interaction analysis. *Analytical Biochemistry* **2016**, *508*, 97–103, doi:10.1016/j.ab.2016.06.025.

214. Biological evaluation of medical devices —Part 5: Tests for in vitro cytotoxicity. In *ANSI/AAMI/ISO 10993-5:2009/(R)2014; Biological evaluation of medical devices —Part 5: Tests for in vitro cytotoxicity*; AAMI, 2009.

215. Dong, K.; Zhang, Y.; Zhang, L.; Wang, Z. Facile preparation of metal–organic frameworks-based hydrophobic anticancer drug delivery nanoplatform for targeted and enhanced cancer treatment. *Talanta* **2019**, *194*, 703–708, doi:10.1016/j.talanta.2018.10.101.

216. Stockert, J.C.; Horobin, R.W.; Colombo, L.L.; Blázquez-Castro, A. Tetrazolium salts and formazan products in Cell Biology: Viability assessment, fluorescence imaging, and labeling perspectives. *Acta Histochemica* **2018**, *120*, 159–167, doi:10.1016/j.acthis.2018.02.005.

217. Ishiyama, M. A highly water-soluble disulfonated tetrazolium salt as a chromogenic indicator for NADH as well as cell viability. *Talanta* **1997**, *44*, 1299–1305, doi:10.1016/S0039-9140(97)00017-9.

218. Tominaga, H.; Ishiyama, M.; Ohseto, F.; Sasamoto, K.; Hamamoto, T.; Suzuki, K.; Watanabe, M. A water-soluble tetrazolium salt useful for colorimetric cell viability assay. *Analytical Communications* **1999**, *36*,

47–50, doi:10.1039/a809656b.

219. Ginouves, M.; Carme, B.; Couppie, P.; Prevot, G. Comparison of Tetrazolium Salt Assays for Evaluation of Drug Activity against Leishmania spp. *Journal of Clinical Microbiology* **2014**, *52*, 2131–2138, doi:10.1128/JCM.00201-14.

220. Riss, T.L.; Moravec, R.A.; Niles, A.L.; Duellman, S.; Benink, H.A.; Worzella, T.J.; Minor, L. *Cell Viability Assays*; 2004;

221. Huo, D.; Liu, S.; Zhang, C.; He, J.; Zhou, Z.; Zhang, H.; Hu, Y. Hypoxia-Targeting, Tumor Microenvironment Responsive Nanocluster Bomb for Radical-Enhanced Radiotherapy. *ACS Nano* **2017**, *11*, 10159–10174, doi:10.1021/acsnano.7b04737.

222. Huang, X.; Teng, X.; Chen, D.; Tang, F.; He, J. The effect of the shape of mesoporous silica nanoparticles on cellular uptake and cell function. *Biomaterials* **2010**, *31*, 438–448, doi:10.1016/j.biomaterials.2009.09.060.

223. Chithrani, B.D.; Ghazani, A.A.; Chan, W.C.W. Determining the Size and Shape Dependence of Gold Nanoparticle Uptake into Mammalian Cells. *Nano Letters* **2006**, *6*, 662–668, doi:10.1021/nl052396o.

224. Nakamura, T.; Akita, H.; Yamada, Y.; Hatakeyama, H.; Harashima, H. A Multifunctional Envelope-type Nanodevice for Use in Nanomedicine: Concept and Applications. *Accounts of Chemical Research* **2012**, *45*, 1113–1121, doi:10.1021/ar200254s.

225. Yang, X.-Z.; Du, J.-Z.; Dou, S.; Mao, C.-Q.; Long, H.-Y.; Wang, J. Sheddable Ternary Nanoparticles for Tumor Acidity-Targeted siRNA Delivery. *ACS Nano* **2012**, *6*, 771–781, doi:10.1021/nn204240b.

226. Poon, Z.; Chang, D.; Zhao, X.; Hammond, P.T. Layer-by-Layer Nanoparticles with a pH-Sheddable Layer for in Vivo Targeting of Tumor Hypoxia. *ACS Nano* **2011**, *5*, 4284–4292, doi:10.1021/nn200876f.

227. Wyman, T.B.; Nicol, F.; Zelphati, O.; Scaria, P. V.; Plank, C.; Szoka, F.C. Design, Synthesis, and Characterization of a Cationic Peptide That Binds to Nucleic Acids and Permeabilizes Bilayers. *Biochemistry* **1997**, *36*, 3008–3017, doi:10.1021/bi9618474.

228. Guo, X.D.; Wiradharma, N.; Liu, S.Q.; Zhang, L.J.; Khan, M.; Qian, Y.; Yang, Y.-Y. Oligomerized alpha-helical KALA peptides with pendant arms bearing cell-adhesion, DNA-binding and endosome-buffering domains as efficient gene transfection vectors. *Biomaterials* **2012**, *33*, 6284–6291, doi:10.1016/j.biomaterials.2012.05.033.

229. Subbarao, N.K.; Parente, R.A.; Szoka, F.C.; Nadasdi, L.; Pongracz, K. The pH-dependent bilayer destabilization by an amphipathic peptide. *Biochemistry* **1987**, *26*, 2964–2972, doi:10.1021/bi00385a002.

230. Ouahab, A.; Cheraga, N.; Onoja, V.; Shen, Y.; Tu, J. Novel pH-sensitive charge-reversal cell penetrating peptide conjugated PEG-PLA micelles for docetaxel delivery: In vitro study. *International Journal of Pharmaceutics* **2014**, *466*, 233–245, doi:10.1016/j.ijpharm.2014.03.009.

231. Jin, Y.; Song, L.; Su, Y.; Zhu, L.; Pang, Y.; Qiu, F.; Tong, G.; Yan, D.; Zhu, B.; Zhu, X. Oxime Linkage: A Robust Tool for the Design of pH-Sensitive Polymeric Drug Carriers. *Biomacromolecules* **2011**, *12*, 3460–

3468, doi:10.1021/bm200956u.

232. Sykes, E.A.; Dai, Q.; Sarsons, C.D.; Chen, J.; Rocheleau, J. V.; Hwang, D.M.; Zheng, G.; Cramb, D.T.; Rinker, K.D.; Chan, W.C.W. Tailoring nanoparticle designs to target cancer based on tumor pathophysiology. *Proceedings of the National Academy of Sciences* **2016**, *113*, doi:10.1073/pnas.1521265113.

233. Wei, W.; Zhang, X.; Zhang, S.; Wei, G.; Su, Z. Biomedical and bioactive engineered nanomaterials for targeted tumor photothermal therapy: A review. *Materials Science and Engineering: C* **2019**, *104*, 109891, doi:10.1016/j.msec.2019.109891.

234. Chen, J.; Zhu, Y.; Wu, C.; Shi, J. Nanoplatform-based cascade engineering for cancer therapy. *Chemical Society Reviews* **2020**, *49*, 9057–9094, doi:10.1039/D0CS00607F.

235. Yang, H.; Tang, C.; Yin, C. Estrone-modified pH-sensitive glycol chitosan nanoparticles for drug delivery in breast cancer. *Acta Biomaterialia* **2018**, *73*, 400–411, doi:10.1016/j.actbio.2018.04.020.

236. Palanikumar, L.; Al-Hosani, S.; Kalmouni, M.; Nguyen, V.P.; Ali, L.; Pasricha, R.; Barrera, F.N.; Magzoub, M. pH-responsive high stability polymeric nanoparticles for targeted delivery of anticancer therapeutics. *Communications Biology* **2020**, *3*, 95, doi:10.1038/s42003-020-0817-4.

237. Luan, S.; Zhu, Y.; Wu, X.; Wang, Y.; Liang, F.; Song, S. Hyaluronic-Acid-Based pH-Sensitive Nanogels for Tumor-Targeted Drug Delivery. *ACS Biomaterials Science & Engineering* **2017**, *3*, 2410–2419, doi:10.1021/acsbiomaterials.7b00444.

238. Li, H.-J.; Du, J.-Z.; Du, X.-J.; Xu, C.-F.; Sun, C.-Y.; Wang, H.-X.; Cao, Z.-T.; Yang, X.-Z.; Zhu, Y.-H.; Nie, S.; et al. Stimuli-responsive clustered nanoparticles for improved tumor penetration and therapeutic efficacy. *Proceedings of the National Academy of Sciences* **2016**, *113*, 4164–4169, doi:10.1073/pnas.1522080113.

239. Liu, B.; Thayumanavan, S. Importance of Evaluating Dynamic Encapsulation Stability of Amphiphilic Assemblies in Serum. *Biomacromolecules* **2017**, *18*, 4163–4170, doi:10.1021/acs.biomac.7b01220.

240. Palanikumar, L.; Choi, E.S.; Oh, J.Y.; Park, S.A.; Choi, H.; Kim, K.; Kim, C.; Ryu, J.-H. Importance of Encapsulation Stability of Nanocarriers with High Drug Loading Capacity for Increasing in Vivo Therapeutic Efficacy. *Biomacromolecules* **2018**, *19*, 3030–3039, doi:10.1021/acs.biomac.8b00589.

241. Anselmo, A.C.; Mitragotri, S. Nanoparticles in the clinic: An update. *Bioengineering & Translational Medicine* **2019**, *4*, doi:10.1002/btm2.10143.

242. Zhang, J.; Yang, C.; Pan, S.; Shi, M.; Li, J.; Hu, H.; Qiao, M.; Chen, D.; Zhao, X. Eph A10-modified pH-sensitive liposomes loaded with novel triphenylphosphine–docetaxel conjugate possess hierarchical targetability and sufficient antitumor effect both in vitro and in vivo. *Drug Delivery* **2018**, *25*, 723–737, doi:10.1080/10717544.2018.1446475.

243. Momekova, D.; Rangelov, S.; Lambov, N. Long-Circulating, pH-Sensitive Liposomes. In; 2017; pp. 209–226.

244. Nunes, S.S.; de Oliveira Silva, J.; Fernandes, R.S.; Miranda, S.E.M.; Leite, E.A.; de Farias, M.A.; Portugal,

R.V.; Cassali, G.D.; Townsend, D.M.; Oliveira, M.C.; et al. PEGylated versus Non-PEGylated pH-Sensitive Liposomes: New Insights from a Comparative Antitumor Activity Study. *Pharmaceutics* **2022**, *14*, 272, doi:10.3390/pharmaceutics14020272.

245. Jain, S.; Deore, S.V.; Ghadi, R.; Chaudhari, D.; Kuche, K.; Katiyar, S.S. Tumor microenvironment responsive VEGF-antibody functionalized pH sensitive liposomes of docetaxel for augmented breast cancer therapy. *Materials Science and Engineering: C* **2021**, *121*, 111832, doi:10.1016/j.msec.2020.111832.

246. Gheybi, F.; Alavizadeh, S.H.; Rezayat, S.M.; Hatamipour, M.; Akhtari, J.; Faridi Majidi, R.; Badiee, A.; Jaafari, M.R. pH-Sensitive PEGylated Liposomal Silybin: Synthesis, In Vitro and In Vivo Anti-Tumor Evaluation. *Journal of Pharmaceutical Sciences* **2021**, *110*, 3919–3928, doi:10.1016/j.xphs.2021.08.015.

247. Xu, H.; Cui, W.; Zong, Z.; Tan, Y.; Xu, C.; Cao, J.; Lai, T.; Tang, Q.; Wang, Z.; Sui, X.; et al. A facile method for anti-cancer drug encapsulation into polymersomes with a core-satellite structure. *Drug Delivery* **2022**, *29*, 2414–2427, doi:10.1080/10717544.2022.2103209.

248. de Oliveira Silva, J.; Fernandes, R.S.; Ramos Oda, C.M.; Ferreira, T.H.; Machado Botelho, A.F.; Martins Melo, M.; de Miranda, M.C.; Assis Gomes, D.; Dantas Cassali, G.; Townsend, D.M.; et al. Folate-coated, long-circulating and pH-sensitive liposomes enhance doxorubicin antitumor effect in a breast cancer animal model. *Biomedicine & Pharmacotherapy* **2019**, *118*, 109323, doi:10.1016/j.biopha.2019.109323.

249. Ou, W.; Jiang, L.; Gu, Y.; Soe, Z.C.; Kim, B.K.; Gautam, M.; Poudel, K.; Pham, L.M.; Phung, C.D.; Chang, J.-H.; et al. Regulatory T Cells Tailored with pH-Responsive Liposomes Shape an Immuno-Antitumor Milieu against Tumors. *ACS Applied Materials & Interfaces* **2019**, *11*, 36333–36346, doi:10.1021/acsami.9b11371.

250. Chen, Y.; Cheng, Y.; Zhao, P.; Zhang, S.; Li, M.; He, C.; Zhang, X.; Yang, T.; Yan, R.; Ye, P.; et al. Co-delivery of doxorubicin and imatinib by pH sensitive cleavable PEGylated nanoliposomes with folate-mediated targeting to overcome multidrug resistance. *International Journal of Pharmaceutics* **2018**, *542*, 266–279, doi:10.1016/j.ijpharm.2018.03.024.

251. Zhang, J.; Du, Z.; Pan, S.; Shi, M.; Li, J.; Yang, C.; Hu, H.; Qiao, M.; Chen, D.; Zhao, X. Overcoming Multidrug Resistance by Codelivery of MDR1-Targeting siRNA and Doxorubicin Using EphA10-Mediated pH-Sensitive Lipoplexes: In Vitro and In Vivo Evaluation. *ACS Applied Materials & Interfaces* **2018**, *10*, 21590–21600, doi:10.1021/acsami.8b01806.

252. Dogra, P.; Adolphi, N.L.; Wang, Z.; Lin, Y.-S.; Butler, K.S.; Durfee, P.N.; Croissant, J.G.; Noureddine, A.; Coker, E.N.; Bearer, E.L.; et al. Establishing the effects of mesoporous silica nanoparticle properties on in vivo disposition using imaging-based pharmacokinetics. *Nature Communications* **2018**, *9*, 4551, doi:10.1038/s41467-018-06730-z.

253. Li, Z.; Guo, J.; Qi, G.; Zhang, M.; Hao, L. pH-Responsive Drug Delivery and Imaging Study of Hybrid Mesoporous Silica Nanoparticles. *Molecules* **2022**, *27*, 6519, doi:10.3390/molecules27196519.

254. Zhang, B.; Chen, X.; Fan, X.; Zhu, J.; Wei, Y.; Zheng, H.; Zheng, H.; Wang, B.; Piao, J.; Li, F. Lipid/PAA-coated mesoporous silica nanoparticles for dual-pH-responsive codelivery of arsenic trioxide/paclitaxel

against breast cancer cells. *Acta Pharmacologica Sinica* **2021**, *42*, 832–842, doi:10.1038/s41401-021-00648-x.

255. Kumar, K.; Moitra, P.; Bashir, M.; Kondaiah, P.; Bhattacharya, S. Natural tripeptide capped pH-sensitive gold nanoparticles for efficacious doxorubicin delivery both in vitro and in vivo. *Nanoscale* **2020**, *12*, 1067–1074, doi:10.1039/C9NR08475D.

256. Cheng, R.; Jiang, L.; Gao, H.; Liu, Z.; Mäkilä, E.; Wang, S.; Saiding, Q.; Xiang, L.; Tang, X.; Shi, M.; et al. A pH-Responsive Cluster Metal–Organic Framework Nanoparticle for Enhanced Tumor Accumulation and Antitumor Effect. *Advanced Materials* **2022**, *34*, 2203915, doi:10.1002/adma.202203915.

257. Tan, G.; Zhong, Y.; Yang, L.; Jiang, Y.; Liu, J.; Ren, F. A multifunctional MOF-based nanohybrid as injectable implant platform for drug synergistic oral cancer therapy. *Chemical Engineering Journal* **2020**, *390*, 124446, doi:10.1016/j.cej.2020.124446.

258. Li, K.; Li, D.; Zhao, L.; Chang, Y.; Zhang, Y.; Cui, Y.; Zhang, Z. Calcium-mineralized polypeptide nanoparticle for intracellular drug delivery in osteosarcoma chemotherapy. *Bioactive Materials* **2020**, *5*, 721–731, doi:10.1016/j.bioactmat.2020.04.010.

259. Liu, Y.; Pan, Y.; Cao, W.; Xia, F.; Liu, B.; Niu, J.; Alfranca, G.; Sun, X.; Ma, L.; Fuente, J.M. de la; et al. A tumor microenvironment responsive biodegradable CaCO 3 /MnO 2 - based nanoplatform for the enhanced photodynamic therapy and improved PD-L1 immunotherapy. *Theranostics* **2019**, *9*, 6867–6884, doi:10.7150/thno.37586.